GREENER HYDROFORMYLATION WITH NANOFILTERABLE RHODIUM CATALYSTS IN A STIRRED MEMBRANE REACTOR

By

Zhuanzhuan Xie

Submitted to the graduate degree program in Chemical & Petroleum Engineering and the Graduate Faculty of the University of Kansas in partial fulfillment of the requirements for the degree of Doctor of Philosophy.

_____

Chairperson: Bala Subramaniam

_____

Raghunath V. Chaudhari

_____

Darryl Fahey

_____

Aaron Scurto

_____

Jon Tunge

Date Defended: April 12, 2013

The Thesis Committee for Zhuanzhuan Xie

certifies that this is the approved version of the following thesis:

GREENER HYDROFORMYLATION WITH NANOFILTERABLE RHODIUM CATALYSTS IN A STIRRED MEMBRANE REACTOR

_____

Chairperson: Bala Subramaniam

Date approved: April 18, 2013

Abstract

Hydroformylation for producing industrial chemical intermediates such as aldehydes and alcohols from olefinic substrates is a 15 billion lb/year industry and a potential route for increasing the carbon chain of light olefins such as ethylene and propylene to produce longer chain olefins. Novel, resource-efficient technologies that conserve feedstock and energy while producing the desired product continue to be interest to industry. This dissertation advances a novel continuous reactor concept involving gas-expanded liquids and nanofilterable catalysts with potential for practical viability.

It has been shown by previous researchers in our group that the use of simple homogeneous Rh/TPP catalyst for 1-octene hydroformylation in CO_2-expanded liquid (CXL) media provides exceptional TOF (~316 h^{-1}) and regioselectivity (*n*/*i* ~9) at mild pressure (~40 bar) and temperature (30-60 ℃) when compared to conventional media. Systematic phase equilibrium and reaction studies performed in this dissertation show that CXLs provide a way of increasing (i.e., tuning) H_2/CO ratio in the liquid phase at fixed syngas feed composition, low syngas partial pressures (i.e. avoiding syngas inhibition) and mild conditions (40-60 ℃, tens of bars).

A novel process concept for continuous hydroformylation in CXLs was demonstrated using bulky phosphite ligands that are effectively retained in the stirred reactor by a nanofiltration membrane. The reactor was operated at 50 ℃ with a syngas pressure of 6 bar to avoid CO inhibition of reaction rate and selectivity. The nanofiltration pressure was provided by ~32 bar CO_2 that also created CXL phase resulting in enhanced turnover frequency (~340 h^{-1}), aldehydes selectivity (>90%) and high regioselectivity (*n/i* ~8) at nearly steady operation for up to 50 h (cumulative TON of 17,680). Further, the use of

pressurized CO_2 also reduced the viscosity of the conventional liquid phase by 30 to 50% thereby improving the mass transfer properties. Constant permeate flux was maintained during the 50 h run with Rh leakage being less than 0.5 ppm.

Novel Rh complex catalysts bound to soluble versions of inexpensive functionalized polysiloxanes ligands were also investigated for the hydroformylation of higher olefins (C_{5+}) to enable nanofiltration in a continuous membrane reactor. Polysiloxanes containing two different functional groups (amine- and phosphine-) were used for Rh complexation. Both types of Rh complexes, when tested in batch and continuous hydroformylation experiments, show good activity and chemoselectivity for a variety of olefinic substrates. The phosphine-functionalized ligand exhibited higher activity (TOF = 165 h^{-1}) than the amine-functionalized one (TOF = 17 h^{-1}) at 6 bar and 50 ℃. Continuous operation with Rh complexes (with the phosphine-functionalized ligand) lasting several days in a stirred reactor equipped with nanofiltration membrane showed steady hydroformylation activity (TOF = 103 h^{-1}; cumulative TON = 12,240 after 120 hours) and high chemoselectivity (> 91%) towards the aldehydes. The Rh concentrations in the reactor effluent were less than a few ppm, which can be easily recovered by absorption and exceeds the economic viability criterion established by earlier work in our group. This technology concept has potential applications in homogeneous catalytic processes to improve resource utilization and catalyst containment for practical viability.

Acknowledgements

First of all, I would like to deeply thank my advisor, Professor Bala Subramaniam, for his patience and encouragement throughout the years. Whenever I struggled with my coursework or research, he's always there to provide me guidance and support. He is not only a great resource of knowledge and creativity that I benefit from, but also an excellent role model that I look up to.

I would like to also thank the rest of my committee members: Professor Raghunath Vitthal Chaudhari, Dr. Darryl Fahey, Professor Aaron Scurto and Professor Jon Tunge. They have provided me critical evaluations and valuable inputs in my research work to help me learn and improve.

I gratefully acknowledge funding from United States Department of Agriculture (Grant 2011-10006-30362) and the Center for Environmentally Beneficial Catalysis (CEBC).

Thanks to Dr. William Kirk Snavely, for his assistance and guidance in helping me building up and improving the experimental apparatus and for his wonderful friendship.

Thanks to Dr. Jing Fang, Dr. Swarup Maiti and Dr. Bibhas Sarkar for their partnership in my research. We have a great time collaborating and contributing together.

Thanks to my colleagues and friends in CEBC: Meng Li, Wenjuan Yan, Qing Pan, Steve Tang, Madhav Ghanta, Dr. Jackson Ford, Xin Jin, etc. Your friendship and company always warm my heart.

Thanks to Ed Atchison and Alan Walker, for their kind assistance in instrumentation.

Last but certainly not the least, thanks to my family. My parents, my brother, my husband and my dear daughter Amy. Without their love and support, I would have never been able to finish my degree.

Table of Contents

List of Figures

List of Tables

Chapter 1 : Introduction and Literature Review

1.1 Rh-Catalyzed hydroformylation reaction

Hydroformylation is one of the most important homogeneous industrial processes. It was first discovered by Otto Roelen[1] in 1938. In this reaction, olefins react with a mixture of hydrogen and carbon monoxide gas (synthesis gas or "syngas") under a metal catalyst (Figure 1.1). A formyl group (-CHO) and a hydrogen atom are added to the carbon-carbon double bond of the olefin. The main products are linear (*n*-) and branched (*iso or i*-) aldehydes as well as internal olefins. The aldehydes formed can be further hydrogenated or oxidized to corresponding alcohols and acids and make valuable commercial products.[2]

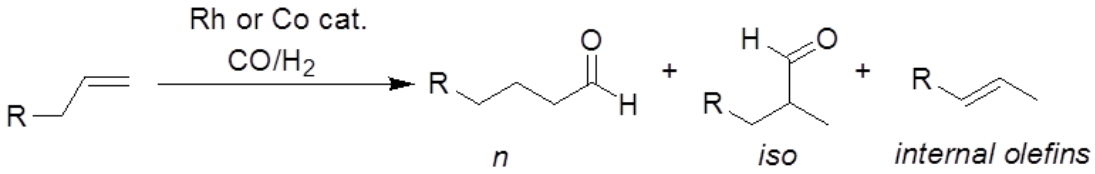

Figure 1.1: Hydroformylation reaction scheme

In current chemical industry, this reaction is mostly accomplished with a rhodium (Rh-) or cobalt (Co)-based catalyst.[3] In general, Co-based catalysts operate at very harsh conditions. For example, the most common cobalt catalyst cobalt carbonyl hydrides require pressures of 200-350 bar and temperatures of 150-180 ℃ in order to prevent decomposition of the catalyst.[4] Recycling of the Co catalyst usually applies a series of unit operations and generates significant amount of waste.[5] The application of Rh-based catalysts provides a potentially better process with mild operating conditions (80 –130 ℃, 15 – 40 bars),[6] higher efficiency and product selectivity. However, Rh is a precious metal and therefore costs more

than 1000 times higher than Co. In order to take advantages of all the benefits of Rh, catalyst separation and recycle is key in commercialization.

For lower olefins such as ethylene or propylene, Rh-catalyzed hydroformylation process has been well established for the products can be easily separated from the catalyst while retaining catalyst stability.[7-9] The catalysts are stable at low temperature therefore can be recovered during product distillation, and recycled to the feed stream with unreacted olefins.[3] For olefins containing more than four carbons, however, the catalyst will decompose during product distillation due to the higher boiling points of higher aldehydes.

One approach in Rh recovery for higher olefins is by employing biphasic systems.[10-12] Two immiscible phases are used: one organic phase containing the reactants and products; one aqueous phase containing the catalysts. In these biphasic processes, the two phases are separated after reaction. The catalysts should remain in the aqueous phase and be circulated back to the reactor. The organic phase that contains most of the products is continuously removed for further purifications. The solubility of higher olefins is low in water, which may cause issues in reaction rates and raise challenge in mass transfer. The extent to which the catalyst can be recovered is also questionable.

Another approach to prevent Rh loss is to immobilize the homogeneous Rh catalysts on various kinds of solid supports to heterogenize the process.[12-15] Several groups of supports were investigated, including silica-based supports (SiO_2,[13] MCM-41,[16] SBA-15,[17] etc.), zeolites,[18] nanoparticles,[19-20] active carbons,[21-22] etc. However, this idea of heterogenizing the homogenous Rh catalyst suffers from several drawbacks. The reaction activity and selectivity reduced significantly compared to homogeneous reactions, attributed to the fact that Rh was bound to the ligands in much less active forms than in homogeneous catalysts.

Rh leaching from the supports and deactivation are also major problems in the heterogenized catalysts.

In recent years, using membrane-base nanofiltration to separate Rh catalysts has started to draw interests.[23-24] Rh is attached to a bulky polymer ligand that's soluble in the reaction mixtures. A nanofiltration membrane with low molecular weight cut off (MWCO) is used for retaining the bulked-up yet still homogeneous Rh catalyst to enable continuous operations. Janssen et al.[25] used a cross-flow ceramic nanofiltration membrane reactor with polyhedral oligomeric silsesquioxanes (POSS) enlarged triphenylphosphine ligand to immobilize Rh for 1-octene hydroformylation. The catalyst activity remained stable for almost two weeks with little Rh leaching. Fang et al.[26] applied a polyimide membrane and a polymer-bound phosphite ligand[27] (JanaPhos) for continuous hydroformylation of 1-octene. Stable catalyst activity and selectivity were observed for up to two days with Rh concentration in the permeate less than 20 ppb. The application of membrane technology combined with modified ligand is very efficient in preventing Rh loss. However, the high syngas pressure used as driving force for nanofiltration will usually lead to CO inhibition that results in low regioselectivity of the aldehydes.

Therefore, the development of continuous hydroformylation processes for higher olefins (C_{5+}) using homogeneous Rh catalysts remains a major challenge in industrial scale processing.

1.2 Hydroformylation in gas-expanded liquids

Gas-expanded liquid (GXL) is defined as a continuum of tunable solvents generated by mixing liquid solvents and compressed near-critical gases such as CO_2 and light olefins[28]

(Figure 1.2). The properties and applications of GXLs have been reviewed substantially in recent journals and books.[28-34] GXLs provide many unique benefits over traditional reaction media. They operate at much lower pressure than supercritical fluids (tens of bars comparing to hundreds of bars). Permanent gases (such as H_2, CO and O_2) show higher solubility in GXLs comparing to traditional organic solvents.[35-39] They provide enhanced transport properties with increased diffusivity and decreased viscosity.[40-44] Moreover, by using inert gas such as carbon dioxide as expanding gas, the flammability region is largely reduced,[45] which makes the process safer when operating.

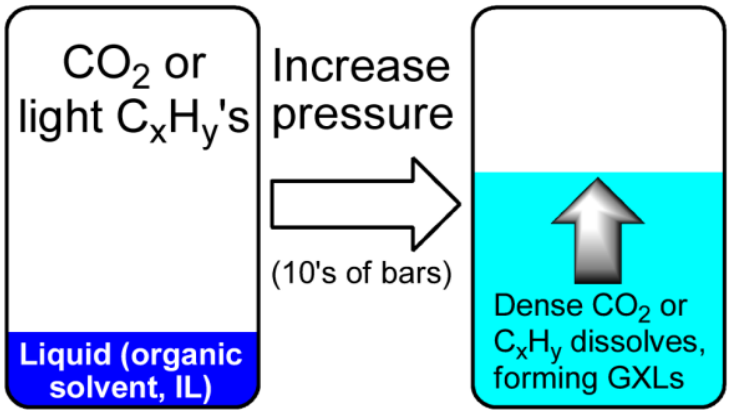

Figure 1.2: Illustration of GXLs

In recent years, CO_2 was found to provide several benefits when applied in hydroformylation reactions[46-49] at tens of bars pressure. The resulting mixtures are called CO_2-expanded liquids (CXLs).

Hallett et al.[49] used CXLs to recover catalyst and products when running hydroformylation of 1-octene in organic-aqueous tunable solvents (OATS). CO_2 is used as an antisolvent to separate the organic and aqueous phases. From their studies, CO_2 has the potential to achieve a greater than 99.9% Rh recovery by separating OATS into a product-rich organic phase and a catalyst-rich aqueous phase.

CO_2-expanded ionic liquids (ILs) have been applied in performing hydroformylation reactions.[50-51] The volume expansion of ionic liquids by dense CO_2 is low compared to organic solvents. For example, at 70 °C and 120 bar, the volume expansion of [HMIm][Tf_2N] by CO_2 is only 25% while the CO_2 solubility at these conditions is approximately 70 mol%[52]. By depositing a thin layer of the mixture of ionic liquid and soluble homogeneous catalyst on high surface area supports such as silica, alumina or mesoporous zeolites, a Supported Ionic Liquid Phase[53-54] (SILP) is created. SILPs eliminate the disadvantage of high viscosity of regular ILs. Dense CO_2 can be used as a solvent with SILPs to reduce the leaching of ILs from the solid supports and provide other benefits relating to transport properties.

Jin et al.[46-47] discovered that CXLs improve both turnover frequency (TOF) and aldehyde regio-selectivity (*n/i*) in 1-octene hydroformylation by using several groups of catalysts including Rh(acac)$(CO)_2$, Rh(acac)$[P(OPh)_3]_2$, Rh(acac)(CO)$[P(OAr)_3]$, and two phosphorous ligands, PPh_3 and biphephos. At 60 ℃ and 64 bar using Rh(acac)$(CO)_2$ and PPh_3 catalyst, the TOF increased from 195 to 290 h^{-1}, and the *n/i* ratio increased from 4 to 11 by replacing 58 bar of syngas (out of 64 bar) with CO_2 (i.e., 6 bar syngas, 58 bar CO_2) in the CXLs run. They also reported that lower temperatures favored the aldehydes selectivity and higher H_2 concentration favored reaction rate.

Fang et al.[55] performed a preliminary economic and environmental analysis, which compares a CXL-based Rh-catalyzed hydroformylation concept with a conventional industrial Co-catalyzed process. The CXL process includes a membrane-based reactor that used a nanofiltration membrane for Rh containment. The results show that the CXL process has much less environmental impact with nearly 40 times lower toxicity index compared to

the benchmarked conventional process. The economic analysis also shows that the CXL process requires 50% less capital cost than the conventional process. Further, when Rh recovery is higher than 99.8%, the production cost of CXLs process is 15% less than conventional process. The criterion for economic viability requires the cost of Rh makeup to be no more than 1.3% of the nonanal product value. A later study[26] employed a stirred vessel equipped with a nanofiltration membrane to demonstrate the capability of the membrane to retain bulky Rh complexes. Rh leaching in the permeate was less than 20 ppb at steady state, making the Rh makeup cost only 0.4% of the nonanal product value and thereby exceeding the economic viability criterion. This result along with those of others,[56-58] provide strong evidence that the utilization of CXLs combined with membrane filtration has the potential to be a practically viable technology for Rh-catalyzed continuous hydroformylation of higher olefins.

The development of new hydroformylation technology concepts may also find application as an atom economical C-C coupling reaction route utilizing emerging feedstocks such as bioethanol, biosyngas and ethane/propane (from natural gas).[59] For example, the bioethanol may be converted by dehydration to ethylene, which is then hydroformylated to linear propanal that is converted to propanol. The propanol is then dehydrated providing access to C_3 olefins. In this manner, successive hydroformylation, reduction and dehydration steps help increase the chain-length of the olefins.

1.3 Objective and overview of this work

The goal of this project is to develop a practically viable continuous hydroformylation process that takes advantage of CXL media and nanofltration membrane to enhance activity,

selectivity and Rh preservation. The membrane-based nano/ultra-filtration reactor is used for effective retention of a polymer-bound rhodium complex catalyst and the use of CXL media is expected to provide high activity and selectivty. The C_8 olefin 1-octene is chosen as a model compound for this study. The desired product in this case is the linear aldehyde n-nonanal. Specific objectives are as follows:

- Conduct phase behavior studies of 1-octene hydroformylation reaction systems in neat and CXL media, focusing on the tunability of H_2 and CO concentrations in the CXL phase in particular.
- Investigate CXL effects on hydroformylation reaction activity and selectivity through strirred batch reaction studies (T = 50-60 ℃, pressure up to 60 bar).
- Demonstrate a continuous nanofiltration membrane reactor that is suitable to carry out homogeneous hydroformylation reactions with bulky Rh complexes in CXL media ensuring that the Rh pass-through is minimal (<5 ppm in permeate) and meets or surpasses an established benchmark for economic viability (Rh recovery > 99.8%).[55]
- Explore alternative, inexpensive polymer ligands (compared to JanaPhos) for Rh retention in a continuous reactor.
- Update economic and environmental analyses based on the continuous CXL-based process.

To begin with, a phase equilibrium study was performed to better understand the intrinsic solubilities of syngas in the continuum of CO_2-expanded 1-octene, nonanal and mixtures were measured under pressures and temperatures encountered in homogeneous catalytic hydroformylation (up to 80 ℃, 80 bar). In collaboration with researchers at the

Max Planck Institute (Magdeburg, Germany), thermodynamic models were developed to describe vapor-liquid equilibria of the binary, ternary and quaternary model systems associated with 1-octene hydroformylation reaction mixtures, including those expanded by dense CO_2.

From the phase equilibrium studies, it was found that the H_2/CO ratio in the liquid phase varies with the addition of CO_2. A detailed study was carried out to discern the effects of CXL on the H_2/CO ratio in the liquid phase and also on the activity and selectivity of hydroformylation reactions.

In order to retain and re-use Rh catalyst, a continuous, membrane-based nano/ultra-filtration reactor was built to enable homogeneous hydroformylation reaction in CO_2-expanded media. A polymer ligand[27] synthesized in-house was used to enlarge and retain Rh in the membrane reactor. Continuous hydroformylation with high activity, selectivity and minimal Rh leaching was demonstrated successfully for several days.

Alternative ligands (inexpensive, simple-synthesis process, high activity and selectivity) for Rh-catalyzed hydroformylation, made of polysiloxanes, were also investigated in both batch and continuous reactions. The polysiloxane ligands show promising results with good activity, selectivity and low Rh leaching for extended runs.

Last but not least, economic and environmental analyses were performed to assess the practical viability of this process. The Rh-catalyzed continuous CXL process with membrane reactor was compared to an industrial process using Co as catalyst. The CXL process shows lower environmental impact than the industrial process. The profit margin of the CXL process is either equal to or greater than industrial process if Rh recovery meets the economic viability requirement.

Chapter 2 : Phase Behavior of Neat and Gas-expanded Hydroformylation Reaction Mixtures

2.1 Introduction

Accurate knowledge of the thermodynamic properties of reaction mixtures is essential to rational catalyst and process development. For systems using CXL media, knowledge of the extent of volume expansion of typical hydroformylation reaction mixtures by compressed CO_2 at the reactor operating conditions (pressure and temperature) is essential for rational reactor design and operation. For hydroformylation reactions, information on syngas (CO + H_2) solubility in CXLs is essential for reliable modeling of kinetic and mass transfer effects on observed hydroformylation rates.

Previously, vapor liquid equilibria of the following systems were measured in the variable volume view cell at temperatures ranging from 40 to 80 ℃ and pressures up to 90 bar: CO + 1-octene, CO_2 + 1-octene, CO + 1-octene + CO_2, CO + nonanal, CO_2 + nonanal, CO + nonanal + CO_2, H_2 + 1-octene, H_2 + 1-octene + CO_2, H_2 + nonanal and H_2 + nonanal + CO_2.[37] It was found that the presence of CO_2 enhanced the solubilities of both CO and H_2 in the liquid phase. The enhancement factor is up to 1.54 for CO and 1.82 for H_2. The enhancement of CO and H_2 solubilities is slightly higher in nonanal than in 1-octene. These systems were simulated using Peng-Robinson equation of state (PR EoS) with van der Waals mixing rules and binary interaction parameters. The modeled VLE data matched the experimental data adequately, with much better fits for the 1-octene systems compared to the more polar nonanal systems.

In this study, volumetric expansion studies and phase equilibrium measurements were carried out for typical 1-octene reaction systems (T = 40-60 ℃, P up to 65 bar) in order to design experiment and identify effects of CXL under those conditions.

2.2 Experimental

2.2.1 Materials

1-Octene (98%), nonanal (>95%) and toluene (anhydrous, 99.8%) were purchased from Sigma-Aldrich. 1-Octene was further purified by passing through molecular sieve to remove water and stored under nitrogen. Syngas (49.5% H_2 with the balance being CO) and CO_2 (99.999%) were purchased from Linweld.

2.2.2 Apparatus and methods

2.2.2.1 Volumetric expansion of hydroformylation reaction mixtures by compressed gases

For measuring the volumetric expansion of a typical hydroformylation reaction mixture of known composition, a Jerguson® view cell (50 cm^3, Clark Reliance Co.) was used. The apparatus and operating procedures are similar as descried elsewhere.[46] The apparatus was modified to be able to introduce both syngas and CO_2 (Figure 2.1). An air-actuated magnet-driven stirring bar was added to intensify gas-liquid mixing and avoid mass transfer limitations.

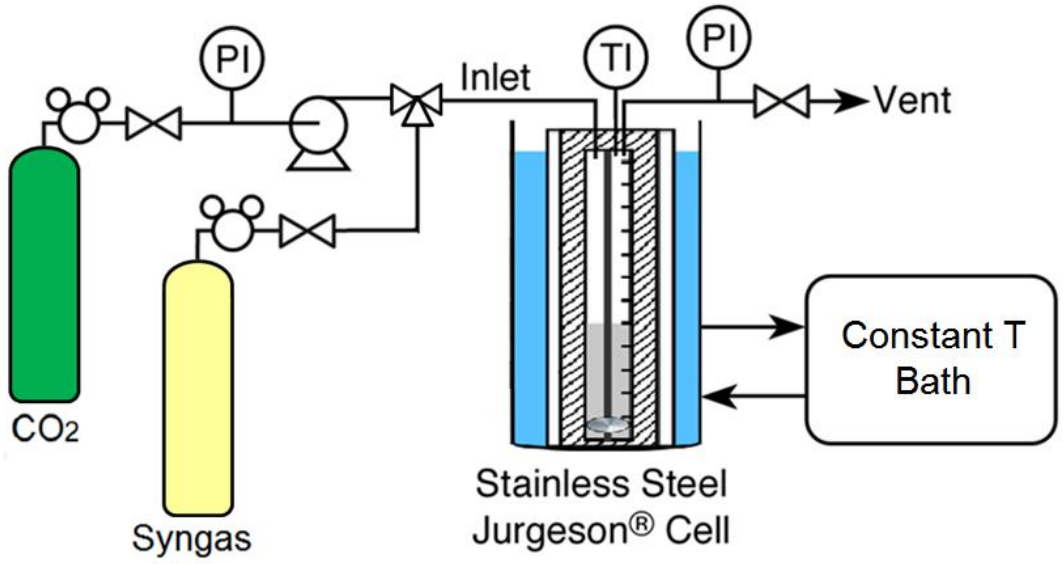

Figure 2.1: Apparatus for volumetric expansion study

The expansion ratio was calculated using Equation 1. The volumetric increase of the expanded liquid phase was compared to the liquid volume at initial state (V_0, P_0) when there was no CO_2 or syngas addition under the same temperature.

$$\frac{V}{V_0} = \frac{V(T,\ P)}{V(T, P_0)} \qquad \text{(Equation 1)}$$

2.2.2.2 Experimental measurements of syngas compositions in neat hydroformylation reaction mixtures

For measuring the vapor-liquid phase equilibrium of CO_2-expanded hydroformylation mixtures, including the solubilities of CO and H_2 in the CXL phase, a Supercritical Fluid Technologies® (SFT) variable-volume equilibrium cell equipped with on-line sampling of the vapor and liquid phases was used.[37] The scheme of this apparatus is shown in Figure 2.2.

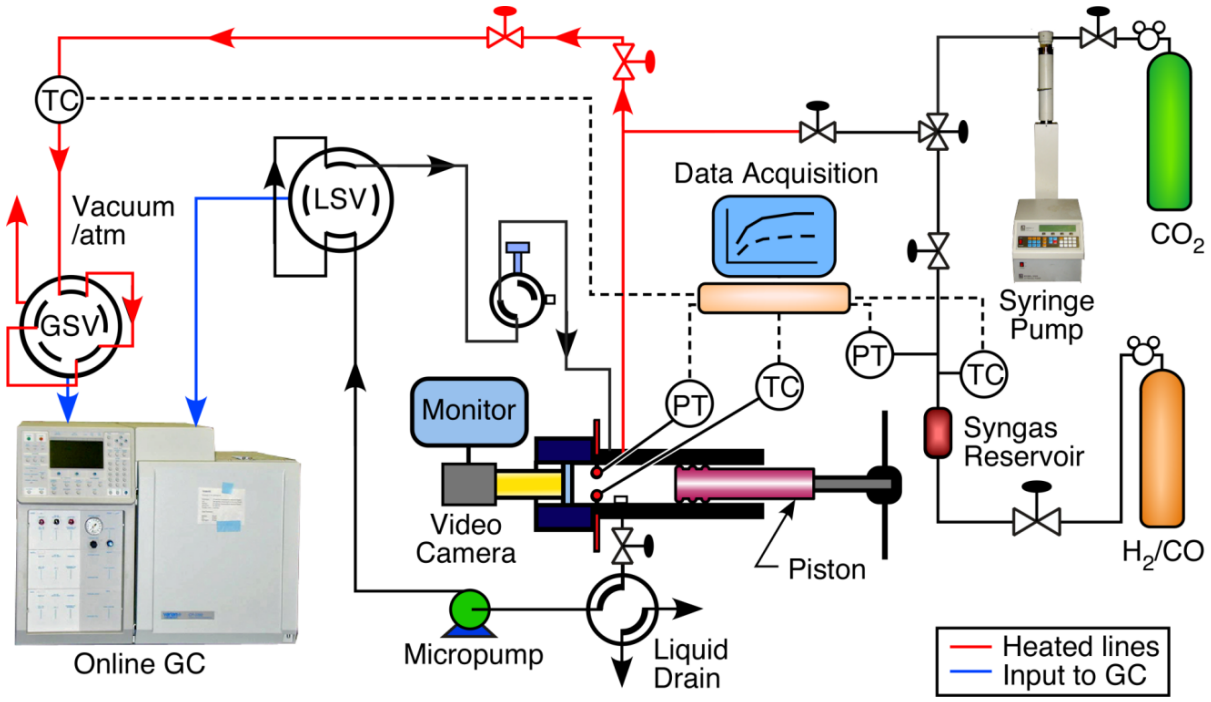

Figure 2.2: Apparatus for phase equilibrium measurements

The SFT Phase Monitor II consists of a manually controlled syringe pump integrated within a 30 ml view cell. The volume of the view cell can be varied from 3 ml to 30 ml. Fluid mixing is achieved through rare earth magnets coupled to an internally mounted impeller as well as the circulation of the fluid. An internal Resistance Temperature Detector (RTD) is used to measure the temperature. A fuzzy logic controller (AI-100, Total Temperature Instrumentation, Inc.) uniformly controls the heating of the view cell up to 150 ℃ with an uncertainty of ± 0.5 ℃. The pressure gauge is composed of a pressure transducer and an Analog Input Panel Meter (Red Lion Controls, Inc.) with an uncertainty of ± 0.1 bar in pressures ranging from vacuum to 200 bar.

In a typical run, a predetermined amount of the pure liquid or liquid mixture was injected into the cell using a syringe, brought to the set temperature, and pressurized to a set pressure by the addition of syngas (molar H_2/CO = 1) and/or CO_2. A micro-pump was

employed to circulate the liquid through the vapor phase to facilitate mixing and to allow the system to reach equilibrium. At equilibrium, samples were withdrawn from both the vapor and liquid phases, and analyzed by online Gas Chromatography (GC). The most significant contribution to the experimental error is from GC measurements, on the order of a few percent. Three measurements were performed for each data point and the standard deviation is always less than 5%. The details and calibration data for GC analysis is shown in Appendix A.

2.3 Results and discussion

2.3.1 Volumetric expansion of 1-octene hydroformylation reaction mixtures

Volumetric expansion studies were performed using model reaction mixtures corresponding to a typical 1-octene hydroformylation experiment at 80% 1-octene conversion using toluene as solvent (0.3 mL 1-octene + 1.4 mL nonanal + 3.5 mL toluene). Three different starting volumes were used in the expansion studies: 5, 10 and 15 mL at 40 ℃.

As seen from Figure 2.3, the volume of the liquid mixture increased exponentially in all cases upon CO_2 pressurization, increasing linearly at lower pressures and exponentially as the pressure approaches the CO_2 critical pressure (73.8 bar). The expansion ratios (estimated using Equation 1) were almost identical for the different starting volumes of the mixture dominated by toluene. This implies that the expansion data for such compositions are reliable for determining reactor holdup volumes during either batch or continuous operation.

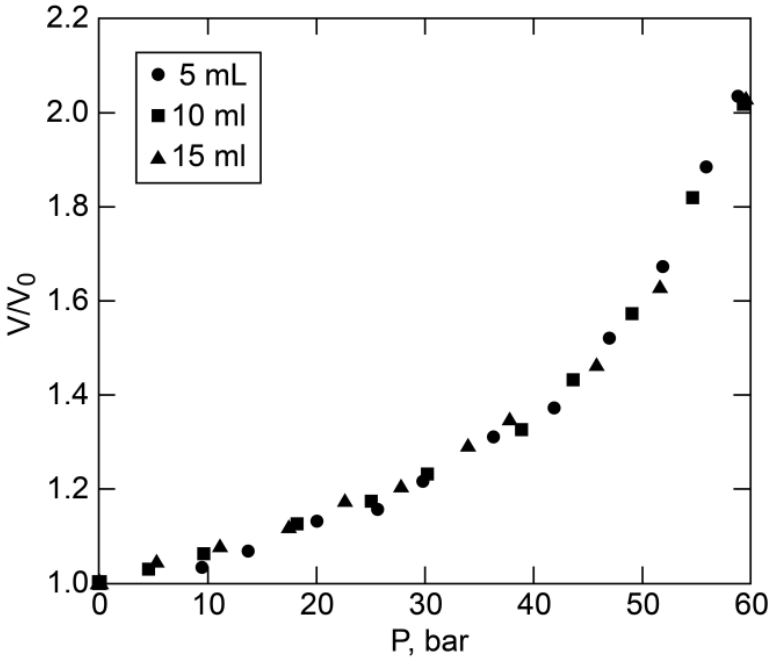

Figure 2.3: Volumetric expansion of 1-octene hydroformylation reaction mixtures with CO_2, with starting volumes of 5, 10 and 15 mL at 40 ℃

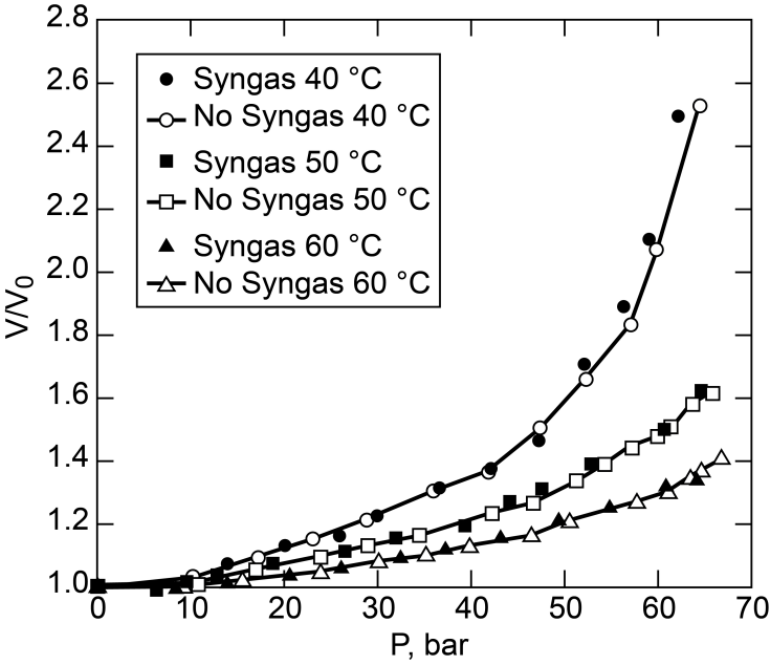

Figure 2.4: Effect of temperature and syngas partial pressure (6 bar syngas) on the volumetric expansion of 1-octene hydroformylation reaction mixtures by CO_2.

Volumetric expansion studies were also performed at several temperatures (40, 50 and 60 ℃), with and without 6 bar syngas (H_2/CO ratio = 1) in the gas phase (Figure 2.4). As expected, the volumetric expansion was greater and more sensitive to pressure at the lower temperature (40 ℃), as compared to the higher temperatures (50 or 60 ℃). At a given pressure, the CO_2 solubility in the CXL phase decreases with an increase in temperature. Also, the pressure dependence of the expansion ratio reflects that of the tunability of CO_2 density with pressure, which is more sensitive closer to its critical temperature (31.1 ℃). Further, the presence of 6 bar syngas did not have a measurable effect on the overall expansion (which is dominated by CO_2 dissolution) even though the syngas solubility should increase at higher CO_2 pressures. For determining the syngas solubility, separate VLE studies were performed in a variable volume cell as described in the following section. From previous studies[47] and the observations from this work, the Rh/TPP catalyst complex remained soluble in the liquid under current operating conditions. We have recently modeled such quarternary systems involving CO_2 in order to reliably predict such expansions.[60]

2.3.2 Experimental measurements of syngas compositions in CO_2-expanded reaction mixtures

In order to understand the effect of CO_2 addition on the relative CO and H_2 solubilities, phase equilibria of typical 1-octene reaction mixtures were investigated. The equilibrium solubilities of CO and H_2 were measured in a CO_2-expanded liquid mixture consisting initially of 0.3 mL 1-octene, 1.4 mL nonanal and 3.5 mL toluene, same as the initial mixture used in the volumetric expansion studies. The H_2 to CO molar ratio in syngas feed is 1/1.

The H_2 and CO compositions in the liquid phase at 50 ℃ with and without CO_2 are shown in Table 2.1. The standard deviations are less than 5% for all data points.

Table 2.1: CO and H_2 mole fractions (x) in neat and CXL reaction mixtures at 50 ℃

	Syngas Only			CXL (6 bar syngas + CO_2)		
P, bar	x, H_2	x, CO	H_2/CO	x, H_2	x, CO	H_2/CO
6	0.0011	0.0019	0.60	-	-	-
25	0.0048	0.0079	0.60	0.0012	0.0019	0.62
38	0.0073	0.0124	0.59	0.0013	0.0021	0.65
56	0.0105	0.0177	0.59	0.0016	0.0022	0.72

From Table 2.1, it is seen that when pressurized with syngas alone, both H_2 and CO compositions increased with syngas pressure, with the H_2/CO ratio remaining more or less constant (0.59-0.60). This is simply a reflection of the fact that both solubilities follow Henry's law and that the solubility of CO is greater than H_2 in the organic phase. The Henry's law constants for H_2 and CO solubilities in 1-octene were estimated using measured vapor-liquid equilibrium data between 40-60 ℃ and compared with literature data[61] (Table 2.2). Clearly, the Henry's law constants obtained in this work match well with previously reported values.

Table 2.2: Henry's law constant (K_H, MPa m^3/kmol) of H_2 and CO in 1-octene

	This Work*			Literature[61]	
Temperature, ℃	40	50	60	80	90
H_2	23.65	23.64	23.64	21.58 ± 0.38	21.12 ± 0.47
CO	11.71	11.56	11.38	11.76 ± 0.37	11.42 ± 0.23

*The K_H values from this work have an uncertainty of ±5%

In contrast, replacing syngas in excess of 6 bar with CO_2 increased the H_2/CO ratio in the liquid phase. As seen in Table 2.1

Table 2.1, the H_2/CO ratio in the neat reaction mixture is 0.59 with 56 bar syngas but increases to 0.72 with 6 bar syngas + 50 bar CO_2. Further, the H_2/CO enhancement in CXLs is achieved at CO mole fractions that are 4 to 8 times lower compared to pressurization with syngas alone at similar total pressures. In other words, it is possible to achieve similar or higher H_2/CO ratios at much lower CO compositions in the CXL phase compared to pressurization of the liquid phase with syngas alone. Such a unique and tunable combination of H_2/CO ratio and low CO mole fraction in CXL phases favors hydroformylation as shown in the following chapter.

Clearly, H_2 is more soluble in the CO_2-expanded reaction mixture than in the mixture pressurized with syngas alone, causing the H_2/CO to increase as more CO_2 is added. At higher pressures, the dense CO_2 dissolves substantially in the liquid phase creating a CXL phase with increased free volume.[62] We therefore hypothesize that the smaller molecular radius of H_2 (74.1 picometer) relative to CO (112.8 picometer)[63] might contribute to the easier accommodation of H_2 in increasingly expanded CXL phases, giving rise to a non-linear increase in the individual gas solubilities that deviates from the ideal Henry's law

behavior. This hypothesis has to be confirmed by molecular modeling studies (similar to those given in the work of Houndonougbo et al.[62]).

Another possibility for the increased H_2/CO ratio may be the change of polarity in the liquid phase by the addition of CO_2. From literature data,[64] it is possible that the solubility of H_2 is affected by solvent polarity. Figure 2.5 show the H_2 solubilities in five different solvents: (1) *n*-hexane, (2) toluene, (3) tetrahydrofuran, (4) *1,4*-dioxane, and (5) *N,N*-dimethylformamide at 25 ℃. Table 2.3 listed the polarity indices of these five solvents.[65] It is clear that at similar syngas pressures, the nonpolar H_2 solubility is the highest in the nonpolar *n*-hexane and lowest in the most polar solvent *N,N*-dimethylformamide. In other words, the H_2 solubility decreases with an increase in solvent polarity.

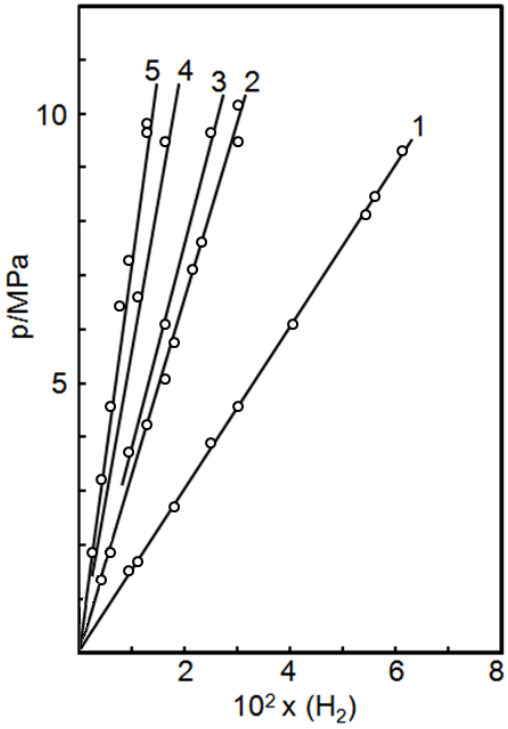

Figure 2.5: Solubility of hydrogen in (1) *n*-hexane, (2) toluene, (3) tetrahydrofuran, (4) *1,4*-dioxane, and (5) *N,N*-dimethylformamide at 25 ℃.[64]

Table 2.3: Polarity index of various solvents[65]

Entry	Solvent	Polarity Index
1	*n*-hexane	0
2	toluene	2.4
3	tetrahydrofuran	4
4	*1,4*-dioxane	4.8
5	*N,N*-dimethylformamide	6.4

In CXLs, the liquid phase polarity decreases upon addition of nonpolar CO_2. Since H_2 is much less polar than CO, the enhancement to H_2 solubility in CXLs could be higher compared to CO solublity.

2.4 Prediction of multicomponent phase behavior of CXLs using CEoS/GE models

In a collaborative effort with researchers at th Max Planck Institute of Complex Technical Systems (Magdeburg, Germany), the VLE phase behavior of these multicomponent systems (up to quinary systems) associated with 1-octene hydroformylation in CO_2-expanded solvents were successfully predicted using Cubic Equation of State/ excess Gibbs free energy (CEoS/GE) models without the need for regression parameters in most systems.[60]

$$AARD_i = \frac{1}{ND}\sum_j^{ND}\left(\frac{\left|z_{i,\exp} - z_{i,cal}\right|}{z_{i,\exp}}\right)_j, \; z=x \text{ or } y, \; i=1, 2,\ldots N \qquad \text{(Equation 2)}$$

$$ATAARD = \left[\sum_{i=1}^{NC} AARD(i)\right] \Big/ NC \qquad \text{(Equation 3)}$$

For quantitative comparison of the relative performances of the various models, the average absolute relative deviation (AARD) between experimental and predicted values (Equation 2) was employed. In this equation, *x* and *y* stand for the molar fraction of component *i* in the liquid and vapor phases, separately. *ND* stands for number of data.

The general fugacity coefficient equation is as follows.

$$\ln \hat{\varphi}_i = \frac{F_{1,i}}{b_m}(Z-1) - \ln(Z-B_m) + \frac{A_m}{B_m}\frac{F_{2,i}}{(w-u)}\ln\left(\frac{Z_m+wB_m}{Z_m+uB_m}\right) \quad \text{(Equation 4)}$$

Where $F_{1,i} = \frac{\partial n b_m}{\partial n_i}$, $F_{2,i} = \frac{1}{b_m}F_{1,i} - \frac{1}{na_m}\left(\frac{\partial n^2 a_m}{\partial n_i}\right) = -\frac{B_m}{A_m}\frac{\partial n \varepsilon_m}{\partial n_i}$ are dependent on mixing rules. After an initial evaluation of 36 CEoS/GE models, four combinations with the lowest total average absolute relative deviations (TAARD) (Equation 3) were selected for further testing. The four combinations of selection are: Peng-Robinson with predictive Soave Redlich-Kwong mixing rule (PR-PSRK), modified Soave-Redlich-Kwong with Modified Huran-Vidal with 2nd-order simplification mixing rule (MSRK-MHV2), Soave-Redlich-Kwong with Modified HV by Orbey and Sandler mixing rule (SRK-HVOS) and modified Soave-Redlich-Kwong with Linear Combination HV and MHV1 (MSRK-LCVM). The systems that were studied are listed in Appendix B.

In general, the SRK-HVOS and the PR-PSRK models were found to be the most accurate for predicting the investigated systems. The AARD was less than 10% for most of the components using these two models. An example of the AARD for quarternary system (H_2 + CO + CO_2 + 1-octene) at a temperture range of 40-60 ℃ is shown in Figure 2.6. For this system, only the PR-PSRK model had an AARD value lower than 0.4 for all components, while the other three models performed especially worse when predicting liquid phase H_2 and CO solubilities. The relativily high AARD values for H_2 and CO

solubilities in the liquid phase and octene solubility in the vapor phase were due to the relatively small absolute values of these concentrations in the systems.

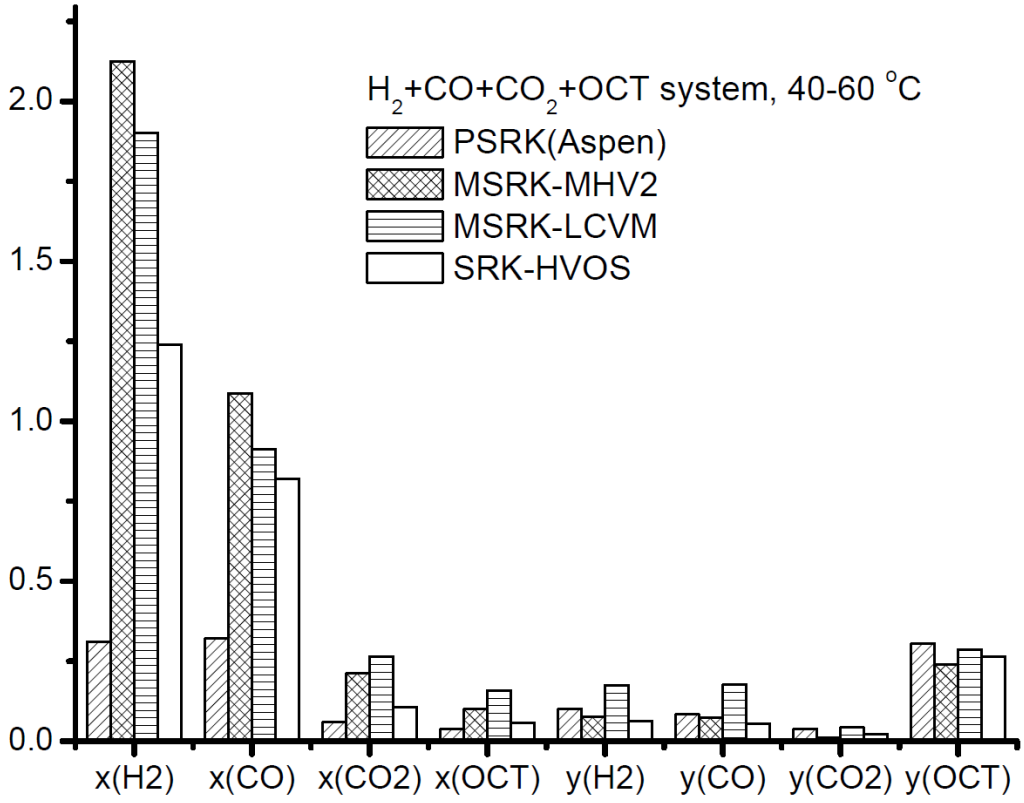

Figure 2.6: AARD analysis of H_2 + CO + CO_2 + 1-octene system at 40-60 ^oC

A comparison of the ATAARD values associated with the VLE predictions for the various systems using the four selected models are listed in Table 2.4. It was found that the SRK-HVOS and PR-PSRK models in general displayed similar performances for almost all cases, with ATAARD values less than 0.3 for 7 out of the 10 systems. Based on the ATAARD values, the MSRK-LCVM and MSRK-MHV2 models were relatively less accurate. The SRK-HVOS and PR-PSRK models are therefore recommended for predicting multicomponent CXL phase behavior for the 1-octene based hydroformylation mixtures.

Table 2.4: Comparison of ATAARD values for various models and systems

System	PR-PSRK (Aspen)	MSRK-MHV2	SRK-HVOS	MSRK-LCVM
CO + CO_2 + OCT	0.0355	0.0903	0.0468	0.0741
CO + CO_2 + NAL	0.2388	0.3006	0.2524	0.2049
H_2 + CO_2 + OCT	0.1173	0.1526	0.1428	0.1673
H_2 + CO_2 + NAL	0.3045	0.2916	0.2880	0.1989
H_2 + CO + OCT	0.1738	0.6263	0.2260	0.3220
H_2 + CO + NAL	0.1724	1.1214	1.2038	1.1571
H_2 + CO + CO_2 + OCT	0.1569	0.4904	0.3287	0.4901
H_2 + CO + CO_2 + NAL	0.2473	0.4334	0.2413	0.2297
H_2 + CO + OCT + NAL	2.3028	2.9896	2.2050	12.5834
H_2 + CO + CO_2 + OCT + NAL	0.4741	0.5950	0.4539	0.4404

The results show that CEoS/GE models can be used as a versatile tool for the prediction of multi-component phase behavior of CXLs. Such a priori predictions are essential to guide the rational selection of CXLs for specific applications and also multi-component VLE experiments involving CXLs with relatively fewer data for validation purposes. More details of the modeling work is shown in Appendix B.

2.5 Conclusions

Volumetric expansions of representative hydroformylation reaction mixtures (ternary, quaternary and quinary systems) with CO_2 show the following qualitative features: (a) the

expansion ratio (V/V_0) was more or less invariant with the starting liquid volume; (b) As expected, the expansion decreased with an increase in temperature; (c) the expansion ratios were similar with or without 6 bar syngas partial pressure.

Syngas solubility studies show that (a) the enhancement of H_2 solubility in CXL is higher than CO; (b) the H_2/CO ratio in CXLs increased at higher CO_2 partial pressure (at a fixed syngas pressure of 6 bar).

The experimental VLE data of ternary, quaternary and quinary systems were successfully modeled by predicted using Cubic equation of state/ excess Gibbs free energy (CEoS/GE) models without the need for regression parameters in most systems.

Chapter 3 : 1-Octene Hydroformylation in Gas-Expanded Liquids

3.1 Introduction

It is well known that the concentrations of the syngas components (CO and H_2) in the liquid phase are major determinants of the reaction pathways and therefore the product selectivity. Figure 3.1 shows a commonly accepted mechanism[66] for Rh-catalyzed hydroformylation.

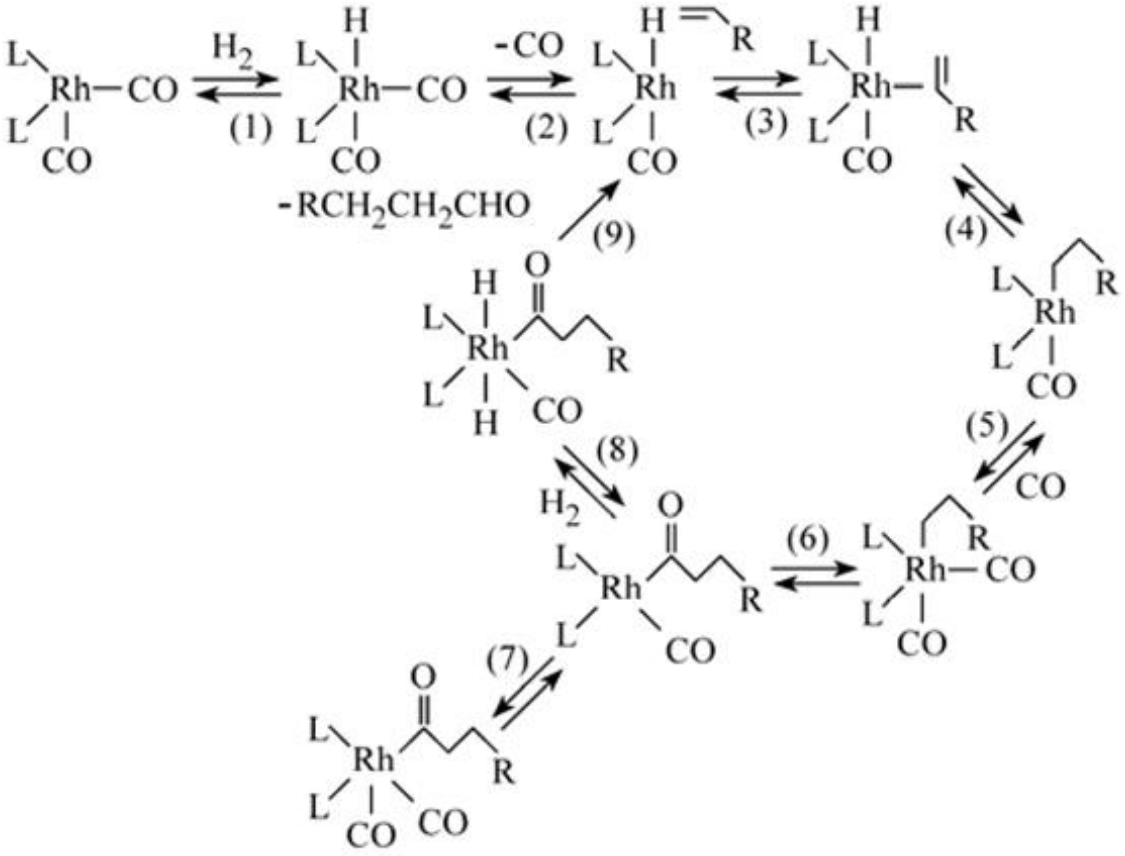

Figure 3.1: Simplified mechanism for Rh-catalyzed hydroformylation[66]

In this mechanism, step 8 is considered to be the rate-limiting step. In this step, hydrogen is added to the Rh-acyl complex, which then undergoes the hydride transfer to form

aldehydes. Further, the H_2 insertion in step 1 is essential to activate the catalyst and to commence the catalytic cycle. Therefore, an increase in H_2 concentration in the liquid phase favors the overall hydroformylation rate. On the other hand, an increase in CO concentration often leads to reduced reaction rates and aldehyde regioselectivity (*n/i*). This effect is manifested in two steps: CO dissociation in step 2, where high CO concentration is known to cause excessive ligand substitution[67] and reduces the regioselectivity; and the CO complexation in step 7, which in the presence of excess CO inhibits the H_2 insertion and forms an active catalytic intermediate, and thereby lowers the reaction rate.[68-70]

In general therefore, higher H_2 concentrations and lower CO concentrations in the reaction phase are required to achieve higher rates and linear aldehyde selectivity. Because CO is generally more soluble than hydrogen in most conventional solvents,[71] the resulting H_2/CO ratio in the liquid phase is less than that in the feed syngas. However, when CO_2 is added to either 1-olefin or nonanal (to create a CXL), we observe that the enhancement of H_2 solubility is more than CO in the CXLs (see Chapter 2).[37,47] This means that the H_2/CO ratio in the liquid phase should be greater in CXLs (based on the organic solvent and extent of CO_2 addition) compared to the ratio without adding CO_2.

It is known that a higher H_2/CO ratio in the syngas feed results in increased TOFs and linear aldehyde yield in supercritical CO_2.[72-73] Similar effects can be achieved by using CXL at a much lower CO_2 pressure and fixed (1/1 H_2/CO molar ratio) syngas feed composition. The observed beneficial effects of CXLs on hydroformylation activity and on selectivity are attributed to the favorable tunability of H_2/CO ratio in the CXL phase. Moreover, by using CXL, CO inhibition is alleviated and therefore the adverse effect on *n/i* ratio is avoided at

higher total pressure. This chapter clarifies these intriguing effects observed with CXLs through systematic reaction studies.

3.2 Experimental

3.2.1 Materials

The purchased materials used in this work are listed in Table 3.1. The purchased materials were used as is unless otherwise noted.

Table 3.1: Materials used in this work

Material	Purity	Company	Additional Comments
1-Octene	>98%	Sigma-Aldrich	Purified by passing through molecular sieve to remove water; stored under nitrogen
n-Nonanal	>95%	Sigma-Aldrich	
Toluene	Anhydrous, 99.8%	Sigma-Aldrich	Stored under argon
Triphenylphosphine (TPP)	99%	Sigma-Aldrich	
Acetylacetonatorhodium(I) dicarbonyl [$Rh(CO)_2(acac)$]	99%	Alfa Aesar	Stored under argon
Syngas	49.5% H_2 with 50.5% CO	Linweld	
CO_2	99.999%	Linweld	

3.2.2 Apparatus and methods

The equipment used for batch reactions is shown in Figure 3.2.

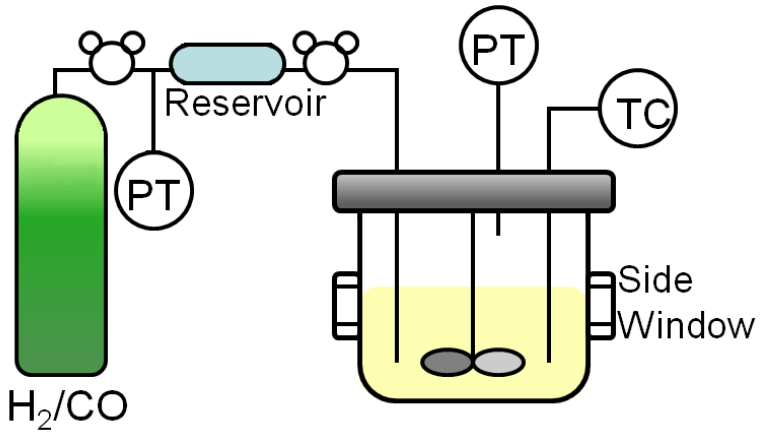

Figure 3.2: Apparatus for batch hydroformylation studies

The TOF and chemoselectivity are calculated using Equations 5 and 6, respectively. The TOF in the batch run is estimated based on the number of moles of syngas converted corresponding to 20 % 1-octene conversion (assuming a 1:1 stoichiometry). The number of moles of syngas converted is obtained from the syngas consumed in the external reservoir (based on the syngas pressure at a constant temperature) while maintaining the syngas pressure constant in the reactor.

$$TOF\ (\mathrm{h}^{-1}) = \frac{\text{Moles of syngas consumed corresponding to 20\% 1-octene conversion}}{(\text{Moles of Rh})\,(\text{corresponding batch time})} \qquad (5)$$

The *chemoselectivity* is defined as the number of moles of aldehydes formed relative to the number of moles of 1-octene reacted at the end of the 6 hour batch runs. The *regio selectivity* (*n/i*) is estimated as the molar ratio of the linear to branched aldehydes in the product following the 6 hour batch run.

$$Chemoselectivity\ (\%) = \frac{\text{Moles of aldehyde products formed}}{\text{Moles of 1-octene converted}} \text{ x } 100\% \qquad (6)$$

3.3 Results and Discussion

3.3.1 Effect of CXLs on hydroformylation activity and selectivity with Rh/TPP catalysts

Hydroformylation reactions catalyzed by homogeneous Rh complexes are significantly affected by the concentrations of CO and H_2 in the liquid phase. In general, higher H_2 concentrations favor turnover frequencies (TOFs)[74] while higher CO concentrations inhibit both TOF as well as regioselectivity. It is therefore of interest to investigate how the tunability of H_2 and CO concentrations in CXLs affects the hydroformylation reaction. The catalyst complex employed in this investigation is composed of $Rh(CO)_2(acac)$ and TPP. In all our experimental runs reported here, the molar 1-octene/Rh ratio was 988. A high P/Rh ratio of 205 is used to avoid ligand deficiency and ensure complete utilization of Rh in forming the catalyst complex. Toluene was used as solvent. Depending on the extent of toluene expansion by CO_2 at the operating pressure (Figure 2.3), the initial volume of the toluene used was varied to ensure a constant initial liquid volume for all batch runs. The stirrer speed was maintained at 1000 rpm to eliminate gas-liquid mass transfer limitations.[62] All data were repeatable within experimental error (5%).

As seen in Table 3.2, higher syngas pressures are detrimental to both activity (TOF) and regioselectivity. The TOF decreased by 37% and the *n/i* ratio decreased by more than two-fold as the syngas pressure was increased from 6 to 56 bar. As seen in Table 2.1, the CO concentration in the liquid phase increases by nearly an order of magnitude in this pressure range. In contrast, when syngas in excess of 6 bar was replaced with CO_2, the TOF increased from ~66 h^{-1} at 6 bar syngas (without CO_2 addition) to ~79 h^{-1} at 38 bar (6 bar syngas + 32

bar CO_2) despite an approximately 20% dilution of the liquid phase by CO_2 dissolution (see Figure 2.4). However, a further increase in total pressure to 56 bar (6 bar syngas + 50 bar CO_2) caused the TOF to decrease to ~68 h^{-1} as further increases in CO_2 addition might change the density and polarity of the liquid phase. Most notably, the *n/i* ratio increased from 7.2 at 6 bar syngas to 10.4 at 56 bar CXL (6 bar syngas + 50 bar CO_2). Further, at even at a similar H_2/CO ratio (~0.60) in the reaction phases at 28 bar total pressure, the TOF and *n/i* ratio in CXLs are greater by approximately 50% and 225%, respectively, compared to pressurization of the liquid phase with syngas alone. These enhancements are attributed to the four-fold lower CO concentrations in the CXL phase compared to pressurization with syngas alone (see Table 2.1).

Table 3.2: Effect of CXLs on H_2/CO, TOF and *n/i* at 50 ℃

Total Pressure, bar	TOF, h^{-1}		*n/i*		H_2/CO	
	Syngas Only	CXL (6 bar Syngas +CO_2)	Syngas Only	CXL (6 bar Syngas +CO_2)	Syngas Only	CXL (6 bar Syngas +CO_2)
6	65.8	-	7.2	-	0.60	-
28	55.4	83.9	4.1	9.9	0.60	0.62
38	48.5	78.9	3.5	10.1	0.59	0.65
56	41.5	68.2	3	10.4	0.59	0.72

1-octene/Rh = 988; P/Rh = 205; ligand: -PPh_3. For CXL runs, total pressure = 6 bar syngas + CO_2 pressures. Solvent: Toluene. Identical liquid volume for neat solvent and CXL runs. Reaction time = 6 hours.

Indeed, in the liquid phase, the increase in absolute concentration of CO with pressure has a greater impact on the *n/i* ratio than does the H_2/CO ratio. This can be seen from

Table 2.1 and Table 3.2. As shown in Table 3.2, for pure syngas, as pressure increases from 6 to 56 bar, the H_2/CO ratio remains fairly constant at 0.60 while the *n/i* ratio drops significantly, from 7.2 to 3. The drop in *n/i* corresponds to an order-of-magnitude increase in the mole fraction of CO in the liquid phase (0.0019 to 0.0177).

For CXLs, the H_2/CO ratio may play a more significant role in *n/i* ratio. Across the same range of pressures, the mole fraction of CO is relatively stable (0.0019 to 0.0022), with a 20% increase in H_2/CO ratio (0.60 to 0.72), as seen in Table 2.1. Since the partial pressure of syngas in the CXL is maintained at 6 bar, the mole fraction of CO in the CXL phase is comparable to that of pure syngas at 6 bar (0.0019). The stable mole fraction of CO corresponds to a relatively constant *n/i* ratio (9.9 to 10.4) as seen in Table 3.2. Yet, these *n/i* ratios in CXLs represent a nearly 40% increase compared to that achieved with pure syngas at 6 bar (7.2) and may be attributed to the simultaneous increase in the H_2/CO ratio in CXLs.

As seen from Table 2.1, while the CO concentration increases by approximately 15%, the H_2 concentration increases by nearly 45% in this pressure range, resulting in an increase in the H_2/CO ratio. Remarkably, the increase of H_2/CO ratio in the reaction phase is achieved with syngas of a fixed composition (*i.e*. without adding extra hydrogen in the gas phase). Thus, CXLs provide a convenient way to enhance the H_2 concentration in the reaction phase without causing CO inhibition. These two effects are known to be beneficial to both the rate and regioselectivity, as seen from the increased TOF and *n*/*i* ratio in the case of CXLs compared to the use of syngas alone (see Table 3.2).

At 60 ℃, similar results were observed (Table 3.3). Both TOF and *n/i* decrease when the liquid phase is pressurized only with syngas. When replacing the syngas in excess of 6 bar with CO_2 pressure, the TOF was higher when compared to pressurization with only syngas.

The pressure effect on TOF at 60 ℃ was less pronounced than at 50 ℃, probably because the kinetic rate constant is much higher at 60 ℃ and offsets the reduction in rate caused by the dilution effect. The *n/i* ratio increased more than threefold in CXLs compared to pressurization with syngas alone. These results clearly demonstrate that the injection of CO_2 into the liquid phase (a) increased the H_2/CO ratio in the CXL phase even at relatively low syngas partial pressures (6 bar), (b) reduced CO inhibition observed when using equivalent pressures of syngas alone, and (c) enhanced the TOF and *n/i* ratio.

Table 3.3: Effect of CXLs on TOF and *n/i* at 60 ℃

Total Pressure, bar	TOF, h^{-1}		*n/i*	
	Syngas Only	CXL (6 bar Syngas +CO_2)	Syngas Only	CXL (6 bar Syngas +CO_2)
6	165.9	-	7.8	-
27	140.5	170.6	3.9	9.4
38	134.6	150.2	3.7	10.7
56	115.6	121.3	3.4	12.9

1-octene/Rh = 988; P/Rh = 205; ligand: -PPh_3. For CXL runs, total pressure: 6 bar syngas + CO_2 pressures. Solvent: Toluene. Identical liquid volume for neat solvent and CXL runs. Reaction time = 6 hours.

The generally accepted mechanism for CO inhibition of the regioselectivity during hydroformylation by Rh/TPP complex was proposed by Pruett and Smith (Figure 3.3).[67] From Figure 3.3, we infer that in addition to PPh_3, CO is also a ligand for the Rh complex. The progressive substitution of PPh_3 by CO attachment to the Rh center is believed to worsen the regioselectivity. Thus, for a given catalytic system, it is plausible that at certain

CO concentrations in the liquid phase the three PPh_3 ligands could all be displaced by CO. Beyond this threshold CO concentration, the beneficial effect of CXLs will no longer be evident. To test this hypothesis, we also carried out experiments using syngas partial pressures of 9 and 12 bar. The results are shown in Table 3.4 and Table 3.5.

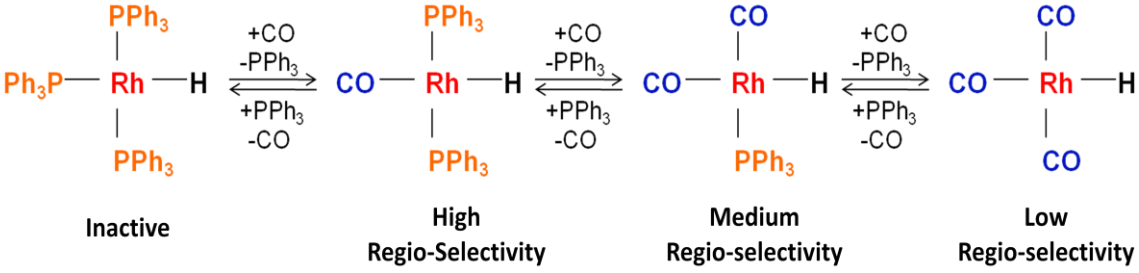

Figure 3.3: Influence of CO as a Rh/TPP ligand on hydroformylation regioselectivity[67]

Table 3.4: Effect of CXLs with 9 bar syngas partial pressure at 60 ℃

	Total Pressure, bar	TOF, h^{-1}	*n/i*
Syngas Only	9	162.1	6
CXL (9 bar syngas + CO_2)	30	169.1	6.6
	41	156.7	7.3
	59	123.3	8.2

1-octene/Rh = 988, P/Rh = 205, ligand: -PPh_3, solvent: toluene. For CXL runs, total pressure: 9 bar syngas + CO_2 pressures. Liquid volume remained constant.

Table 3.5: Effect of CXLs with 12 bar syngas partial pressure at 60 ℃

	Total Pressure, bar	TOF, h^{-1}	*n/i*
Syngas Only	12	154.5	5.0
CXL (12 bar syngas + CO_2)	33	148.8	5.7
	44	139.9	5.9
	62	125.8	6.4

1-octene/Rh = 988, P/Rh = 205, ligand: -PPh_3, solvent: toluene. For CXL runs, total pressure: 12 bar syngas + CO_2 pressures. Liquid volume remained constant.

When syngas partial pressure is increased from 6 to 9 bar in the CXL experiments, the enhancement in both TOF and *n/i* were similar (Table 3.4) compared to 6 bar syngas partial pressure at identical CO_2 partial pressures (Table 3.3). When the syngas partial pressure is further increased to 12 bar, the observed TOFs in CXLs are less compared to the run with only syngas at 12 bar (Table 3.5). Further, the increases in *n/i* ratio with CXLs are moderate, from ~5 with syngas alone to 6.4 at the highest CO_2 pressure of 50 bar. Thus, the observed increases in the *n/i* ratio with CXLs are much less at higher syngas pressures (9 and 12 bar) compared to those at a syngas partial pressure of 6 bar (Table 3.3). The deterioration in the CXL enhancement effect at higher syngas pressure is attributed to the resulting higher CO concentration in the liquid phase, which is detrimental to the regioselectivity. Clearly, the syngas pressure of 6 bar is more suitable for use with CXLs. Lower syngas pressures typically lead to syngas starvation in the liquid phase and loss of selectivity toward isomer formation.

3.3.2 1-Octene hydroformylation in propane-expanded liquids

Comparing to CO_2 (P_c = 73.8 bar, T_c = 31 ℃), propane has higher critical temperature and lower critical pressure (P_c = 42.5 bar, T_c = 96.6 ℃). Therefore, propane has the potential to be a pressurizing gas that's suitable for reactions operates at higher temperatures and therefore increase the activity. It is also possible that propane-expanded liquid (PXL) could achieve the similar effect as CXL at lower operating pressures. To test out these hypotheses, 1-octene hydroformylation reactions were carried out in PXL.

3.3.2.1 Expansion studies of PXLs

As was stated in Chapter 2, volumetric expansion studies are essential for reaction design. The volumetric expansion of a 1-octene/toluene mixture (1/1 vol/vol) was carried out in the apparatus shown in Figure 2.1 following the same procedures as described in Chapter 2. The results are shown in Figure 3.4. The expansion of the liquid decreased when the temperature increased from 60 to 80 ℃. Comparing to CXL (Figure 2.4), the same V/V_0 ratio was achieved at a much lower pressure in PXL. It takes 66 bar of CO_2 or 8 bar of propane to reach a V/V_0 of 1.4.

At 60 ℃, the Rh/TPP (P/Rh = 40 mol/mol) catalyst precipitated out at around 9 bar of propane pressure. When the temperature increased to 80 ℃, the solubility of the catalyst increased under the same propane pressure. The Rh/TPP complex didn't precipitate out until around 12 bar. However, the expansion rate at which the catalyst complex precipitated out was the same (~1.45). This indicated that the solubility of the catalyst depends on the propane concentration in the liquid rather than temperature. When the amount of the TPP

decreased (P/Rh = 10), the propane pressure at which the catalyst complex precipitated out increased to 13.5 bar.

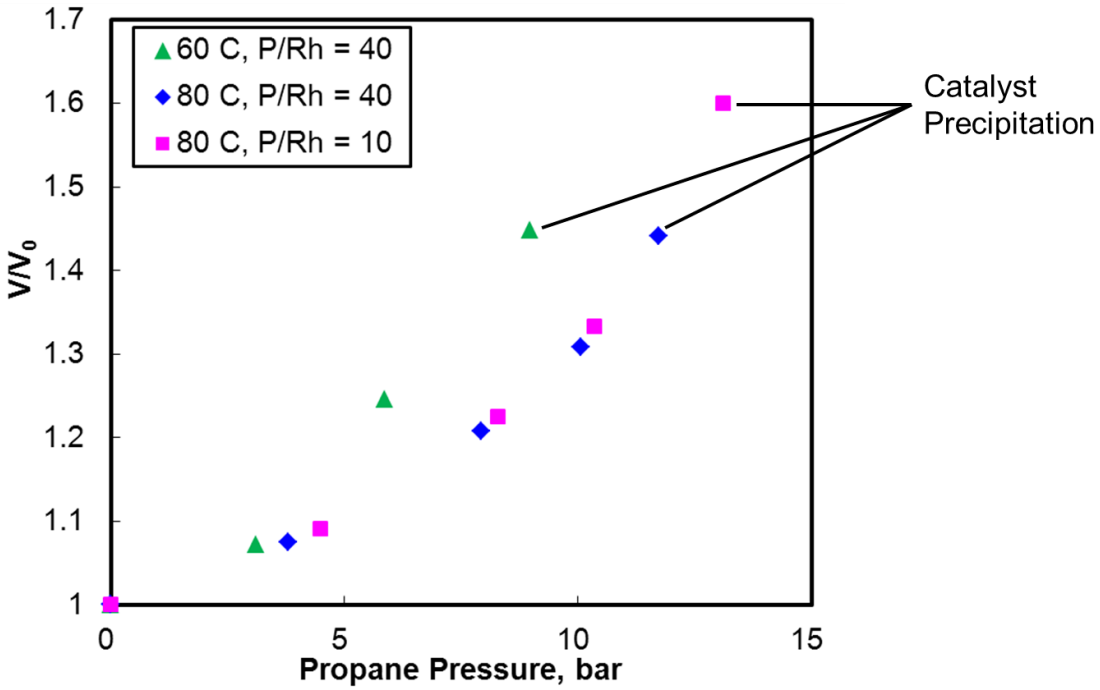

Figure 3.4: Volumetric expansion of 1-octene/toluene (1/1 vol/vol) mixture in propane at 60 and 80 ℃.

The main product of 1-octene hydroformylation is the linear aldehyde n-nonanal. It is necessary to see whether or not the expansion and the catalyst solubility changes with reaction when *n*-nonanal is formed. Figure 3.5 shows the results of volumetric expansion and catalyst precipitation at propane-expanded *n*-nonanal at 80 ℃. For comparison purpose, the expansion of 1-octene/toluene mixture with a P/Rh of 40 that was shown in Figure 3.4 is plotted again in Figure 3.5. As seen in Figure 3.5, the expansion of *n*-nonanal is less than the 1-octene/toluene mixture. However, the TPP solubility is much higher in nonanal than in 1-octene/toluene mixture. The catalyst complex (molar P/Rh = 210), did not precipitate out

until 21 bar in propane-expanded *n*-nonanal. This is an advantage in the actual hydroformylation reaction as the catalyst will stay dissolved as conversion proceeds..

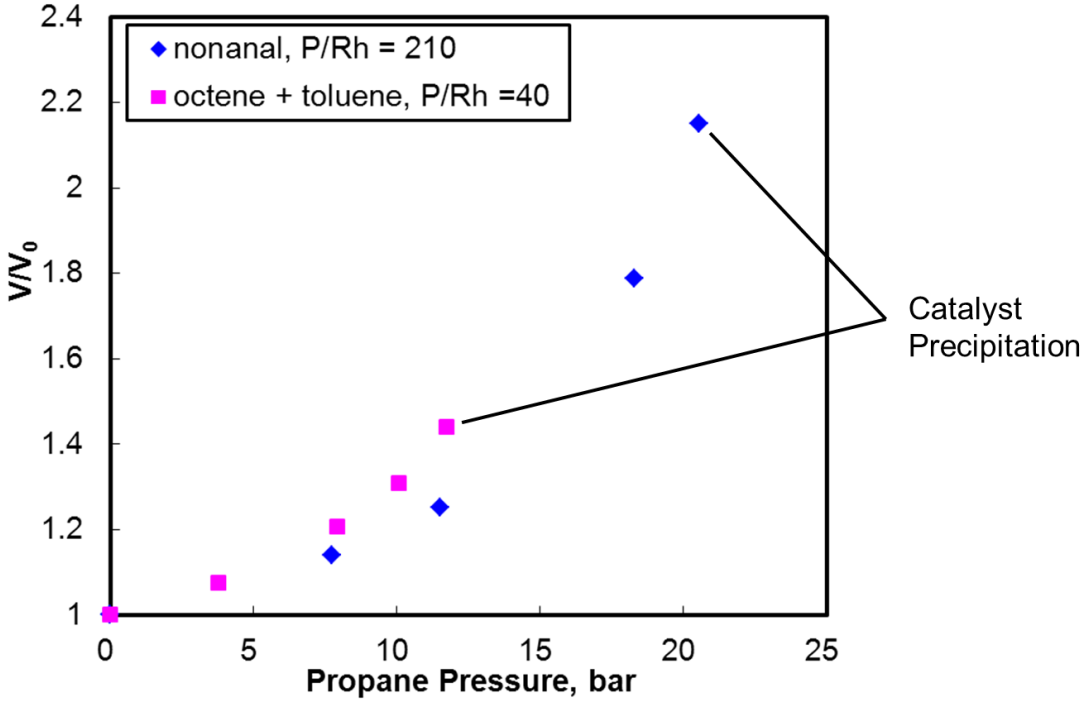

Figure 3.5: Volumetric expansion of n-nonanal in propane at 80 ℃.

3.3.2.2 1-Octene hydroformylation in PXLs

From the volumetric expansion studies as shown above, PXL has similar expansion effect as CXL at much lower operating pressures. It will be interesting to see whether PXL has a similar effect on 1-octene hydroformylation reaction activity and selectivity as CXL. Therefore, 1-octene hydroformylation reactions were carried out in PXL at 60 ℃ (Table 3.6) using Rh/TPP catalyst.

The reaction conditions are as follows: syngas partial pressure = 6 bar, 1-octene/Rh = 988, P/Rh = 205, solvent: toluene, reaction time = 6 hours. In PXL runs, the syngas partial pressures were maintained at 6 bar with various propane partial pressures. In sharp contrast to CXLs, TOF decreased when propane was added. There was little enhancement in *n/i* for

the reactions in PXLs. At 5 and 7 bar pressures of propane, the TOFs were 135.7 h^{-1} and 126.6 h^{-1}, respectively. Both these values are lower than the TOFs observed when using 6 bar syngas only (167.9 h^{-1}). The enhancement of *n/i* ratio was very little comparing to CXL reactions (Table 3.3). When more propane was added to the system (≥ 14 bar), the aldehyde selectivity significantly decreased. The aldehyde selectivity was only 26.7 at 16 bar propane pressure. Most of the 1-octene conversion was towards an unidentified heavy product, which is possibly in a polymer form. This is probably due to the fact that the Rh/TPP catalyst precipitated out under these propane pressures (Figure 3.4).

Table 3.6: 1-Octene hydroformylation in PXL at 60 ℃

Pressure, bar	6 (syngas only)	11 (5 bar propane)	13 (7 bar propane)	20 (14 bar propane)	22 (16 bar propane)
V/V_0	-	1.15	1.3	2.5	3.4
TOF, hr^{-1}	167.9	135.7	126.6	-	-
Conversion, %	85.4	75	70.9	66.1	67.5
S (aldehyde), %	92.8	96.3	96.2	63.1	26.7
S (octane), %	3.3	4.5	1.6	3	1.6
S (isomers), %	3.9	2.2	2.2	4.8	2.7
S (heavy), %	0	0	0	29.1	68.9
n/i	8.1	8.2	8.6	11.2	9.9

In order to prevent the catalyst from precipitating, a higher temperature of 80 ℃ was used. The reactions were carried out under otherwise similar reaction conditions for 4 hours.

In PXL runs, the syngas partial pressures were kept at 6 bar, while 7 bar and 10 bar of propane were added separately. The results are shown in Table 3.7. No heavies were formed under these conditions. Aldehyde selectivity was higher than 95% for all three runs. However, no enhancement in regioselectivity was observed. Even though the activity values increased in general compared to 60 ℃, the TOFs decreased when adding 7 bar and 10 bar propane to the reaction system.

Table 3.7: 1-Octene hydroformylation in PXL at 80 ℃

Pressure, bar	6	13 (7 bar propane)	16 (10 bar propane)
V/V_0 (PXL)	-	1.15	1.3
TOF, hr^{-1}	503.6	348.1	295.9
Conversion, %	98.6	98.5	98.6
S (aldehyde), %	95.9	95.8	95.8
S (octane), %	1.7	1.7	1.7
S (isomers), %	2.2	2.3	2.3
n/i	8	7.9	8.2

3.4 Conclusions

In CXL media, H_2/CO ratio can be increased at fixed syngas composition, low syngas partial pressures (thereby avoiding CO inhibition) and mild total pressures (a few tens of bar). For Rh catalyzed 1-octene hydroformylation, the low syngas partial pressure and increased H_2/CO ratio in CXL medium increases both the TOF and regioselectivities compared to neat hydroformylation reaction mixtures. At 6 bar syngas partial pressure and

50 bar CO_2 pressure, the increase in TOF is up to 64% at 50 ℃ and 21% at 60 ℃, while the corresponding increases in regioselectivity (*n/i*) are 250 and 280%, respectively. At higher syngas partial pressures of 9 and 12 bar, the increases in *n/i* ratio with CXL media were relatively less than at 6 bar. This ability of tuning H_2/CO ratio in CXL can in general be applied to hydroformylation of other olefinic substrates as well.

Volumetric expansion of the 1-octene reaction mixtures were higher in propane-expanded liquids compared to CO_2-expanded liquids under the same pressure. Preliminary tests of 1-octene hydroformylation in PXLs showed a decreased reaction rate, with little or no enhancement in *n/i* ratio at both 60 and 80 ℃. A more detailed systematic investigation is required to determine why PXL did not show similar effects as CXL.

Chapter 4 : Continuous Hydroformylation in CXL with Bulky Rh Complexes in A Nanofiltration Membrane Reactor

4.1 Introduction

Previously, a continuous 1-octene hydroformylation in a nanofiltration membrane reactor was demonstrated using syngas as the pressurizing gas.[26] The use of soluble, polymer-bound bidentate ligand[27] not only allowed better binding of the Rh center but also facilitated superior Rh retention by the membrane. Rh leaching in the permeate at steady state was on the order of a few tens of ppb which easily meets the economic viability criterion.[55] However, the requirement of relatively high syngas pressure (30 bar) to facilitate filtration inhibits the reaction rate and reduces the regioselectivity. As discussed in Chapter 3, CXLs provide a way of tuning H_2/CO ratio in the liquid phase at fixed syngas feed composition, low syngas partial pressures (i.e. without causing syngas inhibition) and mild total pressures (tens of bars). TOF and *n/i* ratio both increased in 1-octene hydroformylation performed in CXL media when using a Rh/TPP ligand. This work examines whether the use of CXLs with low syngas partial pressure during continuous reactor operation could overcome the syngas inhibition while also lowering the viscosity of the reaction mixture to improve mixing and nanofiltration rates in the reactor.

4.2 Experimental

4.2.1 Materials

The purchased materials used in this work are the same as listed in Table 3.1. In

addition, the JanaPhos ligand (Figure 4.1) was synthesized in-house using published methods.[27] The molecular weight of the JanaPhos ligand is centered around 10000 g/mol with a polydispersity index of 1.3.

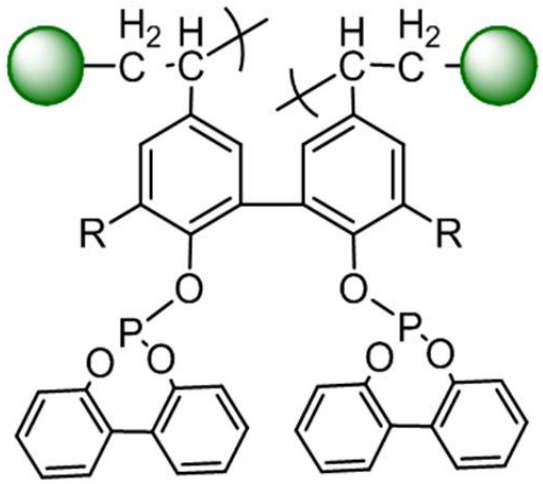

Figure 4.1: Structure of JanaPhos ligand[27]

4.2.2 Continuous nanofiltration membrane reactor suitable for CXL operations

The equipment used for performing continuous hydroformylation in CXLs with *in situ* membrane filtration was a modified version of the equipment used previously,[26] capable of maintaining a constant holdup of a CXL phase in the reactor. Several modifications were performed to accommodate the special features of CXLs.

In previous apparatus, an HPLC pump was used for introducing the liquid solution. The flow was not very stable for extended runs. Hence, it was replaced with an ISCO syringe pump (Model 1000D) which provided steady, uninterrupted flow for the liquid feed.

Secondly, a liquid level controller using fiber optic and a solenoid valve was introduced to the apparatus (Figure 4.2). During continuous runs with conventional liquid phase reaction media, the liquid volume is relatively independent of pressure fluctuations and

hence level control was not a major issue.[26] In contrast, when using gas-expanded liquids, stable level control posed more of a challenge compared to conventional liquid phases, due to the significant pressure dependence of the volume of the expanded phase as shown in the volumetric studies in Chapter 2. Liquid level controllers available in the market are not suitable for level control in our membrane reactor. Fiber optics-based liquid level detection was found to be efficient in a lab-scale reactor.[75] It was successfully demonstrated for measuring volume expansions and phase transitions with supercritical fluids in closed vessels. In this work, fiber optic that provides feedback to a solenoid valve is used as a method for control of liquid control in the CXL phase.

An aluminum clad silica fiber with an inner core size of 200 μm (Fiberguide) was used. As shown in Figure 4.2, one end of the fiber is fixed in the membrane reactor by glue in a 1/16" stainless steel tubing. The light signal from the tip of the fiber was converted to an electric signal by a photodiode and sent to Labview fieldpoints. During the continuous operation, the light signal will change when the liquid level is higher than the tip of the fiber. The solenoid valve will then open to relieve the liquid to sample collectors. When the liquid level drops below the tip of the fiber, the signal changes again and the solenoid valve will be closed to stop liquid from flowing. To improve the light signal, a PVC fiber connector designed in-house was used to increase the interface between the two ends of the fiber and reduce the problems associated with misalignment and shifting. Ocean Optics HL-2000 tungsten halogen light source provides a light signal of around 5 V and reduced the noise level and signal drift. A Swagelok® double pattern metering valve was installed downstream of the solenoid valve to provide additional resistance to flow.

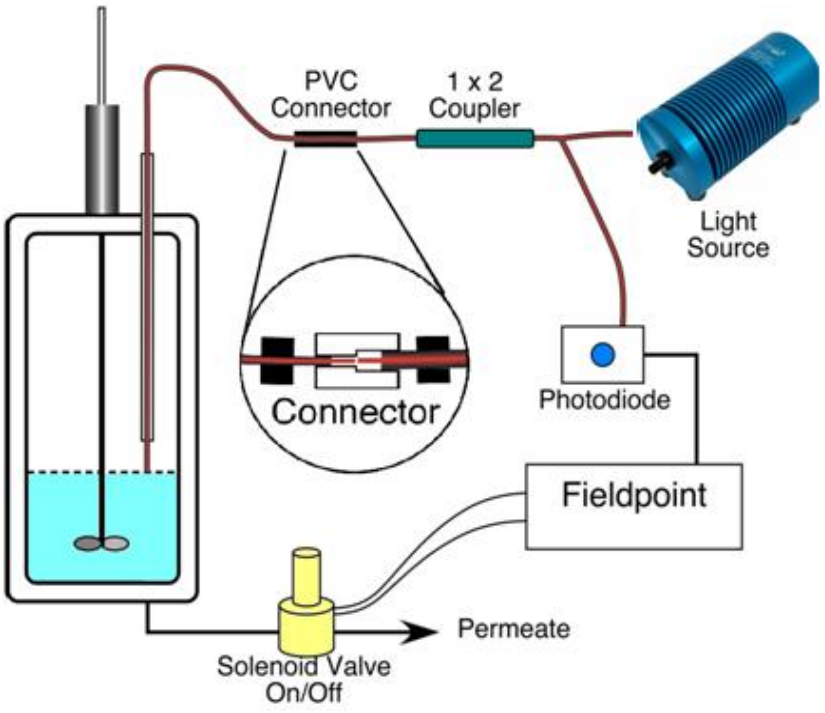

Figure 4.2: Scheme of fiber optic liquid level controller

A continuous filtration experiment using CO_2-expanded toluene was conducted at room temperture. By employing this level control system during the continuous filtration, steady permeate flow rate of approximately 0.33 ± 0.01 mL/min was maintained for 50 hours (Figure 4.3), matching the 0.33 mL/min liquid inlet flow rate set at the syringe pump. The pressure and temperature sensors along with control mechanisms were interfaced with a LabVIEW® data acquisition and control system for continuous data monitoring.

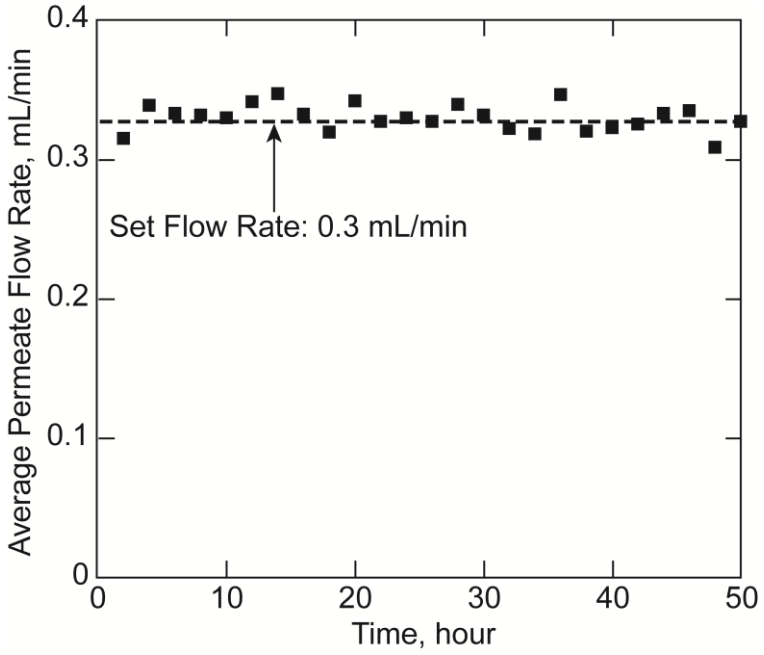

Figure 4.3: Average permeate flow rate with fiber optics-based level control of CXL-toluene in the continuous reactor

Another challenge in the continuous operation using CXL is to determine a proper way to introduce two different gases (syngas and CO_2) independently. Initially, the two gases were premixed in a 2.25 L high-pressure sample cylinder (reservoir). The cylinder was then heated to reactor temperature and the mixture was fed to the reactor during experiments (Figure 4.4).

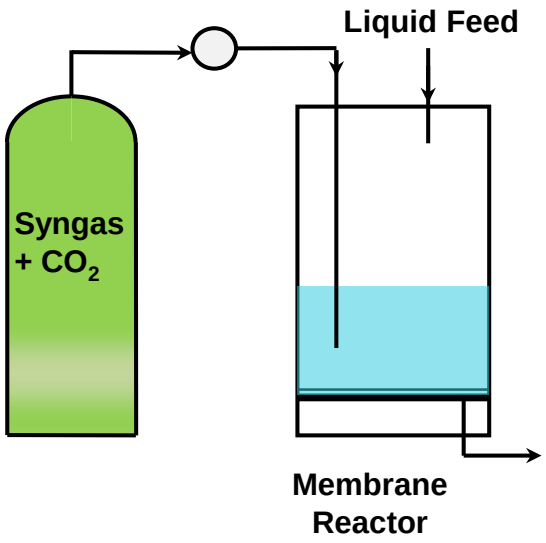

Figure 4.4: Gases introduction by premixing

However, it was recognized later that this method led to the problem of syngas starvation in the liquid phase. Syngas is not only absorbed by the liquid phase but also consumed as a reactant. Therefore, as the reaction proceeds, the partial pressure of syngas in the reservoir decreases, leading to the syngas starvation in the reactor. Figure 4.5 shows the results of a continuous 1-octene hydroformylation when using the premixed gases. In the beginning of the reaction, premixed 6 bar syngas and 24 bar CO_2 were used in the reaction. The aldehyde selectivity was less than 50% and continued to decrease during the first 8 hours. The percentage of 1-octene isomer products increased from around 26% to more than 40%. This significant change of selectivity indicates syngas starvation during the reaction. To verify this, the feed gas was switched to 30 bar syngas only. This caused the aldehyde selectivity to increase to around 70% after another 8 hours. When the feed was switched back to a fresh premixed 6 bar syngas and 24 bar CO_2 mixture, the aldehyde selectivity decreased to less than 40% immediately.

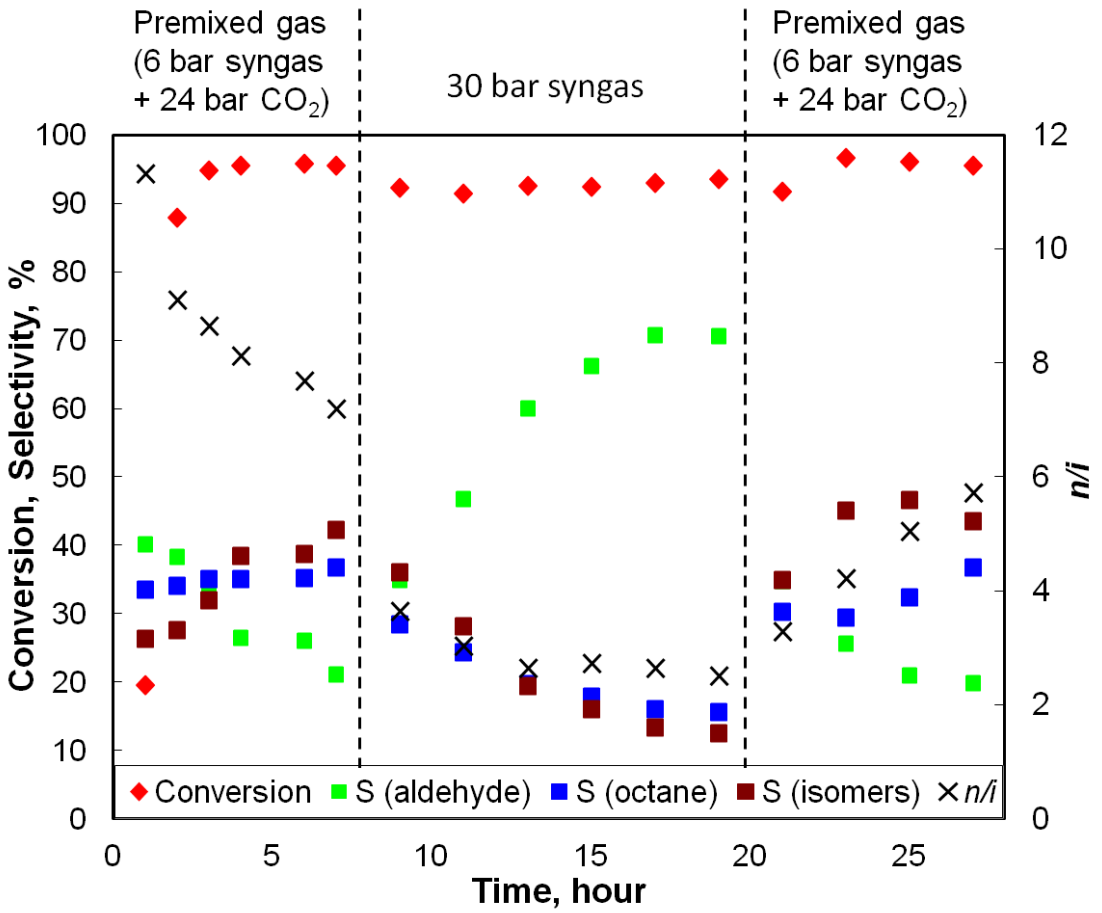

Figure 4.5: Effect of gases feed on continuous 1-octene hydroformylation reaction (50 ℃, 1-octene/Rh = 1000, P/Rh = 6, 1-octene/toluene = 3/7 V/V, stirring rate = 1000 rpm)

To avoid syngas starvation, the syngas/CO_2 partial pressure in the reactor gas phase has to be maintained constant. This is not possible with a combined CO_2+syngas feed since they are absorbed by the liquid phase at different rates. In other words, the CO_2 and syngas have to be admitted independently to maintain their gas phase partial pressures constant. The plumbing of the setup was modified for this purpose (Figure 4.6). The CO_2 is introduced via a mass flow controller (Brooks®) at a constant reactor pressure and at a predetermined mass flow rate calculated based on CO_2 solubility in the liquid under the reaction conditions.[37] The syngas consumed in the liquid phase by reaction is replenished from an external

cylinder to maintain constant syngas partial pressure in the MET cell (upstream pressure control, using the gas regulator). This configuration should maintain a CO_2/syngas ratio.

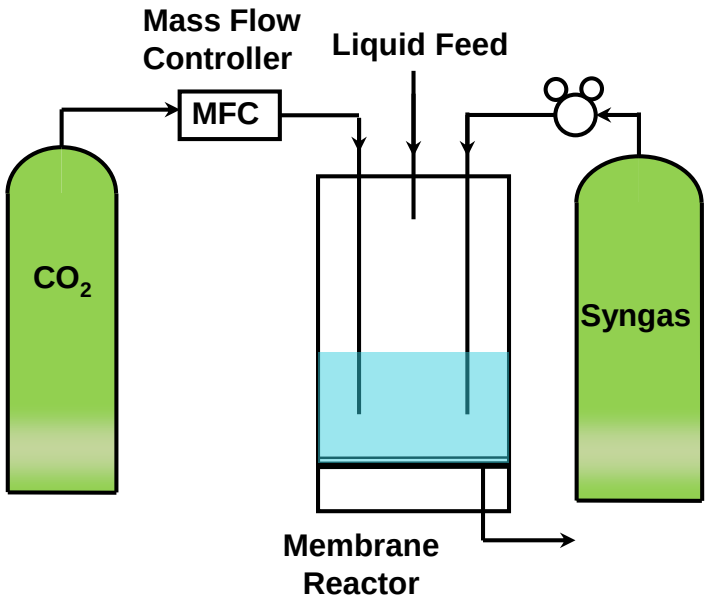

Figure 4.6: Modified gases introduction

The permeate stream was collected by an automatic sample collection system assembled in house using a Cheminert® stream selector, a Valco® actuator and digital valve sequence programmer (Figure 4.7). The liquid permeate coming out of the membrane reactor went through the stream selector into the sample bottle during the pre-set time interval controlled by the valve sequence programmer. The valve actuator rotated at the end of the time interval and switched the permeate stream into the next sample bottle. The sample collecting system is capable of holding up to 10 samples.

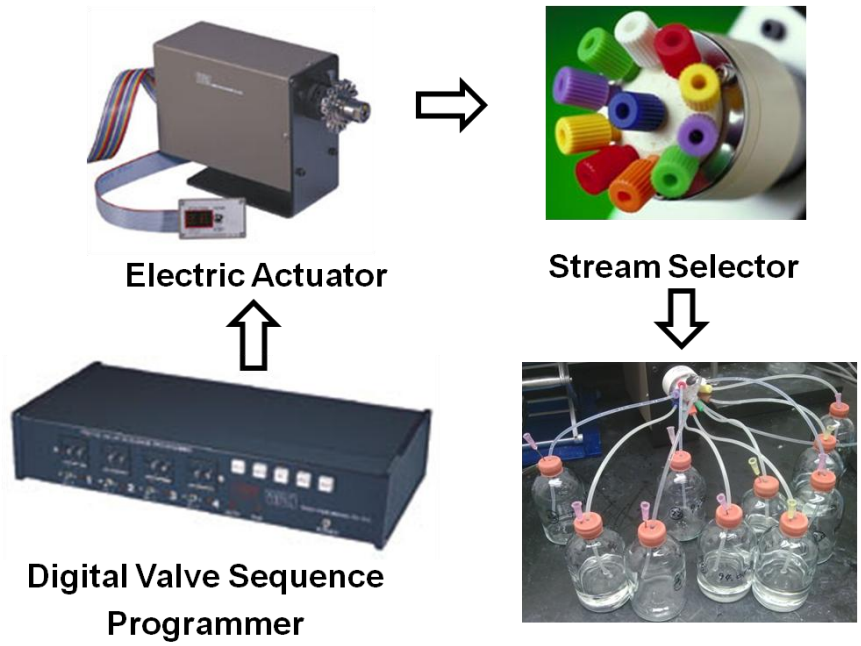

Figure 4.7: Automatic sample collecting system for extended run

Incorporating all the modifications mentioned above, the schematic of the setup is shown in Figure 4.8. The polyimide membrane used for retaining the JanaPhos complex was PuraMem 280 (molecular weight cut-off of 280 g/mol), purchased from Evonik. It has a pressure limit of 60 bar and temperature limit of 50 ℃. A circular piece 9 cm in diameter is cut to fit into the reactor.

A typical continuous hydroformylation run was performed as follows. The membrane reactor was first flushed with CO_2 at 20-30 bar to remove residual air. Approximately 80 mL of the liquid feed stream consisting of 30 vol% 1-octene and 70% vol% toluene was then charged to the reactor by the syringe pump. The reactor was then heated to the desired temperature of 50 ℃. Following temperature equilibration, CO_2 was added to the reactor with stirring until the pressure stabilized at 32 bar. Then syngas was introduced to raise the total reactor pressure to 38 bar (syngas partial pressure = 6 bar) indicating the start of the reaction. Immediately following syngas introduction, a liquid feed rate of 0.33 mL/min and

a CO_2 feed rate of 25 sccm (standard cubic centimeters per minute) were simultaneously established. Permeates were collected automatically and analyzed by gas chromatography (GC/FID, Varian® CP-3800) for estimating 1-octene conversion and product selectivity. The permeate samples were also subjected to inductively coupled plasma atom emission spectroscopy (ICP-AES, Horiba Jobin Yvon® 2000) to quantify the amounts of Rh and P. The GC/FID and ICP-AES analyses are detailed in Appendix A and Appendix D, separately.

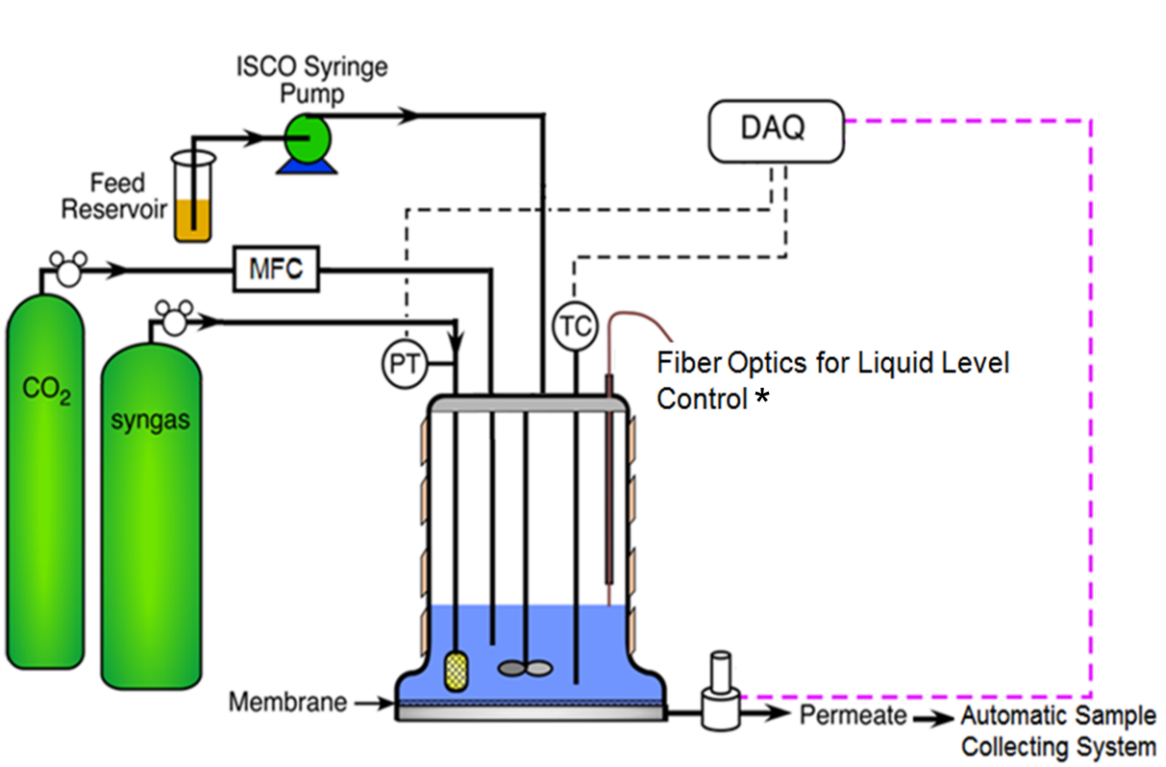

Figure 4.8: Reactor setup for continuous run with membrane filtration.

The turnover frequency during the continuous run (TOF_c) at steady state time t is estimated as follows:

$$TOF_c\ (\mathrm{h}^{-1}) = \frac{(\mathrm{Molar\ 1\text{-}octene\ feed\ rate})\,(1\text{-}\mathrm{octene\ conversion\ at\ time}\ t)}{(\mathrm{Initial\ moles\ of\ Rh\ in\ the\ reactor} - \mathrm{total\ Rh\ loss\ at\ time}\ t)} \qquad (4)$$

The amount of Rh at any time is estimated by subtracting from the initial Rh loading the total Rh loss collected in the permeate measured by inductively coupled plasma atomic emission spectroscopy (ICP-AES).

4.3 Effect of CXLs on hydroformylation activity and selectivity with Rh/JanaPhos complex

It is well known that it is difficult to recover and recycle Rh/TPP catalyst complexes from reaction mixtures. In previous work, the bulky polymer-bound JanaPhos ligand was shown to facilitate effective retention of the Rh complex (~ 20 ppb Rh in the permeate) during a continuous hydroformylation run at 50 ℃ in a stirred reactor equipped with a nanofiltration membrane of 400 molecular weight cutoff (MWCO).[26] A gas pressure of 30 bar was required for filtration with the polyimide nanofiltration membrane. Even though steady activity and selectivity were demonstrated, the observed regioselectivity was only 3.3 at this syngas pressure. To improve the regioselectivity, we investigated the concept of CXL media in which the total filtration pressure is made up of dense CO_2 and a lower syngas pressure to enhance the regioselectivity. To test this concept, $Rh(CO)_2(acac)$ complexed with JanaPhos ligand was first tested in CXLs in batch hydroformylation reactions. The batch experiments were run at 50 and 60 ℃ under 6 bar syngas pressure and 32 bar CO_2. The results are shown in Table 4.1.

Table 4.1: Effect of CXLs on hydroformylation with bidentate ligands (JanaPhos)

T, ℃	50		60	
Pressure, bar	6	38 (CXL)	6	38 (CXL)
Time, hrs	4	4	1.5	1.5
TOF, hr^{-1}	494	484	987	976
Conversion, %	97.9	97.1	97.0	97.2
S (aldehyde), %	85.6	85.9	80.6	80.2
S (octane), %	6.8	6.5	9.2	9.5
S (isomers), %	7.2	7.3	9.9	10
n/i	6.6	7.3	7.7	8.5

The *n/i* ratio observed with the Rh/JanaPhos complex increased to 6.6 (50 ℃) and 7.7 (60 ℃) at the lower syngas pressure of 6 bar. However, at both temperatures, the *n/i* ratio in CXL media increases by ~10% compared to that observed with syngas alone at 6 bar. These enhancements are relatively less compared to those observed with the Rh/TPP complex (Table 3.2 and Table 3.3). Further, the TOFs with Rh/JanaPhos complex actually decrease slightly in CXLs compared to neat media (e.g. 484 h^{-1} in CXL vs 494 h^{-1} in non-CXL phase at 50 ℃). This is partly due to dilution effects and partly because the TOFs with bidentate ligands depend not only on CO dissociation but also on ligand bite angle.[74] Although the effect of CXLs on TOF and *n/i* is more modest in the case of Rh/JanaPhos complex, the CXLs nevertheless provide the necessary pressure (30 bar minimum) for nanofiltration without introducing CO inhibition that occurs when syngas alone at 30 bar is employed.

Additionally, the significant viscosity reduction obtained with CXLs, discussed in the following section, facilitates the nanofiltration process.

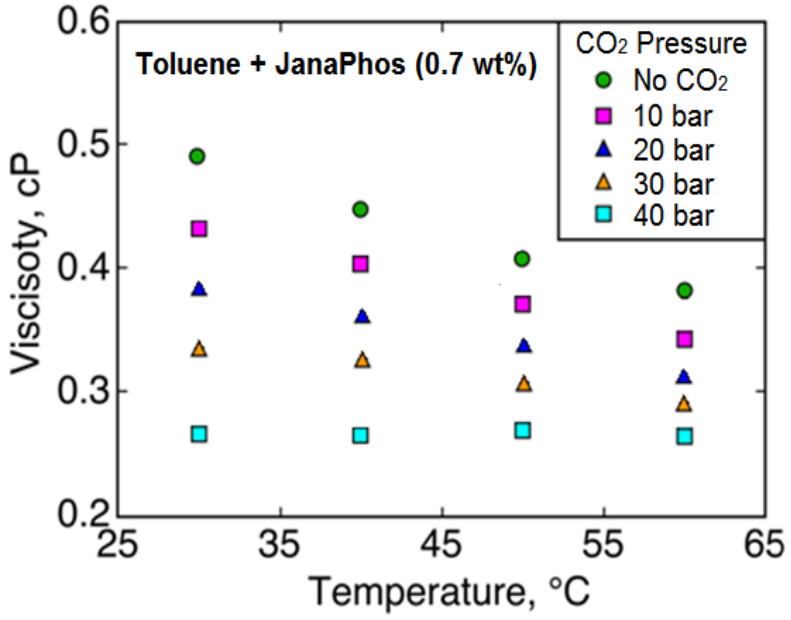

Figure 4.9: Variation of viscosities with temperature for (toluene + 0.7 wt% JanaPhos) mixtures at different CO_2 pressures[76]

The use of CXL should decrease the viscosity of the reaction mixture containing the dissolved polymer ligand. Figure 4.9 shows the viscosities measured for the mixture of toluene and JanaPhos ligand at a concentration of 0.7% by weight, at four temperatures and five CO_2 pressures.[76] At these conditions, the polymer ligand stays dissolved in the CXL (*i.e.* operating conditions are below the cloud point). Such information provides valuable guidance for both the batch as well as continuous hydroformylation studies under homogeneous conditions. From Figure 4.9, it may be inferred that the viscosities decrease with increasing temperature at the same CO_2 pressure and with increasing CO_2 pressure at the same temperature. When pressurizing with up to 40 bar CO_2 at temperatures of 30 ℃ and 60 ℃, viscosities decrease by 50% and 30%, respectively. Remarkably, these viscosity

reductions are greater in magnitude than those achieved with increases in temperature. For example, negligible change in viscosity with temperature was observed at CO_2 pressure of 40 bar. Furthermore, the viscosity reduction achieved in the 30-60 ℃ range with no CO_2 addition is roughly 50% less compared to the viscosity reduction achieved at 30 ℃ by adding 40 bar CO_2. At the desired operating temperature of 50 ℃, the viscosity reduction upon adding 30 bar CO_2 is approximately 33%.

4.4 Continuous reaction with membrane filtration in CXLs

Continuous reaction in CXLs with membrane filtration was carried out for 50 hours and the results are shown in Figure 4.10. In our previous continuous reactor studies with syngas only at 30 bar,[26] the conversion stabilized at 50% and the *n/i* was around 3.3 due to syngas inhibition. In contrast, the conversion increased to more than 70% and the *n/i* was nearly 8 in the case of the CXL run that utilized 6 bar syngas (to alleviate inhibition of TOF and *n/i* ratio) and 32 bar CO_2. Aldehyde selectivity was more than 90%. The conversion appears to stabilize around 70% with a TOF_c value of ~340 h^{-1} (cumulative TON = 17,680 after 52 hours). Clearly, the use of a combination of low syngas partial pressure and CO_2 is beneficial to the regioselectivity as well as reaction activity. Further, the nearly steady TOF_c and permeate flow at constant pressure indicate that the membrane pores are not blocked or fouled during the 50 hour run.

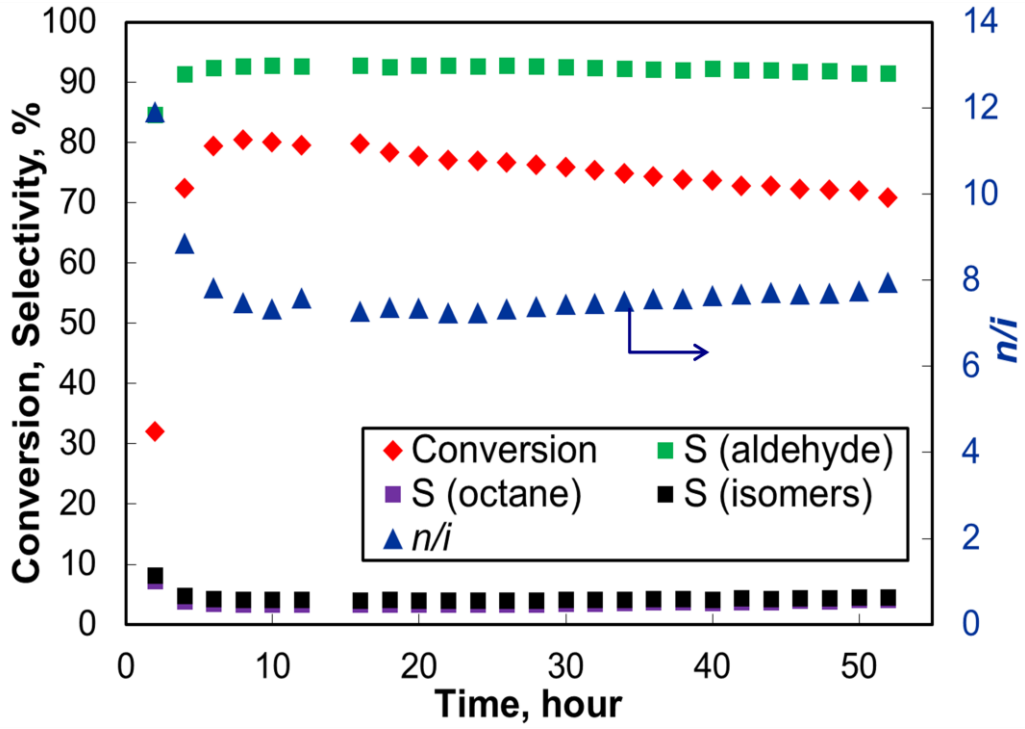

Figure 4.10: Temporal 1-olefin conversion and product selectivities during continuous Rh/JanaPhos catalyzed homogeneous hydroformylation in CXL media performed in a stirred reactor fitted with a nanofiltration membrane. Reaction conditions: 1-octene/toluene = 3/7 (V/V), liquid flow rate = 0.33 mL/min; syngas partial pressure = 6 bar (maintained constant); total pressure = 38 bar; CO_2 flow rate = 25 sccm; T = 50 ℃; Rh concentration = 130 ppm

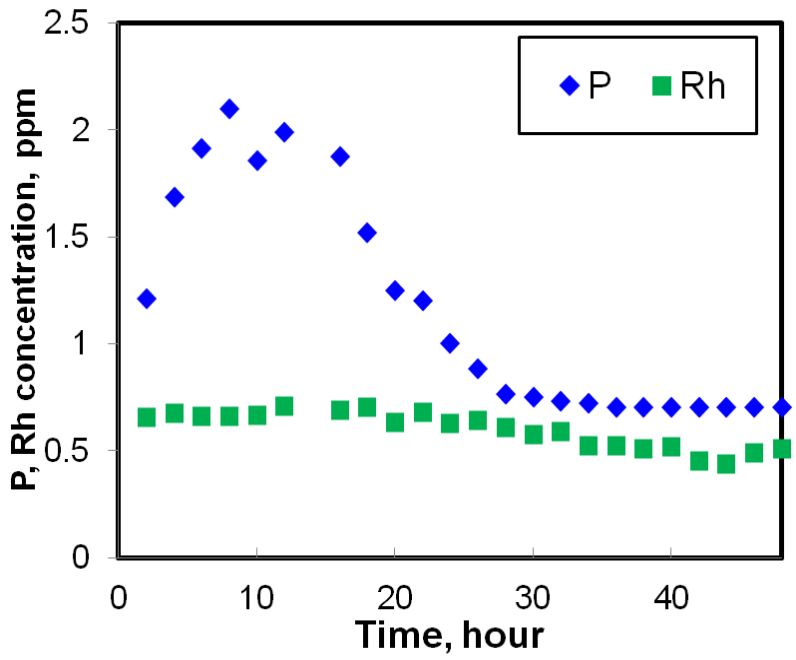

Figure 4.11: Temporal Rh and P concentrations in permeate of continuous reactor based on ICP analyses (operating conditions same as for run shown in Figure 4.10)

ICP analysis of the permeate stream showed a low Rh and P leaching rate in CXLs (Figure 4.11). The P concentration in the permeate stabilized at 0.5 ppm after 25 hours. Rh concentration was less than 0.5 ppm after 25 hours. The total leaching of Rh in 50 h was 0.46 mg (5%). Total leaching of P was 0.89 mg (4.6%). At concentrations of a few ppm, the Rh can be effectively recovered by using suitable absorbents,[77-79] thus providing nearly quantitative Rh recovery. It has been shown previously that a CXL-based process concept as demonstrated in this manuscript would be economically competitive with conventional cobalt-based hydroformylation of higher olefins.[55]

4.5 Conclusions

Continuous homogeneous hydroformylation was demonstrated in CXL media in a stirred reactor equipped with a nanofiltration membrane to effectively retain the bulky Rh catalyst complex. The advantages of low syngas pressure and CXL media on TOF and selectivity are particularly well suited for performing continuous reactions with *in situ* nanofiltration, wherein operating pressures of 30-40 bar are needed to obtain a reasonable transmembrane flux for the 280 MWCO membrane. By maintaining a constant syngas partial pressure of 6 bar and a CO_2 partial pressure of 32 bar in the reactor, we not only avoid syngas inhibition (observed when 30 bar syngas alone is used as pressurizing gas) but also exploit the resulting CXLs to increase the H_2/CO ratio in the reaction phase and the lower the viscosity. Continuous hydroformylation in such a CXL, using soluble bulky phosphite ligands, was successfully conducted for up to 50 hours at 50 ℃. The increased H_2/CO ratio in the CXL phase helps to attain nearly steady TOF_c (~340 h^{-1}) and selectivity (*n/i* = 8, aldehydes > 90%). Constant permeate flux is maintained across the nanofiltration membrane during the 50 h run with low Rh and P leaching (< 1 ppm each in the permeate) at steady state. It should be possible to implement the demonstrated CXL-based continuous reactor concept with *in situ* nanofiltration by replacing existing hydroformylation reactors with the proposed system. Further, the concept should also be applicable in general to homogeneously catalyzed reactions where effective catalyst containment is the key for practical viability.

Chapter 5 : Hydroformylation with Soluble Functionalized Polysiloxanes as Ligands

5.1 Introduction

In the previous chapter (Chapter 4), continuous hydroformylation of 1-octene in a nanofiltration membrane reactor using a soluble polymeric phosphite ligand bound-(JanaPhos) Rh catalyst complex was successfully demonstrated using CO_2 as a pressurizing gas. Stable conversion and selectivity for tens of hours with low Rh leaching (less than 1 ppm of Rh detected in the effluent) were achieved. Reaction activity and selectivity were much improved compared to using syngas only under similar pressures. While JanaPhos ligand has many benefits, it involves tedious synthesis steps and is air- and moisture-sensitive, making cost-effective large-scale synthesis difficult. Hence, we are also exploring alternative, cost-effective polymer ligands that are easy to obtain or synthesize and are also easily retained in solution by nanofiltration membranes. Toward this goal, we have investigated new polymer-anchored Rh-complex catalysts for the hydroformylation of 1-octene and initial tests show very promising results.

Polysiloxanes, commonly referred to as silicones or siloxane polymers, are one of the most widely used modern functional macromolecular materials.[80-81] They consist of a Si-O-Si backbone along with two substituent groups on the Si-atom. The Si-O-Si backbone is inorganic in nature, and addition of the substituent groups (mostly organic) makes these hybrid materials display interesting organic-inorganic properties/characteristics. Polydimethylsiloxane, PDMS, is one example of a simple hybrid polymer having methyl substituents on a Si-O-Si backbone. The variation in the backbone composition (chain

length) serves an important purpose in determining the properties such as density, solubility, thermal stability, viscosity, glass transition temperature etc., while the substituents play key roles in determining and tailoring the physico-chemical properties of the silicone polymer.[82-83] Depending on the nature of the different substituents (phenyl, vinyl, fluoroalkyl, mercaptoalkyl, epoxidyl etc.) several applications of the polysiloxanes are already in practice such as customized surface coatings, electro-optical elastomers, binders, adhesives, membranes, gels and sealants .

The applications of polysiloxanes in catalysis have been numerous in the form of films for holding elemental metals (Au, Cu etc.) for surface patterning,[84] sol-gel based catalyst initiator,[85] and porous membrane for micro-encapsulating chiral complex catalysts.[86] However, the use of functional polysiloxanes as catalyst supports is scarce. The important properties of polysiloxanes such as (a) structural and topical flexibility of chain for easy adoption of optimal conformation of catalytic metal centers, and (b) solubility in organic media, make them suitable candidates as soluble supports. Polysiloxane supported Pd-complexes for Heck coupling was reported by Cypryk et al, where alkylthiol functionalized polysiloxanes were used.[87] In another study, hydroformylation of 1-hexene was demonstrated using a solid hybrid Rh-catalyst with a polysiloxane backbone.[88] Typical results showed 20-80 % conversions, with chemoselectivity to aldehydes decreasing at higher conversion levels with TOF of 150 h^{-1} at 100 ℃. Mukhopadhyay et al[18] used Rh-complex bound to 3-aminopropyl functionalized MCM-41, MCM-48 for the hydroformylation of alkenes. We were motivated to design low MW (on the order of a few thosand Daltons) liquid polysiloxane anchored Rh-complex catalyst by using functionalized polydimethylsiloxane. The motivation for using a liquid polymer is to use membrane

nanofiltration to facilitate easy catalyst retention (by nanofiltration membranes) during a continuous hydroformylation process.

5.2 Preparation of Rh complex with functionalized polysiloxane ligands

Two kinds of functionalized polysiloxanes were tested as ligands for Rh-catalyzed hydroformylation. The first one is a commercially available amine-functionalized polysiloxane ((3-aminopropyl)methylsiloxane-dimethylsiloxane, Figure 5.1) purchased from Gelest. This ligand is readily available and is relatively cheap ($175 for 3kg). It is also much less prone to air oxidation compared to JanaPhos.

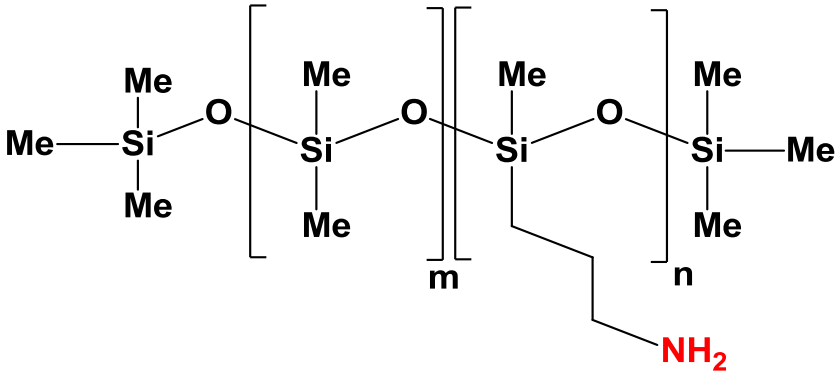

Figure 5.1: Amine-functionalized polysiloxane ligand

The second one is a phosphine-functionalized polysiloxane ligand (Figure 5.2) which requires a one-step synthesis process as shown in Figure 5.3. A commercially available hydroxyl-terminated polysiloxane (silanol terminated polydimethylsiloxane) reacts with (2-diphenylphosphino)ethyldimethylethoxysilane under argon at room temperature for 20 hours to replace the –OH groups with $–PPh_2$ functional groups.

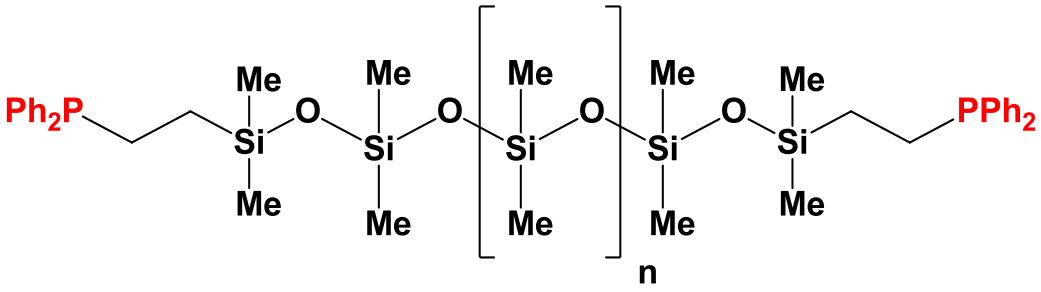

Figure 5.2: Phosphine-functionalized polysiloxane ligand

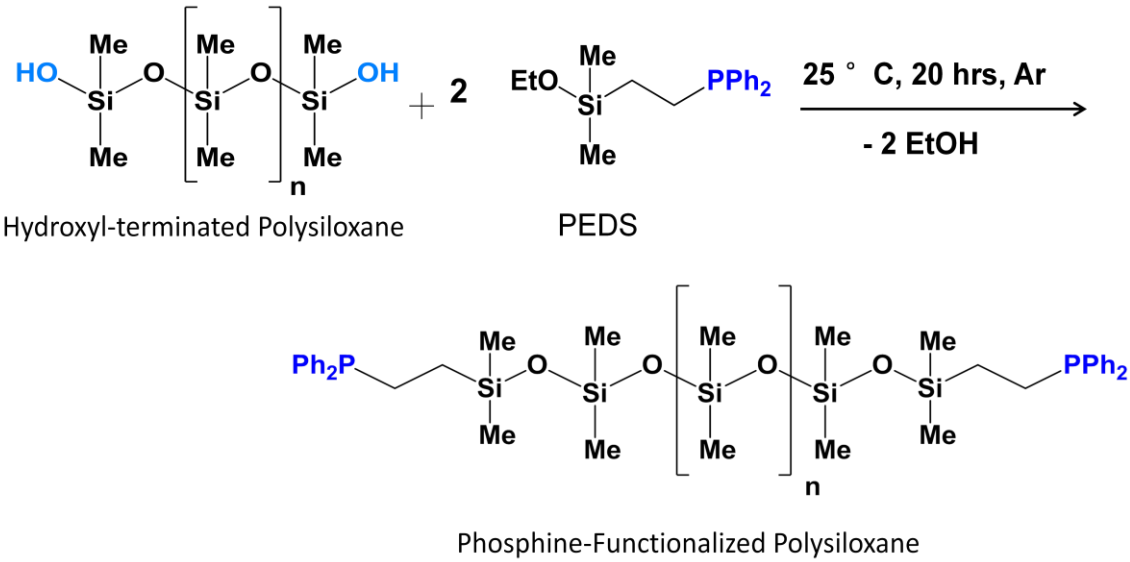

Figure 5.3: Synthesis protocol for phosphine-functionalized polysiloxane

The properties of the amine-funtionalized polysiloxane and the silanol terminated polydimethylsiloxane are listed in Table 5.1.

Table 5.1: Properties of functionalized polysiloxane polymers

Molecular weight (M_n)	2,000-4,500
Viscosity	40-120 Centistokes
Specific gravity	0.8-1.2
Refractive index	1.3-1.5
Functional group content	0.8-2.5%

The functionalized ligands were then complexed with Rh precursors. The amine-functionalized polysiloxane was complexed with $HRhCO(TPP)_3$ (Catalyst A) and the phosphine-functionalized polysiloxane was complexed with $Rh(acac)(CO)_2$ (Catalyst B). The details of the Catalyst A preparation methods are as follows: To a 250 mL toluene solution containing 50 g of (3-aminopropyl)methylsiloxane-dimethylsiloxane copolymer (M_N = 4,000-5,000), a solution 0.7 g of $HRh(CO)(PPh_3)_3$ complex in 50 mL toluene solution was added under a nitrogen blanket. The solution was stirred for 12 h at ambient temperature. After this, the mixture was filtered using membrane nanofiltration with N_2 pressure of 30 bar and a continuous flow of toluene. The permeate was tested for Rh-content periodically until only low concentrations of Rh were found (< 5 ppm).

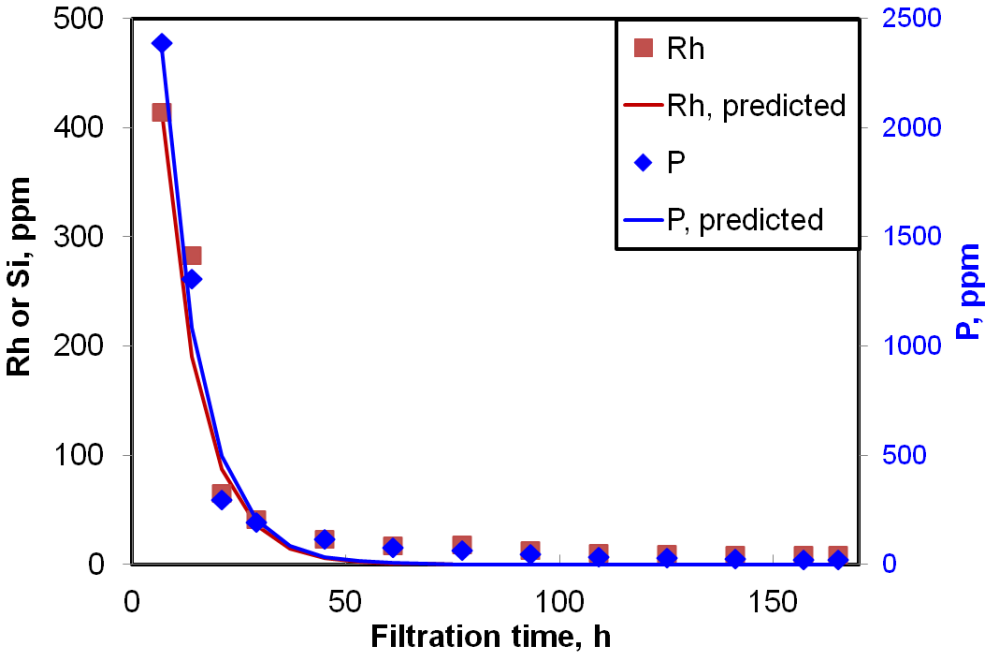

Figure 5.4: Catalyst wash for removing free Rh and P during preparation

To prepare Catalyst B, the reaction mixture for making phosphine-functionalized polysiloxane was mixed with $Rh(acac)(CO)_2$. The solution was then stirred and filtered as

described for Catalyst A. An example of the Rh and P concentrations in the washed-out permeate from Catalyst B are shown in Figure 5.4.

The Rh and P concentration profiles were also simulated using Equation 7, assuming a perfectly mixed CSTR operation:. c_t represents the concentration of Rh or P at any time t; c_i represents the initial concentration of Rh or P; V is the volume of the liquid hold-up in the reactor and v is the liquid flow rate.

$$c_t = c_i \cdot \exp\left(-\frac{t}{\theta}\right), \quad \theta = \frac{V}{v} \qquad \text{(Equation 7)}$$

The predicted Rh and P concentrations (Figure 5.4) match well with the initial Rh and P concentration obtained experimentally in the first 40 hours, indicating that the Rh and P leaching were mainly from the unbound Rh and P species in the retentate mixture.

5.3 Evaluation of soluble functionalized polysiloxane-attached Rh complexes for hydroformylation activity

The two catalysts A and B (retentates following removal of free Rh and P) were first tested separately in batch 1-octene hydroformylation reactions at 50 ℃, 1-octene/Rh = 1000, 1-octene/toluene = 3/7 (V/V) and H_2/CO = 1:1. Reaction time was 6 hours for all runs. The results are shown in Table 5.2. We can see that Catalyst A shows lower activity but similar selectivity compared to the $HRhCO(TPP)_3$ catalyst. This is possibly due to the fact that the N-Rh bond is weaker than the P-Rh bond. In contrast, the catalyst complex B has much higher activity but similar selectivity as the $HRhCO(TPP)_3$ catalyst.

Table 5.2: 1-Octene hydroformylation with various ligands at 50 ℃

Catalyst	P, bar	TOF, h^{-1}	*n/i*	S_{Al}, %
$HRhCO(TPP)_3$	6	73.5	2.9	98.4
A	6	17.3	2.2	89.6
B	6	165.2	2.8	97.6
B	30	139.5	2.6	98.7

Since Catalyst B (phosphine-functionalized) shows good activity in 1-octene hydroformylation, we also tested it with other olefins. As shown in Table 5.3, Catalyst B displays very good activity for the olefins tested (1-decene, 1-dodecene and styrene) at 50 ℃. The syngas consumption profiles were plotted in Figure 5.5. The initial activity of 1-dodecene is the highest among the substrates tested using Catalyst B. As expected, the main product for styrene hydroformylation is the branched aldehyde. The amount of aldehydes formed (measured by GC) matched closely with the amount of syngas consumed, which was consistent with the high chemoslectivity towards the aldehydes. These results imply that Catalyst B has potential for application in various kinds of terminal olefin hydroformylations.

Table 5.3: Olefin hydroformylation using Catalyst B (6 bar, 50 ℃, olefin/Rh = 1000, solvent: toluene, H_2/CO = 1:1, time = 6 hours)

Substrate	Conv., %	TOF, h^{-1}	*n/i*	S(Aldehyde), %	n(Aldehyde), mmol	n(Syngas), mmol
octene	86.9	165.2	2.8	97.6	24.0	24.1
1-decene	89	169.1	2.7	98.2	24.8	25.1
1-dodecene	96	185.4	2.7	97.1	26.4	27.2
styrene	91.6	176.5	0.09	97.1	25.2	25.6

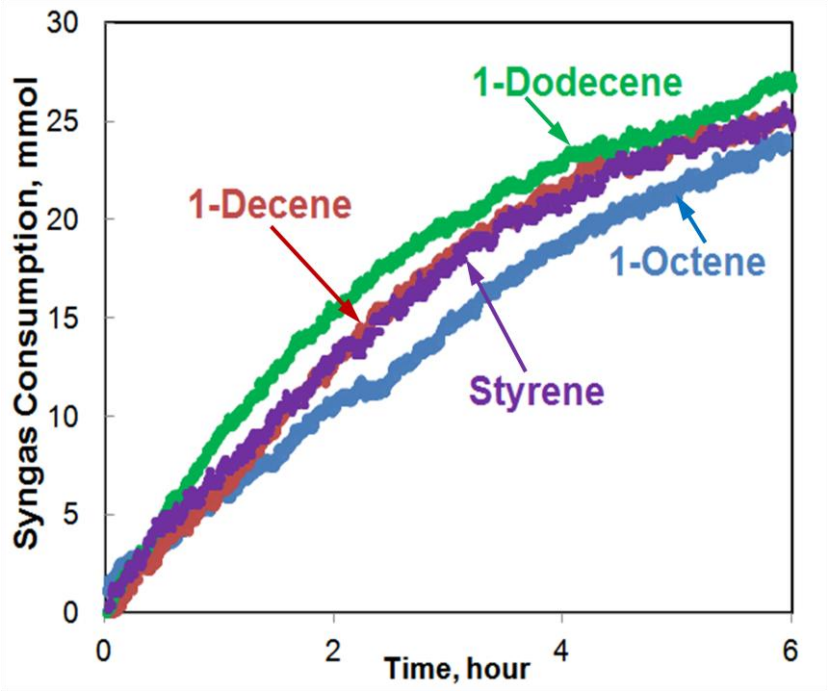

Figure 5.5: Syngas consumption profiles for hydroformylation of various olefins using Catalyst B

5.4 Continuous hydroformylation with soluble functionalized polysiloxane-bound Rh complexes in a nanofiltration membrane reactor

Continuous reactions were also performed using Catalysts A and B in a stirred reactor equipped with a nanofiltration membrane. Figure 5.6 shows time on stream conversion and selectivity for up to 70 hours during continuous hydroformylation of 1-octene with Catalyst A. At a liquid hourly space velocity (LHSV) of 60.5 g 1-olefin /g Rh/h, the steady state TOF_c was 11 h^{-1} (cumulative TON = 770 after 70 hours) with an aldehyde selectivity > 84%.

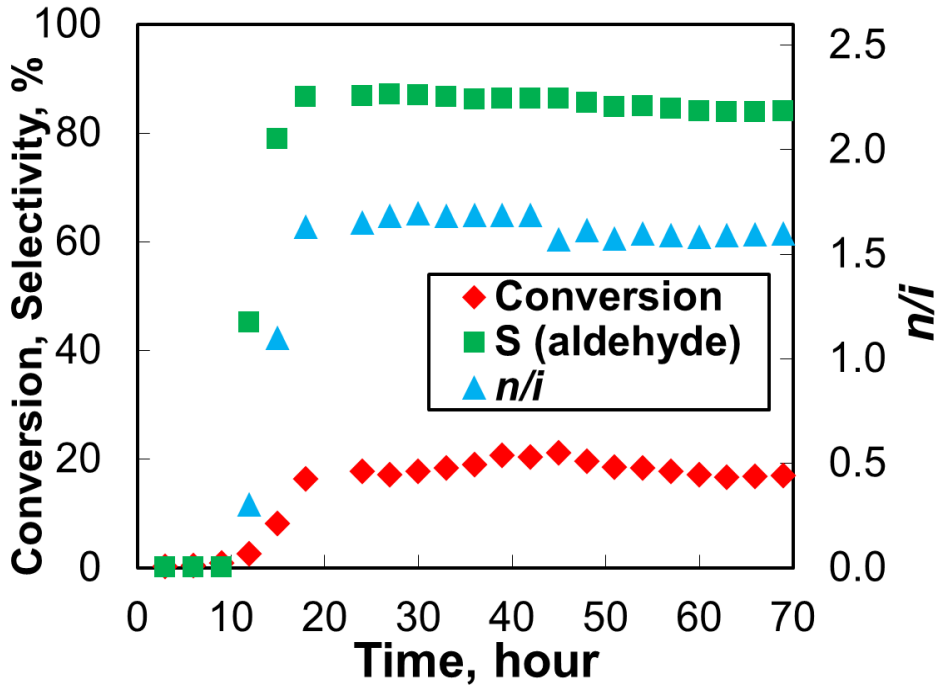

Figure 5.6: Temporal 1-octene conversion and selectivity profiles during continuous Catalyst A catalyzed homogeneous hydroformylation (50 °C, 30 bar; 1-octene/toluene = 1/9 (V/V); H_2/CO = 1:1; LHSV = 60.5 g 1-octene/g Rh/h)

There was almost no activity in the first 10 hours. This was probably due to the long induction period when using Catalyst A. A long induction period of around 3 hours was also observed in batch reaction using Catalyst A under similar conditions (Figure 5.7).

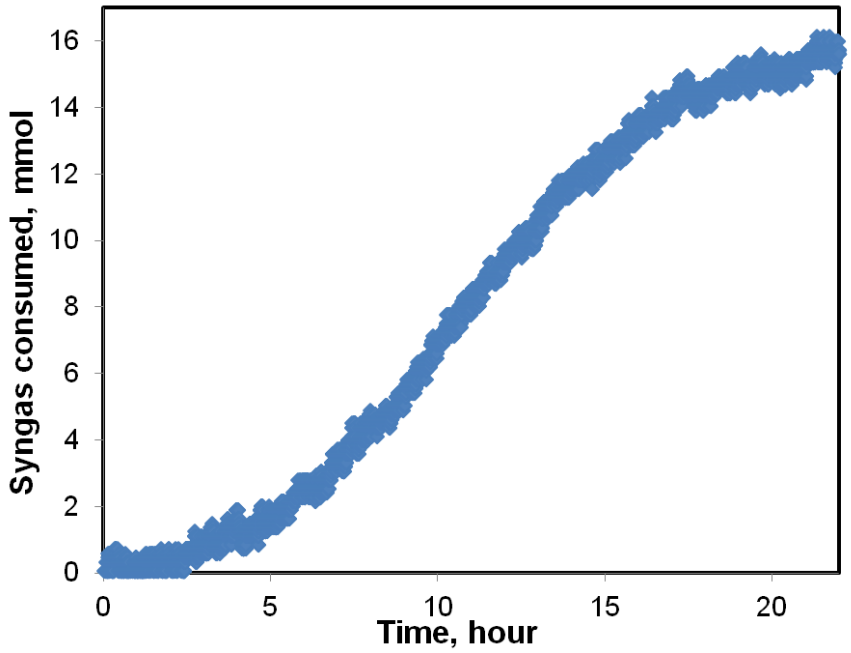

Figure 5.7: Syngas consumption profile during batch study using Catalyst A at 50 ℃ and 30 bar syngas (1-octene/Rh = 500, solvent: toluene, H_2/CO = 1:1, time = 22 hours)

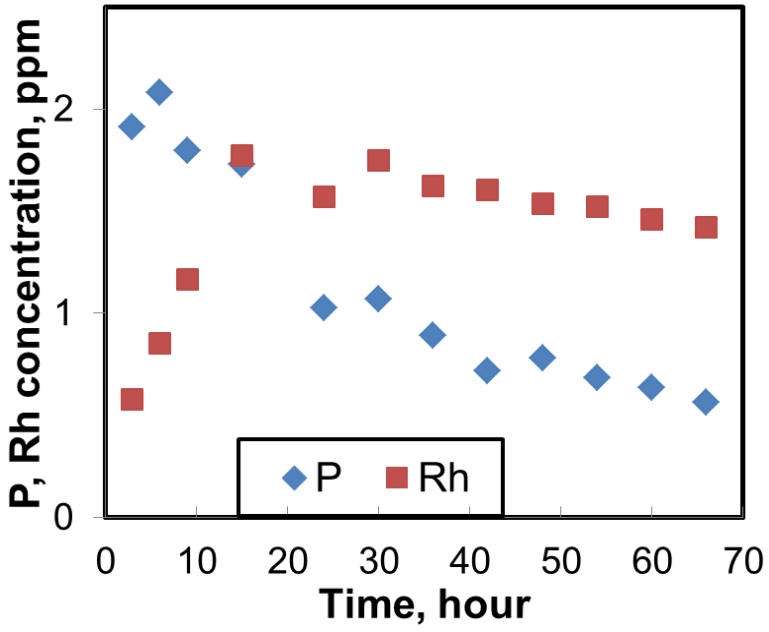

Figure 5.8: Temporal catalyst leaching profiles during continuous Catalyst A catalyzed homogeneous hydroformylation (conditions same as described in Figure 5.6)

Rh concentrations in the permeate were less than 2 ppm during the reaction (Figure 5.8), which corresponds to a total Rh leaching of 0.97 mg (6%) over 70 hours. The conversion is relatively low as also seen in the batch studies (Table 5.2).

Figure 5.9 shows the results of continuous reaction using Catalyst B. Stable conversion, selectivity, and high activity were achieved for up to 120 hours using Catalyst B. At a LHSV of 181.5 g 1-octene/g Rh/h, the steady state TOF_c was 102 h^{-1} with an aldehyde selectivity > 91%. The cumulative TON after 120 hours was 12,240.

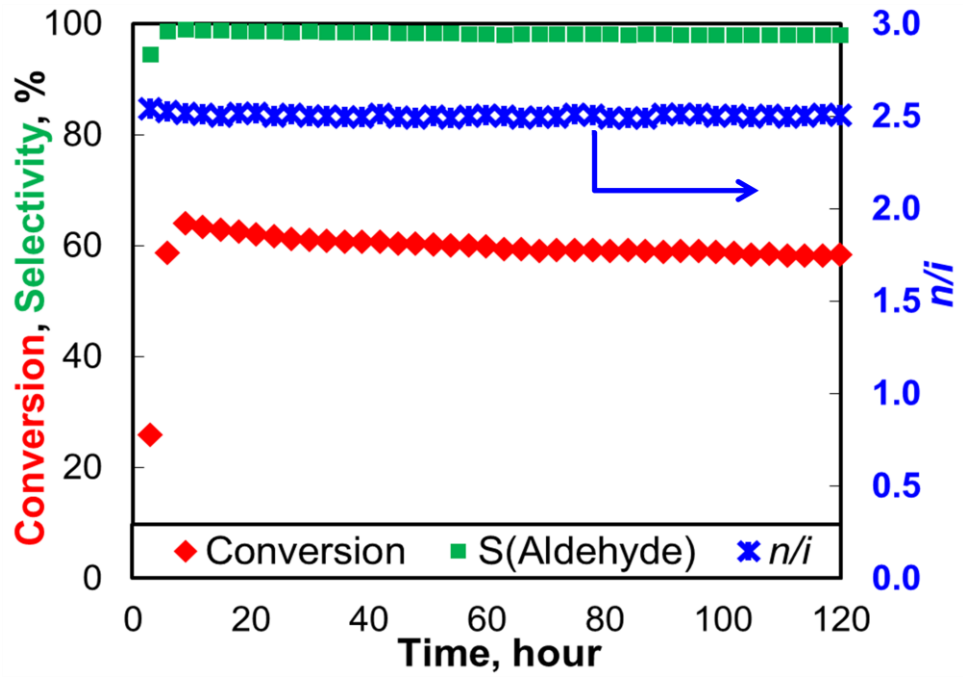

Figure 5.9: Temporal 1-octene conversion and selectivity profiles during continuous Catalyst B catalyzed homogeneous hydroformylation (50 °C, 30 bar; 1-octene/toluene = 3/7 (V/V); H_2/CO = 1:1; LHSV = 181.5 g 1-octene/g Rh/h)

Rh concentration in the permeate (Figure 5.10) was less than 2 ppm at steady state (>40 hrs). The total Rh leaching is 2.3 mg (14.7%) over 120 hours. More than 50% of the Rh leaching occurred during the first 40 hours. It is interesting to note that the conversion only

reduced by 8.8 % throughout the run. This indicates that nearly half of the Rh leached was probably the unbound free Rh, which is known to be less active than the bound Rh.

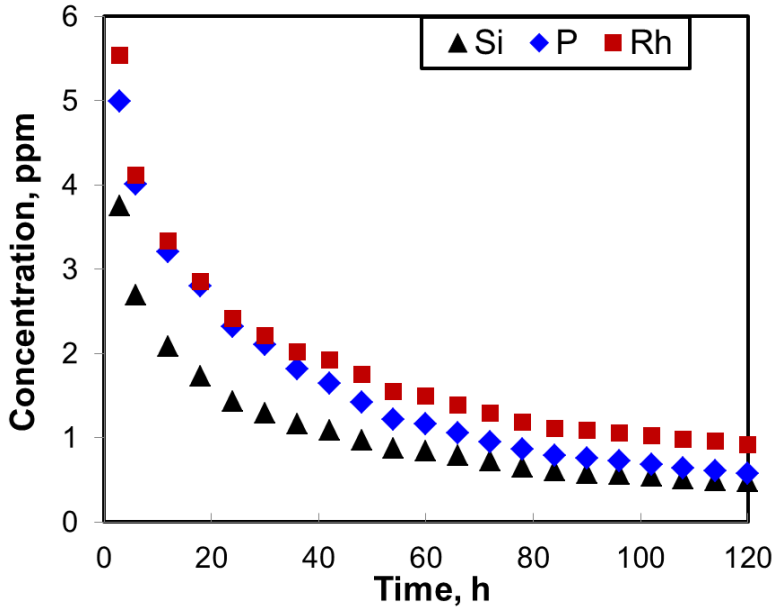

Figure 5.10: Temporal 1-octene conversion and selectivity catalyst leaching profiles during continuous Catalyst B catalyzed homogeneous hydroformylation (conditions same as described in Figure 5.9)

The Si/Rh and Si/P molar ratios in the permeate for continuous reaction using Catalyst B were plotted in Figure 5.11. The relatively higher Si leaching in the beginning of the run indicated the smaller molecular weight portion of the polymer may come through the membrane in the beginning. The stable Si/P ratio after 60 hours indicates that the catalyst leaching at steady state may be due to small pin holes in the membrane, where a very small fraction of the catalyst continued to come through. This problem may be solved by preparing the polymer ligand from a higher molecular weight polysiloxane.

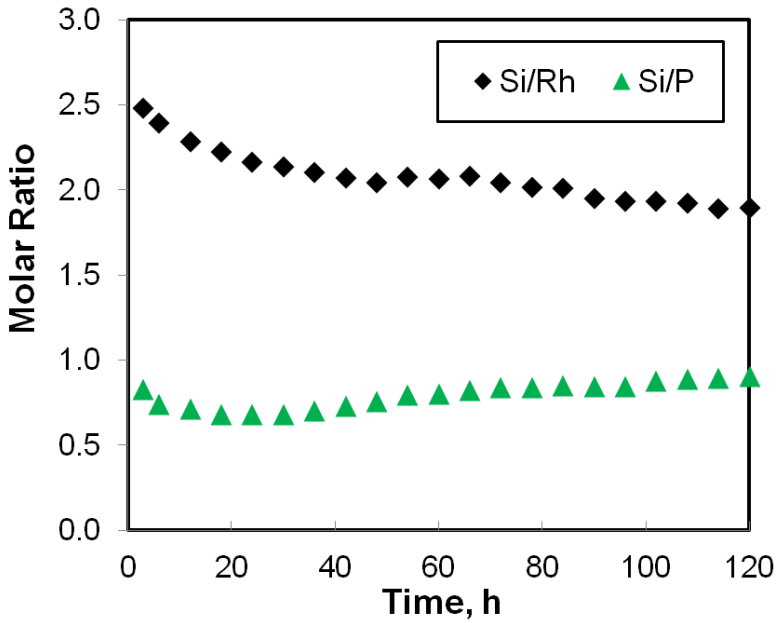

Figure 5.11: Temporal Si/Rh and Si/P molar ratios profiles in permeate during continuous Catalyst B catalyzed homogeneous hydroformylation (conditions same as described in Figure 5.9)

5.5 Conclusions

Polysiloxanes show promise as an inexpensive, stable nano-filterable ligand for hydroformylation reactions displaying excellent activity and chemoselectivity to the aldehydes during continuous runs lasting several days. The advantages of the functionalized polysiloxane ligand include: (a) high stability under hydroformylation conditions, (b) relatively straightforward synthetic steps to functionalize the polymer and synthesize the bound Rh catalyst, and (c) potential use in continuous hydroformylation using membrane filtration. Phosphine functionalized polysiloxane ligand shows better activity than amine functionalized polysiloxane ligand. The Rh-leaching in the effluent with both ligands is less than a few ppm which is recoverable with suitable adsorbents.[77-79]

Chapter 6 : Comparative Economic and Environmental Analyses

6.1 Introduction

Preliminary economic and environmental analyses for the continuous Rh-catalyzed 1-octene hydroformylation process in CXL media using nanofiltration membrane reactor was performed previously.[55] The results were compared to a conventional hydroformylation process using cobalt as catalyst.[89-93] Since then, the CXL process has been modified for better control and catalyst recovery. Updated economic and environmental analyses were conducted using the newly obtained experimental data and improved process. The conventional process was also updated based on more specific data from literature. All the data were updated to the year 2012.

6.2 Process simulations

Both CXL and conventional processes were simulated using Aspen HYSYS. The Peng-Robinson equation of state with van der Waals mixing rules was used to predict relevant thermodynamic properties. The following assumptions were made:

- Annual production capacity was 150 kton per year for both processes
- Identical feeds (1-octene and syngas with a 1/1 H_2/CO ratio) for both processes
- The unit price for all of the raw materials, utilities and labor were the same for both processes.
- The membrane lasts for at least a month.
- The cost of polymer ligand was negligible compared to the cost of Rh.

- Tetramer, diether and diacetal (heavy byproducts) formed in the conventional process were not subsequently cracked or recycled. Neglegible amounts of heavy byproducts were formed in CXL process.

The conditions used in the HYSYS simulation are listed in Table 6.1.

Table 6.1: Conditions used in HYSYS simulation

Simulation Conditions	Units	Conventional	CXL
Catalyst		$HCo(CO)_4$	$Rh(CO)_2(acac)$/Janaphos (P/Rh = 4)
Catalyst Concentration Based on Olefins	wt%	0.53	0.028
Catalyst Recovery Rate	%	98	99.8
Rxn. Temperature	℃	165	50
Rxn. Pressure	bar	207.5	38
Conversion	%	94	80
Selectivity to Aldehydes	%	80	97
Aldehyde *n/i*		4	8
Syngas/Olefin	mol/mol	2.02	2.02
H_2: CO	mol/mol	1.1	1.1
Solvent		none	CXL-toluene (10 vol% CO_2)

The simulated processes for the conventional and CXL processes are shown in Figure 6.1 and Figure 6.2, respectively. Normally, a mixture of different isomers of octenes is used

as raw material in industrial hydroformylation. However, for fair comparison to the CXL process, 1-octene is assumed to be the raw material for both processes. In the conventional process, the hydroformylation reaction is catalyzed by cobalt carbonyl at 165 ℃ and 207.5 bar in three loop reactors in series. The reaction mixture (octene and cobalt catalyst) is fed into the first reactor. The effluent from the first reactor is fed to the second reactor and so on. Syngas is fed into the three reactors in parallel to maintain constant syngas pressure. The cobalt catalyst is separated from the products and recycled back to the reactors through a serious of unit operations.[91-92] Formic acid is used to regenerate the cobalt carbonyl salt back into cobalt tetracarbonyl and cobalt formate (Equation 8). The cobalt tetracarbonyl is removed via gas stripping. The cobalt formate is treated with high pressure syngas to form cobalt salt and regenerate formic acid (Equation 9).

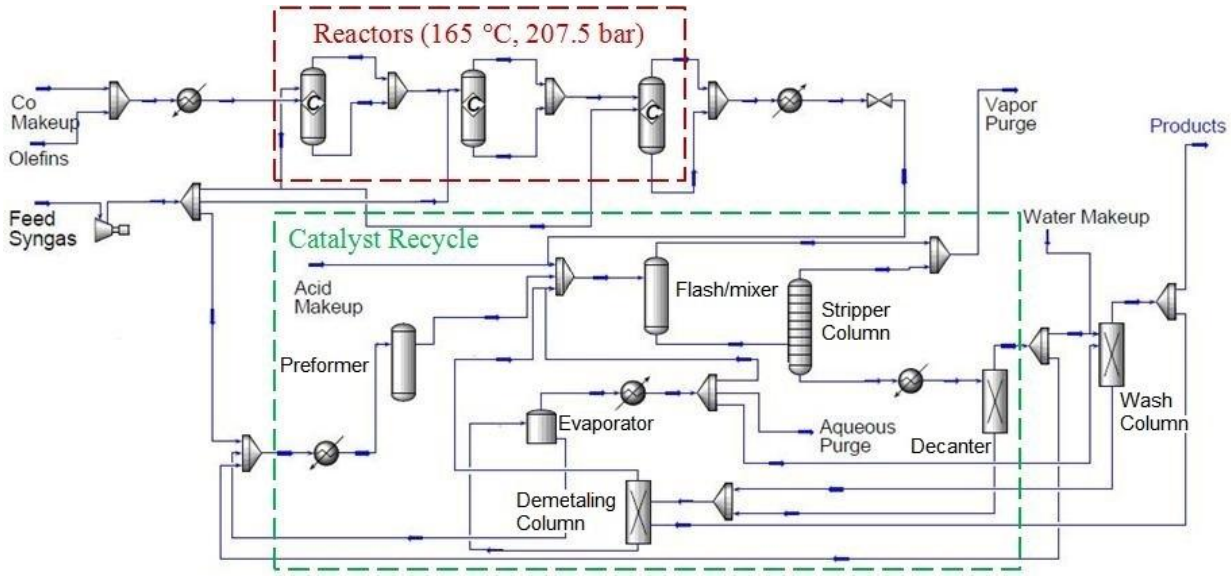

Figure 6.1: Simulated conventional process

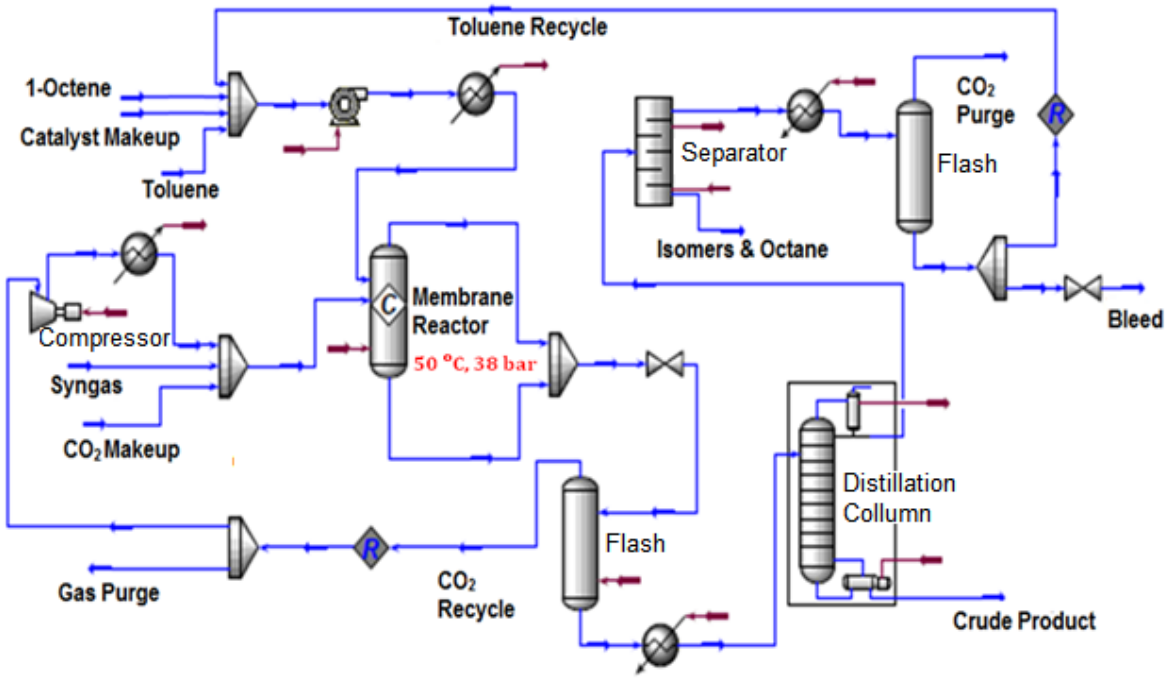

Figure 6.2: Simulated CXL process

$$Co[Co(CO)_4]_2 + 2\ HCOOH \rightarrow 2\ HCo(CO)_4 + Co(COOH)_2 \qquad \text{(Equation 8)}$$

$$3\ Co(COOH)_2 + 8\ CO + 3\ H_2 \rightarrow Co[Co(CO)_4]_2 + 6\ HCOOH \qquad \text{(Equation 9)}$$

In the CXL process (Figure 6.2), the octene hydroformylation reaction is catalyzed by Rh/JanaPhos at 50 ℃ and 38 bar in a membrane reactor. The Rh complex is retained in the membrane reactor during the continuous operation with a Rh loss of 0.2% per hour. The products are separated after reaction. Both CO_2 and toluene are recycled back into the reactor.

The mass and energy flow obtained from HYSYS simulations were used for calculating the economic and environmental impacts.

6.3 Economic analysis

The economic analysis was performed by calculating total capital investment (TCI) and total production cost (TPC) using the methods described in the book of Peters et al.[94] All costs were adjusted for inflation to 2012 dollars using the Chemical Engineering Plant Cost Index (CEPCI).[95]

TCI consists of the fixed-capital investment and the working capital.[94] The working capital is assumed to be 20% of the TCI. The fixed-capital investment includes purchased equipment cost, equipment installation cost, direct and indirect installation costs and auxiliaries/off-site costs. The material for constructing the units was carbon steel. Details of the contribution of each component are listed in Appendix E.

TPC is the sum of total operating costs and total general expenses. Total operating costs include variable production costs (raw materials, catalyst, solvents, utilities, labor, maintenance costs, etc.), fixed charges, and plant overhead costs (research and development costs, distribution and marketing costs, administrative costs). Depreciation is ignored in the present analyses. The cost of raw materials, products, catalysts, and solvents were taken from a variety of sources including the Chemical Market Reporter.[96] Utility costs (cooling water, electricity and steam) were obtained from the Energy Information Administration, Department of Energy.[97] The prices of the raw materials and utilities are also listed in Appendix E. Operating labor expenses are determined by plant capacity and the number of principal processing steps. The mean hourly wage was $47.81, taken from U.S. Bureau of Labor.[98] Details of the contributions to the TPC is shown in Appendix E.

The main components of the total capital investment are shown along with the total cost (Figure 6.3). The details of the costs are listed in Table 6.2. The estimated total capital investment of the conventional process is more than 50% higher than the CXL process. The main contributions to the TCI of the conventional process are the costs of the reactors, the heat exchangers, the separators and distillation columns. Because of the use of three high pressure reactors (207.5 bar) in parallel, the costs of the reactors in the conventional process were almost three times greater than the CXL process, wherein only one membrane reactor (38 bar operating pressure) was used. The much higher reaction temperature (165 ℃) of the conventional process resulted in the heat exchanger cost being more than twice as the CXL process (50 ℃). The series of unit operations for Co catalyst regeneration increases the cost of separators and distillation columns in the conventional process. In the CXL process, the cost of compressor for pumping CO_2 is one of the major contributors to the total captial cost.

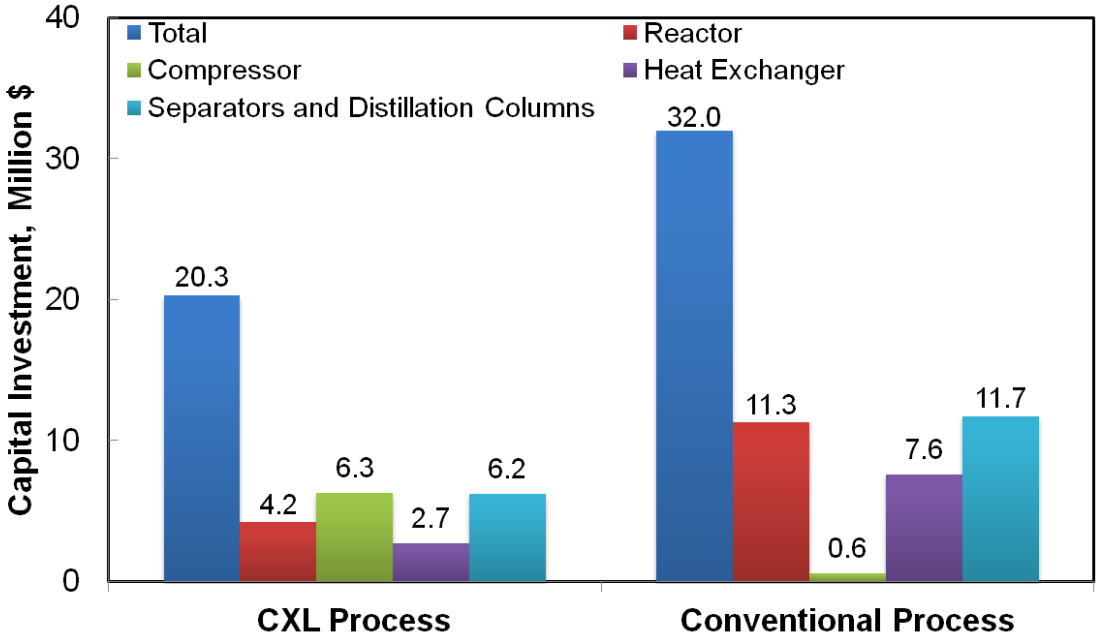

Figure 6.3: Total capital investment for CXL and conventional processes

Table 6.2: Itemnized total capital investment (million $)

Unit	CXL Process	Conventional Process
Reactor	4.2	11.3
Heat Exchangers	2.7	7.6
Distillation Columns	5.4	8.2
Separators	0.8	3.5
Pumps	0.8	0.9
Compressors	6.3	0.6
Filters	0.1	0.0
Total	20.3	32.0

The annual total production cost and the major contributions are shown in Figure 6.4. The details of the production cost are listed in Table 6.3. In year 2012, the average Rh metal price was around $20,800/lb,[99] while Co metal was around $14.8/lb.[100] The annual production cost of CXL process was slightly lower than conventional process assuming that the Rh make-up was 0.2% per hour. At this Rh make-up rate, the ratio (r) of Rh make-up cost per lb of aldehyde produced to nonanal product value ($1.24/lb) was 0.01. The raw material cost was around 70% of the total cost of both processes. Even though the amount of Rh used for CXL process is almost 20 times less than the amount of Co used in the conventional process, the cost of make-up catalyst in CXL process was more than 5 times as the conventional process (Co make-up 2% per hour) because Rh is much more expensive than Co. The ratio of Co make-up cost per lb of aldehyde produced to nonanal product value ($1.3/lb) in the conventional process was 0.002.

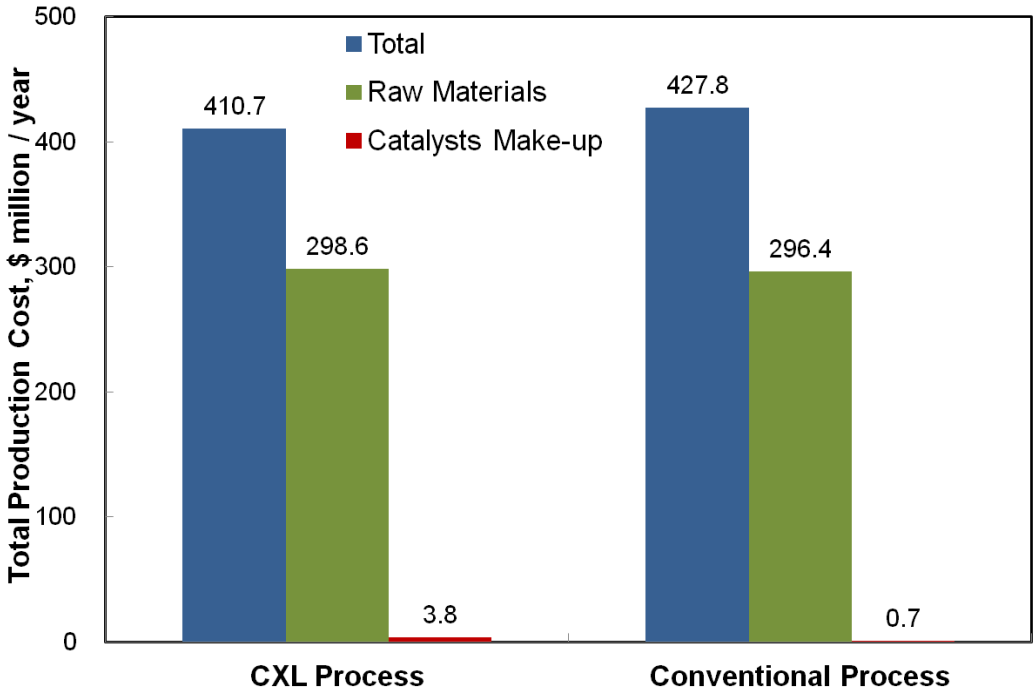

Figure 6.4: Total annual production cost for CXL and conventional processes

Table 6.3: Total annual production cost (million $)

	CXL Process	Conventional Process
Raw Materials	298.6	296.4
Utilities	16.4	19.0
Catalysts Make-up	3.8	0.7
Solvents	0.3	0.0
Other Variable Production Costs	23.5	30.8
Fixed Charges	2.2	8.3
Plant Overhead Cost	3.0	6.0
General Expenses	62.9	66.7
Total	410.7	427.8

A sensitivity analysis of the TPC was performed with various Rh make-up rates at a Rh price of $20,800/lb.[99] As shown in Figure 6.5, the TPC of CXL process was lower than

conventional process for Rh make-up rates of 0.1, 0.2 and 0.5 % per hour at the current Rh price. The TPC of CXL process matched the conventional process when the Rh make-up rate was around 0.94% per hour. At this rate, the ratio (r) of Rh make-up cost per lb of aldehyde produced to the nonanal product value ($1.3/lb) is 0.042.

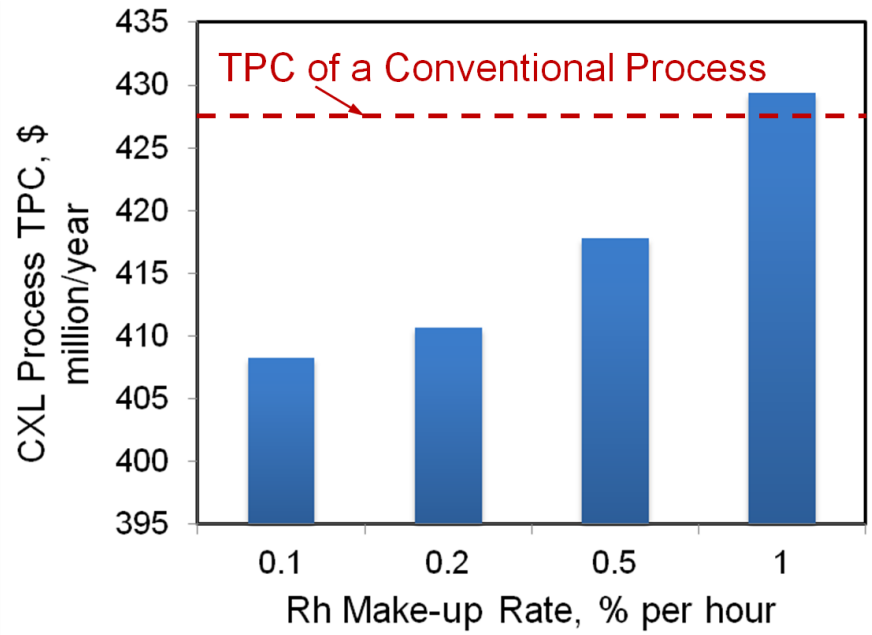

Figure 6.5: Rh make-up rate sensitivity analysis

The estimated r values for various catalysts and process scenarios are shown in Table 6.4. Clearly, all the r values exceed the economic viability critierion (r = 0.042). This indicates that the continuous membrane filtration process is economically viable compared to conventional cobalt catalyzed process.

Table 6.4: Ratio (*r*) of Rh make-up cost per lb of aldehyde produced to nonanal product value ($1.3/lb); Rh cost = $20,800/lb

System	*r*
CXL with JanaPhos	0.006
Syngas only with Catalyst A	0.005
Syngas only with Catalyst B	0.007

In this simulations, the lost Rh was not separated from the product streams. If the ppm level of Rh leached in the permeate is also recovered and recycled, the production cost in the CXL process will be reduced even further.

6.4 Gate-to-gate environmental impact analysis

The ratio of the mass of waste per unit of desired product (*n*-nonanal) is defined as the Environmental factor (E-factor).[101] Waste is defined as everything but the desired products generated in the process, including byproducts, purge gases and emissions. The typical E-factor values for bulk chemicals are < 1-5.[101] The E-factor for the simulated conventional process is 0.64. The E-factor of CXL process is approximately 0.34 due to excellent product selectivity and fewer emissions. In other words, the waste generated from CXL process is approximately half of that generated from the conventional process. When considering that the worldwide hydoformylation capacity is billions of pounds per year, the actual magnitude of potential waste reduction is significant.

Simultaneous Comparison of Environmental and Non-Environmental Process Criteria (SCENE)[102] software was used for the environmental impact analysis. The procedures were the same as described elsewhere.[55] The toxicity index I_{pc} was used as a measure of the extent of toxicity associated with each process. The definition of I_{pc} was also used in the work of Chen et al.[103] As shown in Figure 6.6, the total toxicity index is 3.4 for the conventional process and 2.4 for the CXL process. The CXL process has 33% reduced toxicity than the conventional process. The major contributions to the total toxicity of both processes are the fish toxicity and the human non-carcinogenic inhalation toxicity. The use of formic acid for catalyst regeneration is the main reason for the higher fish toxicity in the conventional process. For both processes, carbon monoxide usage is the main reason for the human non-carcinogenic inhalation toxicity.

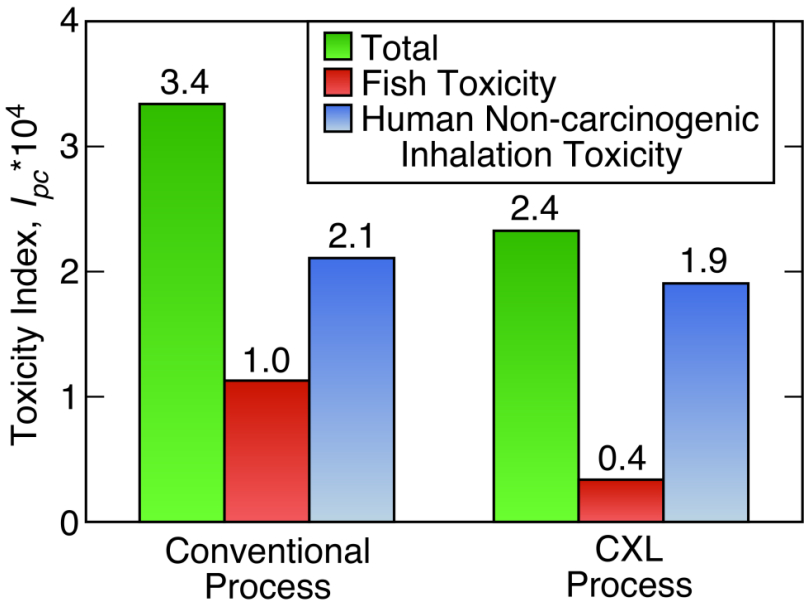

Figure 6.6: Toxicity index for conventional and CXL process

6.5 Conclusion

The E-factor of CXL process (0.34) was nearly half of the conventional process (0.64), indicating a significant reduction in the waste generated in the CXL process. Environmental impact analysis using SCENCE software shows that the total toxicity index of CXL process was approximately 30% less than the conventional process. Based on this analysis, the CXL process is deemed to be environmentally friendlier than the conventional process.

Economic analysis of both processes show an approximately 30% lower total capital investment in the CXL process compared to the conventional process. This disparity is attributed to the higher reaction and catalyst recovery efficiency, lower reaction temperature and pressures used in the CXL process. The total production cost of CXL process was lower than the conventional process when the Rh make-up rate was lower than 0.94% per hour at current Rh price ($20,800/lb). For the CXL process to be more profitable than the conventional process, the economic viability criterion requires that the ratio (r) of Rh make-up cost per lb of aldehyde produced to the nonanal product value ($1.3/lb) is less than 0.042.

Chapter 7 : Conclusions and Recommendations

7.1 Conclusions

The main contributions of this dissertation are as follows:

- A clear understanding of the tunability of syngas solubility in CO_2-expanded liquids and the beneficial effects thereof on enhancing TOF and regioselectivty toward linear aldehydes, even with simple Rh/TPP catalyst complexes.
- The first demonstration of continuous hydroformylation in CXL media in a stirred nanofiltration membrane reactor using 1-octene with soluble Rh-catalyst complex as a model system. The continuous run reflected the previously reported advantages with batch CXL systems producing steady activity, >95% chemoselectivity, *n/i* ratio of nearly 8, and effective Rh retention that exceeded economic viability benchmark.
- Development and demonstration of soluble functionalized polysiloxane-based ligands as inexpensive, nanofilterable alternatives to the JanaPhos ligands in both batch and continuous hydroformylation reactions involving 1-octene and other substrates, with Rh precursors.

These accomplishments are summarized in the following pargraphs.

This dissertation has conclusively shown that CO_2-expanded liquids (CXLs) provide a way of increasing H_2/CO ratio in the liquid phase at fixed syngas feed composition, low syngas partial pressures (i.e. without causing syngas inhibition) and mild total pressures (tens of bars). At a relatively low syngas partial pressure of 6 bar, the H_2/CO ratio in the CXL phase either remains constant at a value of approximately 0.6 (typical in the case non-

CO_2 expanded 1-octene or n-nonanal) or increases to as high as 0.7 at CO_2 partial pressures exceeding 50 bars. For Rh catalyzed 1-octene hydroformylation, the combination of low syngas partial pressure (6 bar) and high H_2/CO ratio (0.6 or greater) in CXL medium avoids CO inhibition, increasing both the TOF and regioselectivities compared to neat hydroformylation reaction mixtures. At 6 bar syngas partial pressure and 50 bar CO_2 pressure, the increase in TOF is up to 64% at 50 ℃ and 21% at 60 ℃, while the corresponding increases in regioselectivity (*n/i*) are 250 and 280%, respectively. At higher syngas partial pressures of 9 and 12 bar, the increases in *n/i* ratio with CXL media were relatively less than at 6 bar. This ability of tuning H_2/CO ratio in CXL can in general be applied to hydroformylation of other olefinic substrates as well.

Continuous homogeneous hydroformylation was demonstrated in CXL media in a stirred reactor equipped with a nanofiltration membrane to effectively retain the bulky Rh catalyst complex. The advantages of low syngas pressure and CXL media on TOF and selectivity are particularly well suited for performing continuous reactions with *in situ* nanofiltration, wherein operating pressures of 30-40 bar are needed to obtain a reasonable transmembrane flux for the 280 MWCO membrane. By maintaining a constant syngas partial pressure of 6 bar and a CO_2 partial pressure of 32 bar in the reactor, we not only avoid syngas inhibition (observed when 30 bar syngas alone is used as pressurizing gas) but also exploit the resulting CXLs to increase the H_2/CO ratio in the reaction phase and the lower the viscosity. Continuous hydroformylation in such a CXL, using soluble bulky phosphite ligands, was successfully conducted for up to 50 hours at 50 ℃. The increased H_2/CO ratio in the CXL phase helps to attain nearly steady TOF_c (~340 h^{-1}) and selectivity (*n/i* = 8, aldehydes > 90%). The cumulative turnover number (TON) is approximately 17,680 after 52 hours.

Constant permeate flux is maintained across the nanofiltration membrane during the 50 h run with low Rh and P leaching (< 1 ppm each in the permeate) at steady state.

Polysiloxanes show promise as an inexpensive, stable nano-filterable ligand for hydroformylation reactions displaying excellent activity and chemoselectivity to the aldehydes during continuous runs lasting several days. Phosphine functionalized polysiloxane ligand shows better activity than amine functionalized polysiloxane ligand. The Rh-leaching in the effluent with both ligands is less than a few ppm which is recoverable with suitable adsorbents.[77-79]

Updated economic analysis, based on plant scale simulation of the continuous CXL process to produce 150 kton/y, shows a more than 30% lower capital investment for the CXL process compared to the conventional Co-catalyzed process of similar capacity. This is due to the higher reaction and catalyst recovery efficiencies, lower reaction temperature and pressures used in CXL process. The total production cost associated with the CXL process was lower than the conventional process when the Rh make-up rate was lower than 0.94% per hour at current Rh price ($20,800/lb). This translates to an economic viability criterion of ($make-up Rh/$ Nonanal) being 0.042 or less.

Updated environmental impact analysis of the simulated and conventional processes revealed that the E-factor (waste generated/desired product) for the CXL process is approximately 0.34, which is almost half of that for the conventional process (0.64), The actual magnitude of potential waste reduction in the CXL process is thus significant when one considers the worldwide capacity of hydroromylation processes (billions of lbs/y). Environmental impact analysis using SCENCE software yielded an overall toxicity index for the CXL process that is approximately 30% less than that for the conventional process.

Based on this comparative gate-to-gate environmental impact analysis, it is deemed that the CXL process is environmental friendlier than the conventional process. Given that the CXL process is more resource-efficent, a cradle-to-gate analysis should yield even better environmental performance.

It should be possible to implement the demonstrated CXL-based continuous reactor concept with *in situ* nanofiltration by replacing existing hydroformylation reactors with the proposed system. Further, the concept should also be applicable in general to homogeneously catalyzed reactions where effective catalyst containment is the key for practical viability.

7.2 Recommendations

1. The current study has shown that using CXL media in continuous membrane filtration is an effective way to achieve high activity, selectivity and Rh retention in Rh-catalyzed 1-octene hydroformylation. Extended runs lasting several days should be carried out to optimize the continuous hydroformylation in CXL media and to study the effect of membrane durability, pressure and temperature on catalytic activity and selectivity.

2. In order to broaden the applications of the CXL-based membrane filtration, it will be extremely beneficial to develop a mathematical model of CXL-based membrane reactor. Rational design and scale-up will be facilitated by such a mathematical model. Detailed kinetic studies for CXL process are also necessary for better understanding of the reaction mechanism.

3. Initial tests on functionalized polysiloxane ligand have shown that phosphine-functionalized polysiloxanes have excellent potential to be inexpensive and effective ligands

for Rh-catalyzed hydroformylation. More detailed studies must be performed to understand the effects of temperature, pressure and P/Rh ratio on hydroformylation reaction using phosphine-functionalized polysiloxane ligand. The ligand preparation can be optimized to improve the quality of the ligand. Further, it will be interesting to apply the CXL concept to the hydroformylation reactions catalyzed by Rh/phosphine-functionalized ligand to confirm whether or not similar enhancements in TOF and selectivity are attainable as with Rh/TPP catalyst.

4. The idea of using gas-expanded liquids to enhance H_2/CO ratio and reduce CO inhibition may also find application in hydroformylation reactions catalyzed by Co-based complexes. Expansion gases such as propane or butane can be used for Co systems since the temperature requirement (>120 ℃) is much higher than that for Rh-catalyzed systems. It will be extremely interesting to see if enhanced TOF and *n/i* are also attainable with Co-catalyzed reactions, considering that Co is almost one thousand times cheaper than Rh.

5. The continuous membrane reactor can be modified to replace the polyimide membrane with a ceramic membrane to withstand the higher temperatures required for Co-catalyzed hydroformylation and other systems.

6. While gate-to-gate environmental analyses were performed for both CXL and conventional processes, a cradle-to-gate analysis should be performed to provide a more thorough evaluation of the environmental impacts of both processes.

References

1. Roelen O, Inventor. Production of oxygenated carbon compounds. DE 849,548. 1938/1952.

2. Chaudhari R. Homogeneous catalytic carbonylation and hydroformylation for synthesis of industrial chemicals. *Top Catal.* 2012;55:439-445.

3. Billig E, Bryan DR. Oxo Process. *Kirk-Othmer concise encyclopedia of chemical technology*. Hoboken, N.J.: Wiley-Interscience; 2000.

4. Frohning CD, Kohlpaintner CW, Bohnen HW. Hydroformylation. In: Cornils B, Herrmann WA. *Applied Homogeneous Catalysis with Organometallic Compounds.* Wiley-VCH, 2002:31-103.

5. Cornils B. In: Falbe J. *New Syntheses with Carbon Monoxide.* Springer, 1980.

6. van Leeuwen PWNM, ed *Homogeneous Catalysis: Understanding the Art*. New York: Springer-Verlag 2004.

7. Frohning CD, Kohlpaintner CW, Bohnen H-W. Carbon Monoxide and Synthesis Gas Chemistry. In: Cornils B, Herrmann WA. *Applied Homogeneous Catalysis with Organometallic Compounds.* 2nd ed. Weinheim, Germany: Wiley-VCH Verlag GmbH, 2008:29-194.

8. Brewester EAV, Pruett RL, Inventors; Union Carbide Corporation, assignee. Cyclic hydroformylation process. US 4247486. 1981.

9. Pruett RL, Smith JA, Inventors; Union Carbide, assignee. Hydroformylation Process. US 3527809. 1970.

10. Gladysz JA. Recoverable catalysts and reagents perspective and prospective. *Chem Rev.* 2002;102:3215-3892.

11. Cornils B, Herrmann WA, Horváth IT, Leitner W, Mecking S, Olivier-Bourbigou H, Vogt D, eds. *Multiphase Homogeneous Catalysis*. Weinheim: Wiley-VCH; 2008; No. 1.

12. Benaglia M, ed *Recoverable and Recyclable Catalysts*. Hoboken, N.J.: Wiley; 2009.

13. Neves ÂCB, Calvete MJF, Pinho e Melo TMVD, Pereira MM. Immobilized catalysts for hydroformylation reactions: A versatile tool for aldehyde synthesis. *Eur J Org Chem.* 2012;6309-6320.

14. Barbaro P, Liguori F. *Heterogenized homogeneous catalysts for fine chemicals production : materials and processes*. Dordrecht ; New York: Springer; 2010.

15. Cole-Hamilton DJ, Tooze RP, eds. *Catalyst separation, recovery and recycling : chemistry and process design*. Dordrecht: Springer; 2006. Catalysis by Metal Complexes Vol. 30.

16. Kresge CT, Leonowicz ME, Roth WJ, Vartuli JC, Beck JS. Ordered mesoporous molecular sieves synthesized by a liquid-crystal template mechanism. *Nature.* 1992;359:710-712.

17. Liu AM, Hidajat K, Kawi S, Zhao DY. A new class of hybrid mesoporous materials with functionalized organic monolayers for selective adsorption of heavy metal ions. *Chem Commun.* 2000;0:1145-1146.

18. Mukhopadhyay K, Mandale AB, Chaudhari RV. Encapsulated $HRh(CO)(PPh_3)_3$ in microporous and mesoporous supports: novel heterogeneous catalysts for hydroformylation. *Chem Mater.* 2003;15:1766-1777.

19. Li P, Thitsartarn W, Kawi S. Highly active and selective nanoalumina-supported Wilkinson's catalysts for hydroformylation of styrene. *Ind Eng Chem Res.* 2009;48:1824-1830.

20. Yoon T-J, Lee W, Oh Y-S, Lee J-K. Magnetic nanoparticles as a catalyst vehicle for simple and easy recycling. *New J Chem.* 2003;27:227-229.

21. Li B, Li X, Asami K, Fujimoto K. Hydroformylation of 1-hexene over rhodium supported on active carbon catalyst. *Chem Lett.* 2003;32:378-379.

22. Ma Z, Liu X, Yang G, Liu C. Hydroformylation of mixed octenes catalyzed by supported rhodium-based catalyst. *Fuel Process Technol.* 2009;90:1241-1246.

23. Janssen M, Mueller C, Vogt D. Recent advances in the recycling of homogeneous catalysts using membrane separation. *Green Chem.* 2011;13:2247-2257.

24. Bergbreiter DE. Using soluble polymers to recover catalysts and ligands. *Chem Rev* 2002;102:3345-3383.

25. Janssen M, Wilting J, Muller C, Vogt D. Continuous rhodium-catalyzed hydroformylation of 1-octene with polyhedral oligomeric silsesquioxanes (POSS) enlarged triphenylphosphine. *Angew Chem Int Ed.* 2010;49:7738-7741.

26. Fang J, Jana R, Tunge JA, Subramaniam B. Continuous homogeneous hydroformylation with bulky rhodium catalyst complexes retained by nano-filtration membranes. *Appl Catal, A.* 2011;393:294-301.

27. Jana R, Tunge JA. A Homogeneous, recyclable rhodium(I) catalyst for the hydroarylation of Michael acceptors. *Org Lett.* 2009;11:971-974.

28. Subramaniam B, Akien GR. Sustainable catalytic reaction engineering with gas-expanded liquids. *Curr Opin Chem Eng.* 2012;1:336-341.

29. Jessop PG, Subramaniam B. Gas-expanded liquids. *Chem Rev.* 2007;107:2666-2694.

30. Hutchenson K, Scurto A, Subramaniam B, eds. *Gas-Expanded Liquids and Near-Critical Media*: American Chemical Society; 2009.

31. Akien GR, Poliakoff M. A critical look at reactions in class I and II gas-expanded liquids using CO_2 and other gases. *Green Chem.* 2009;11:1083-1100.

32. Jessop PG, Leitner W, eds. *Green Solvents*: Wiley-VCH; 2010.

33. Subramaniam B. Gas-expanded liquids for sustainable catalysis and novel materials: Recent advances. *Coordin Chem Rev.* 2010;254:1843-1853.

34. Subramaniam B. Gas Expanded Liquids for Sustainable Catalysis. In: Anastas PT, Zimmerman JB. *Innovations in Green Chemistry and Green Engineering.* Springer New York, 2013:5-36.

35. Lopez-Castillo ZK, Aki SNVK, Stadtherr MA, Brennecke JF. Enhanced solubility of oxygen and carbon monoxide in CO_2-expanded liquids. *Ind Eng Chem Res.* 2006;45:5351-5360.

36. Lopez-Castillo ZK, Aki SNVK, Stadtherr MA, Brennecke JF. Enhanced solubility of hydrogen in CO_2-expanded liquids. *Ind Eng Chem Res.* 2008;47:570-576.

37. Xie Z, Snavely WK, Scurto AM, Subramaniam B. Solubilities of CO and H_2 in neat and CO_2-expanded hydroformylation reaction mixtures containing 1-Octene and nonanal up to 353.15 K and 9 MPa. *J Chem Eng Data.* 2009;54:1633-1642.

38. Hert DG, Anderson JL, Aki SN, Brennecke JF. Enhancement of oxygen and methane solubility in 1-hexyl-3-methylimidazolium bis(trifluoromethylsulfonyl) imide using carbon dioxide. *Chem Commun.* 2005;2603-2605.

39. Zevnik L, Levec J. Hydrogen solubility in CO_2-expanded 2-propanol and in propane-expanded 2-propanol determined by an acoustic sensor. *J Supercrit Fluids.* 2007;41:335-342.

40. Guha D, Jin H, Dudukovic MP, Ramachandran PA, Subramaniam B. Mass transfer effects during homogeneous 1-octene hydroformylation in CO_2-expanded solvent: modeling and experiments. *Chem Eng Sci.* 2007;62:4967-4975.

41. Sih R, Armenti M, Mammucari R, Dehghani F, Foster NR. Viscosity measurements on saturated gas-expanded liquid systems-Ethanol and carbon dioxide. *J Supercrit Fluids.* 2008;43:460-468.

42. Sih R, Dehghani F, Foster NR. Viscosity measurements on gas expanded liquid systems. Methanol and carbon dioxide. *J Supercrit Fluids.* 2007;41:148-157.

43. Sih R, Foster NR. Viscosity measurements on saturated gas expanded liquid systems-Acetone and carbon dioxide. *J Supercrit Fluids.* 2008;47:233-239.

44. Sato Y, Yoshioka H, Aikawa S, Smith RL, Jr. A digital variable-angle rolling-ball viscometer for measurement of viscosity, density, and bubble-point pressure of CO_2 and organic liquid mixtures. *Int J Thermophys.* 2010;31:1896-1903.

45. Scurto AM, Hutchenson K, Subramaniam B. Gas-Expanded Liquids: Fundamentals and Applications. In: Hutchenson K, Scurto AM, Subramaniam B. *Gas-Expanded Liquids and Near-Critical Media.* 1006: American Chemical Society, 2009:3-37.

46. Jin H, Subramaniam B. Homogeneous catalytic hydroformylation of 1-octene in CO_2-expanded solvent media. *Chem Eng Sci.* 2004;59:4887-4893.

47. Jin H, Subramaniam B, Ghosh A, Tunge J. Intensification of catalytic olefin hydroformylation in CO_2-expanded media. *AIChE Journal.* 2006;52:2575-2581.

48. Wang R, Cai H, Jin H, Xie Z, Subramaniam B, Tunge JA. Hydroformylation in CO_2-expanded media. *ACS Symp Ser.* 2009;1006:202-217.

49. Hallett JP, Ford JW, Jones RS, Pollet P, Thomas CA, Liotta CL, Eckert CA. Hydroformylation catalyst recycle with gas-expanded liquids. *Ind Eng Chem Res.* 2008;47:2585-2589.

50. Webb PB, Sellin MF, Kunene TE, Williamson S, Slawin AMZ, Cole-Hamilton DJ. Continuous flow hydroformylation of alkenes in supercritical fluid−ionic liquid biphasic systems. *J Am Chem Soc.* 2003;125:15577-15588.

51. Frisch AC, Webb PB, Zhao G, Muldoon MJ, Pogorzelec PJ, Cole-Hamilton DJ. "Solventless" continuous flow homogeneous hydroformylation of 1-octene. *Dalton T.* 2007;0:5531-5538.

52. Ahosseini A, Ren W, Scurto AM. Understanding biphasic ionic liquid/CO_2 systems for homogeneous catalysis: hydroformylation. *Ind Eng Chem Res.* 2009;48:4254-4265.

53. Riisager A, Fehrmann R, Haumann M, Wasserscheid P. Supported ionic liquid phase (SILP) catalysis: An innovative concept for homogeneous catalysis in continuous fixed-bed reactors. *Eur J Inorg Chem.* 2006;2006:695-706.

54. Gu Y, Li G. Ionic liquids-based catalysis with solids: state of the art. *Adv Synth Catal.* 2009;351:817-847.

55. Fang J, Jin H, Ruddy T, Pennybaker K, Fahey D, Subramaniam B. Economic and environmental impact analyses of catalytic olefin hydroformylation in CO_2-expanded liquid (CXL) media. *Ind Eng Chem Res.* 2007;46:8687-8692.

56. Frisch AC, Webb PB, Zhao G, Muldoon MJ, Pogorzelec PJ, Cole-Hamilton DJ. "Solventless" continuous flow homogeneous hydroformylation of 1-octene. *Dalton T.* 2007;5531-5538.

57. Hemminger O, Marteel A, Mason MR, Davies JA, Tadd AR, Abraham MA. Hydroformylation of 1-hexene in supercritical carbon dioxide using a heterogeneous rhodium catalyst. 3. Evaluation of solvent effects. *Green Chem.* 2002;4:507-512.

58. Datta A, Ebert K, Plenio H. Nanofiltration for Homogeneous Catalysis Separation: Soluble Polymer-Supported Palladium Catalysts for Heck, Sonogashira, and Suzuki Coupling of Aryl Halides. *Organometallics.* 2003;22:4685-4691.

59. Rodriguez BA, Tenn WJ. Direct formation of propanol from a dilute ethylene feed via reductive-hydroformylation using homogeneous rhodium catalysts at low feed pressures. *Appl Catal, A.* 2012;421-422:161-163.

60. Ye K, Freund H, Xie Z, Subramaniam B, Sundmacher K. Prediction of multicomponent phase behavior of CO_2-expanded liquids using CEoS/GE models and comparison with experimental data. *J Supercrit Fluids.* 2012;67:41-52.

61. Jauregui-Haza UJ, Pardillo-Fontdevila EJ, Wilhelm AM, Delmas H. Solubility of hydrogen and carbon monoxide in water and some organic solvents. *Lat Am Appl Res.* 2004;34:71-74.

62. Houndonougbo Y, Jin H, Rajagopalan B, Wong K, Kuczera K, Subramaniam B, Laird B. Phase equilibria in carbon dioxide expanded solvents: Experiments and molecular simulations. *J Phys Chem B.* 2006;110:13195-13202.

63. Haynes WM, ed *CRC Handbook of Chemistry and Physics*. Boca Raton, FL: Chapman and Hall/CRCnetBASE; 1999.

64. Brunner E. Solubility of hydrogen in 10 organic solvents at 298.15, 323.15, and 373.15 K. *J Chem Eng Data.* 1985;30:269-273.

65. Byers JA. http://www.chemical-ecology.net/java/solvents.htm.

66. Evans D, Osborn JA, Wilkinson G. Hydroformylation of alkenes by use of rhodium complex catalysts. *J Chem Soc A.* 1968;0:3133-3142.

67. Pruett RL, Smith JA. Low-pressure system for producing normal aldehydes by hydroformylation of alpha-olefins. *J Org Chem.* 1969;34:327-330.

68. Bhanage BM, Divekar SS, Deshpande RM, Chaudhari RV. Kinetics of hydroformylation of 1-dodecene using homogeneous $HRh(CO)(PPh_3)_3$ catalyst. *J Mol Catal A: Chem.* 1997;115:247-257.

69. Deshpande RM, Bhanage BM, Divekar SS, Kanagasabapathy S, Chaudhari RV. Kinetics of hydroformylation of ethylene in a homogeneous medium: comparison in organic and aqueous systems. *Ind Eng Chem Res.* 1998;37:2391-2396.

70. Divekar SS, Deshpande RM, Chaudhari RV. Kinetics of hydroformylation of 1-decene using homogeneous $HRh(CO)(PPh_3)_3$ catalyst: a molecular level approach. *Catal Lett.* 1993;21:191-200.

71. Purwanto, Deshpande RM, Chaudhari RV, Delmas H. Solubility of hydrogen, carbon monoxide, and 1-octene in various solvents and solvent mixtures. *J Chem Eng Data.* 1996;41:1414-1417.

72. Fujita S-I, Akihara S, Fujisawa S, Arai M. Hydroformylation of 1-hexene using polymer-supported rhodium catalysts in supercritical carbon dioxide. *J Mol Catal A: Chem.* 2007;268:244-250.

73. Koeken ACJ, Benes NE, van den Broeke LJP, Keurentjes JTF. Efficient hydroformylation in dense carbon dioxide using phosphorus ligands without perfluoroalkyl substituents. *Adv Synth Catal.* 2009;351:1442-1450.

74. van Leeuwen PWNM, Casey C, Whiteker G. Phosphines as ligands. In: van Leeuwen PWNM, Claver C. *Rhodium Catalyzed Hydroformylation.* The Netherlands: Springer-Verlag, 2001:76-102.

75. Mueller SG, Werber JR, Al-Dahhan MH, Dudukovic MP. Using a fiber-optic probe for the measurement of volumetric expansion of liquids. *Ind Eng Chem Res.* 2007;46:4330-4334.

76. Fang J. *Towards a benign and viable rhodium catalyzed hydroformylation of higher olefins: Economic and environmental impact analyses, solvent effects and membrane-based catalyst separation.* [Ph.D. dissertation]. Lawrence, Kansas, University of Kansas; 2009.

77. Kramer J, Nollen E, Buijs W, Driessen WL, Reedijk J. Investigations into the recovery of Wilkinson's catalyst with silica-immobilized P-donor ligands. *React Funct Polym.* 2003;57:1-11.

78. Kramer J, Scholten A, Driessen WL, Reedijk J. Recovery of rhodium-containing catalysts by silica-based chelating ion exchangers containing N and S donor atoms. *Inorg Chim Acta.* 2001;315:183-190.

79. Yousif AM, Nishioka M, Wakui Y, Suzuki TM. Rapid adsorption of Rh(III) by polyamine-functionalized cellulose fiber combined with microwave irradiation. *Chem Lett.* 2010;39:1317-1318.

80. Mark JE. Overview of Siloxane Polymers. In: Clarson SJ, Fitzgerald JJ, Owen MJ, Smith SD. *Silicones and Silicone-Modified Materials.* 729: American Chemical Society, 2000:1-10.

81. Clarson SJ, Semlyen JA, eds. *Siloxane Polymers*. New Jersey: Prentice Hall; 1993.

82. Voronkov MG, Mileshkevich VP, Yuzhelevskii YA. *The siloxane bond*. New York: Consultants Bureau; 1978.

83. Yilgör İ, McGrath J. Polysiloxane containing copolymers: A survey of recent developments. *Polysiloxane Copolymers/Anionic Polymerization.* 86: Springer Berlin Heidelberg, 1988:1-86.

84. Graudejus O, Görrn P, Wagner S. Controlling the Morphology of Gold Films on Poly(dimethylsiloxane). *ACS Applied Materials & Interfaces.* 2010;2:1927-1933.

85. Forster T, Schunk SA, Jentys A, Lercher JA. Co and Mn polysiloxanes as unique initiator-catalyst-systems for the selective liquid phase oxidation of o-xylene. *Chemical Communications.* 2011;47:3254-3256.

86. Tas D, Thoelen C, F. J. Vankelecom I, A. Jacobs P. Bifunctional catalytic membrane containing Bronsted acids and sites for enantioselective hydrogenation. *Chemical Communications.* 1997;0:2323-2324.

87. Cypryk M, Pospiech P, Strzelec K, Sobczak JW. Soluble akylthiopolysiloxane-supported palladium catalysts for the Heck reaction. *Phosphorus, Sulfur Silicon Relat Elem.* 2009;184:1586-1598.

88. Lindner E, Auer F, Baumann A, Wegner P, Mayer HA, Bertagnolli H, Reinöhl U, Ertel TS, Weber A. Supported organometallic complexes. Part XX. Hydroformylation of olefins with rhodium(I) hybrid catalysts. *J Mol Catal A: Chem.* 2000;157:97-109.

89. Vargas JM, Inventor; Exxon Chemical Patents Inc., assignee. Hydrogenation catalyst for oxo alcohol process. US 5306848. 1994.

90. Roussel PB, Inventor; Exxon Chemical Patents, Inc., assignee. Process for preforming cobaltous salts using shell-type preformer catalysts. US 5600031. 1995.

91. Hill RR, Roussel PB, Inventors; Exxon Chemical Patents Inc., assignee. Reactivation or regeneration of cobalt preformer catalyst for oxo process. US 5434318. 1995.

92. Beadle SW, Poulin CA, Inventors; Exxon Chemical Patents, Inc., assignee. Use of stripper reactor reflux as an initiator for preforming reaction of cobaltous salts to cobalt carbonyls. US 5457240. 1995.

93. Summerlin WH, Inventor; Exxon Chemical Patents Inc., assignee. Method for removing hydroformylation catalyst. US 5237105. 1993.

94. Peters MS, Timmerhaus KD, West RE. *Plant design and economics for chemical engineers*. 5th ed. New York: McGraw-Hill; 2003.

95. *Chemical Engineering.* March 2013:68. www.che.com.

96. ICIS. http://www.icis.com/chemicals/channel-info-chemicals-a-z/, 2012.

97. U.S. Energy Information Administration. http://www.eia.doe.gov/, 2012.

98. U.S. Bureau of Labor Statistics. http://www.bls.gov/cpi/, 2012.

99. Rhodium price. http://www.kitco.com/charts/rhodium.html, 2012.

100. Cobalt price. http://www.infomine.com/investment/metal-prices/cobalt/, 2012.

101. Sheldon RA. Atom efficiency and catalysis in organic synthesis. *Pure Appl Chem.* 2000;72:1233-1246.

102. Allen DT, Shonnard D. *Green engineering : environmentally conscious design of chemical processes*. Upper Saddle River, NJ: Prentice Hall PTR; 2002.

103. Chen H, Shonnard DR. Systematic Framework for Environmentally Conscious Chemical Process Design: Early and Detailed Design Stages. *Ind Eng Chem Res.* 2004;43:535-552.

104. Xie Z. *Solubilities of CO and H_2 in neat and CO_2-expanded hydroformylation reaction mixtures containing 1-octene and nonanal up to 80 ℃ and 90 bar*. Lawrence, KS: Chemical Engineering, University of Kansas; 2009.

Appendix A : Gas Chromatography Analysis Methods

The GC used in this work is a Varian CP-3800 custom-built in the production facility of Varian Inc. It was designed specifically to quantitatively measure the compounds of interest in our phase equilibrium measurements. The GC plumbing is shown in Figure A.1. The two sampling valves were purchased from Valco Instruments Co. Inc. The 8-port valve V1 is a dual liquid sampling valve with two sampling loops measuring 0.2 μL and 0.5 μL in internal volume. The 0.2 μL sample is injected to the TCD. The 0.5 μL sample is injected through the splitter to the FID. The 10-port valve V2 is a dual gas sampling valve with 200 μL and 250 μL external sample loops. The maximum pressure of the valves is 172 bar (2500 psi) and the maximum temperature is 100 ℃. The liquid sampling valve was not placed in heated zones to prevent the sample from vaporizing before injection. Gases are normally injected at high temperature and low pressure to prevent condensation in the lines. The gas sampling valve was placed in contact with an aluminum heating block. The sample valve temperature was set to 100 ℃.

The injector is Varian CP-1177 split/splitless injector. The temperature was set to 225 ℃. The column oven temperature was set to start from 30 ℃, increase in a rate of 10 ℃ /min till reach 95 ℃, then increase in a rate of 20 ℃ /min till 205 ℃, stay and hold for 10 minutes. The TCD temperature was 225 ℃ with the filament temperature being 350 ℃. The make up flow rate of TCD was 25 ml/min and the reference flow rate was 40 ml/min. The FID temperature was 300 ℃. The make up flow rate of FID was 25 ml/min. The H_2 and zero air flow rates were 30 ml/min and 300 ml/min separately.

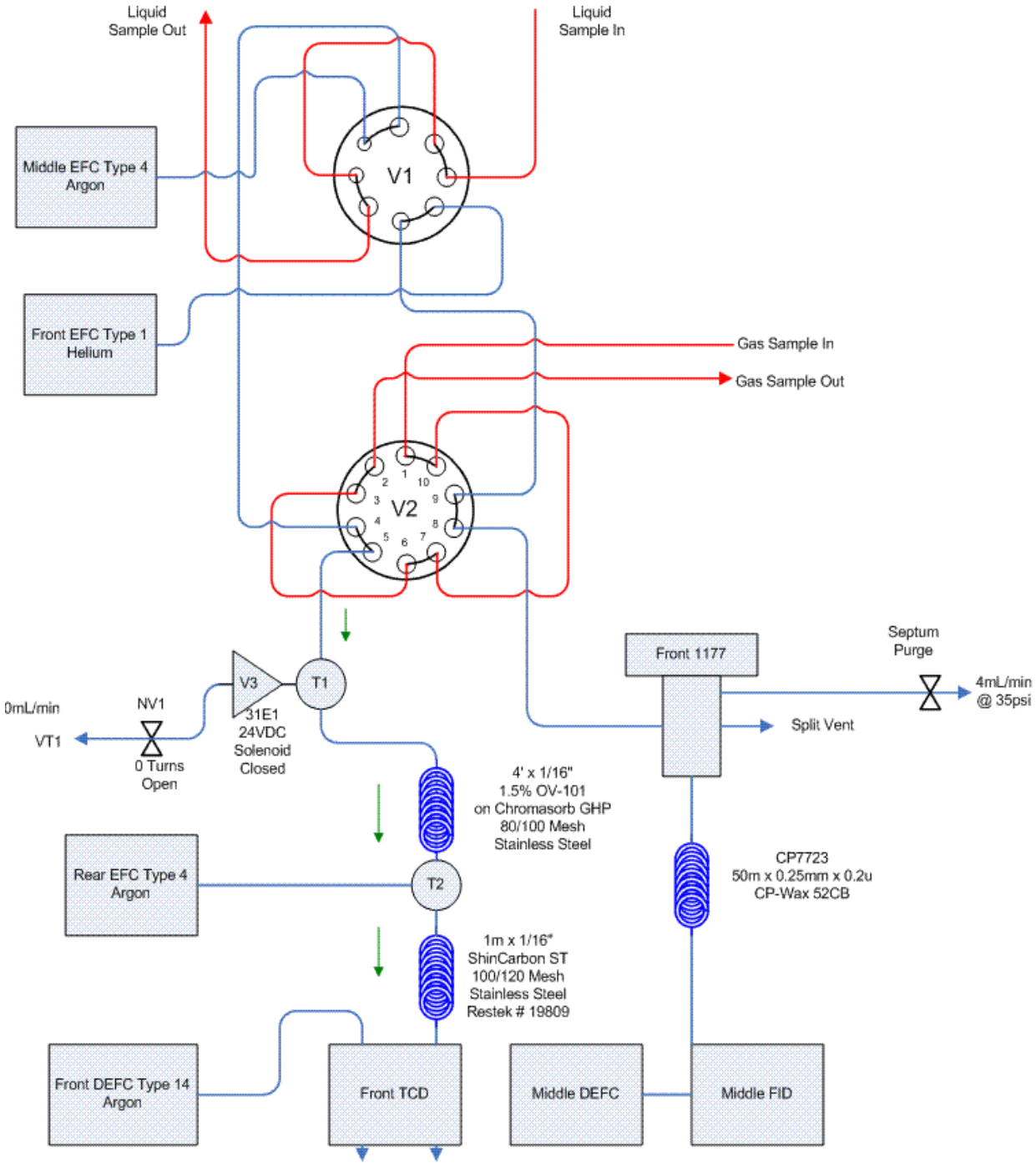

Figure A.1: Schematic of GC plumbing for sampling liquid and vapor phases

The capillary column used for measuring liquid phase composition was a Varian CP-Wax 52CB, 50m $\times$ 0.25 mm $\times$ 0.2 µm. The carrier gas for capillary column was helium. The

packed columns used for measuring gas phase composition were a pre-column (4' × 1/16", 1.5% OV-101 on Chromasorb GHP) from Supelco, and a separation column. The separation column was a Hayesep D 6'×1/8" SS, 80/100 meshed from Hayes Separation Inc. The carrier gas used for packed column injection is argon in order to enable TCD detection of hydrogen, carbon monoxide and carbon dioxide.

Examples of chromatograms of both gas (measured by TCD) and liquid (measured by FID) samples are shown in Figure A.2 and Figure A.3, separately.

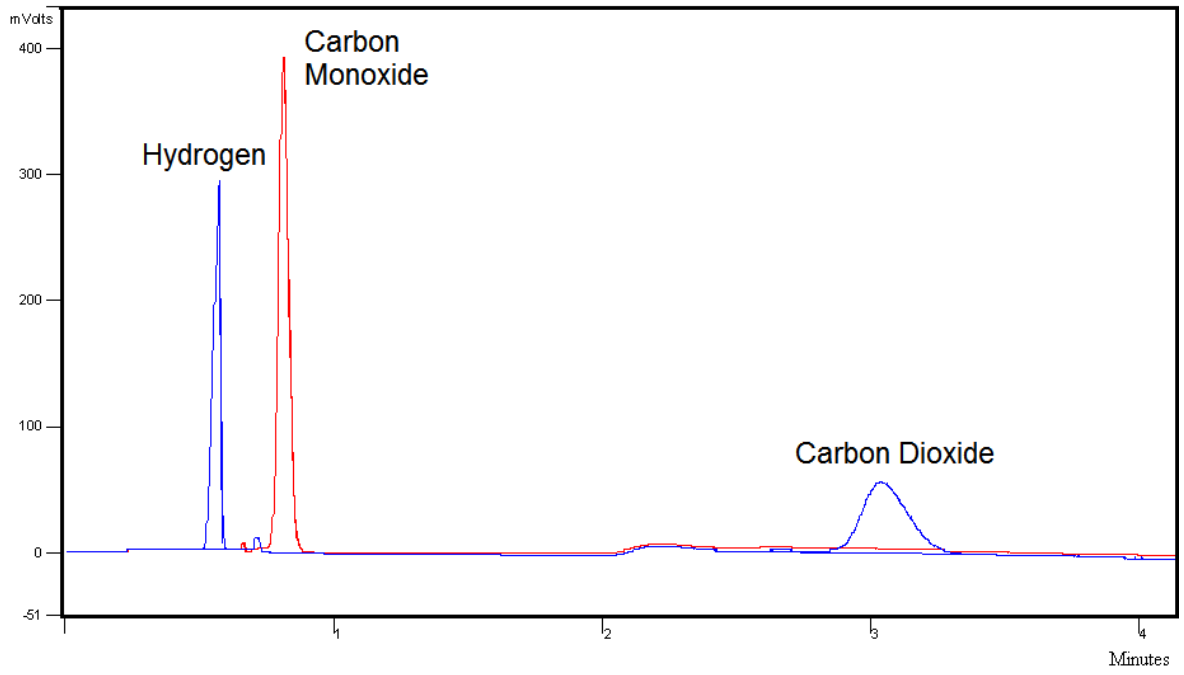

Figure A.2: GC/TCD chromatogram of H_2, CO and CO_2

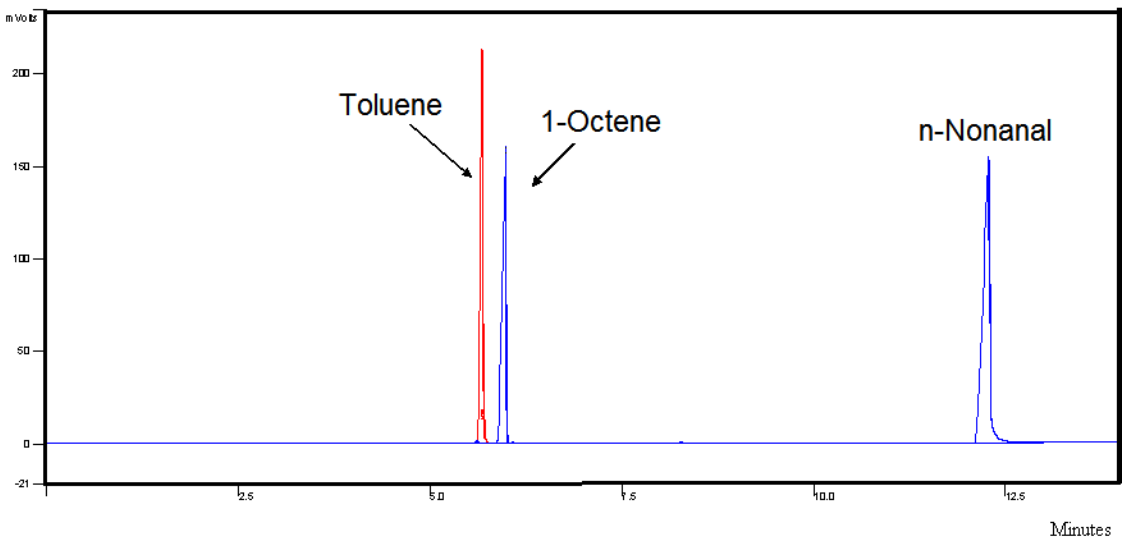

Figure A.3: GC/FID chromatogram of organics

External standardization method was applied to the on-line GC analysis. In this technique, a standard of known composition is chromatographed to generate linear calibration curves for each of the components in the systems being investigated. An identical amount of the sample with unknown composition is then chromatographed. The concentration of a given component is then estimated from the peak areas of that component from the calibration sample and the measured sample.

Calibration curves of gaseous components were generated using the vacuum calibration method as described else where.[104] The calibration curves and data sheets are shown below. The standard deviation was within 5% at each data point.

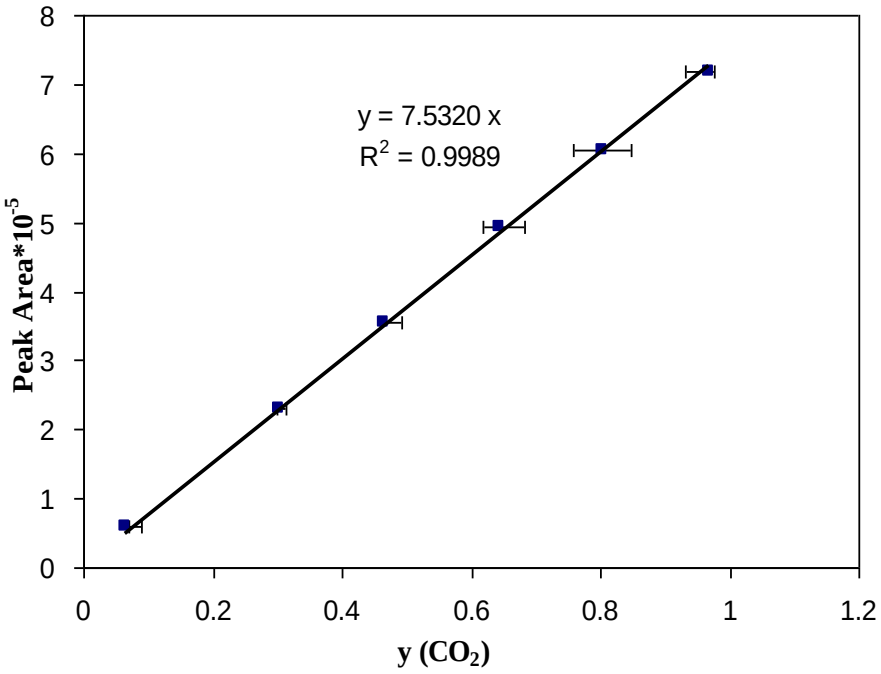

Figure A.4: CO_2 calibration curve

Table A.1: CO_2 calibration data

y, CO_2	PA, average	Standard Deviation
0.064	59317	1065
0.301	230718	778
0.465	354630	134
0.642	492734	3745
0.803	604332	4382
0.967	718515	2053

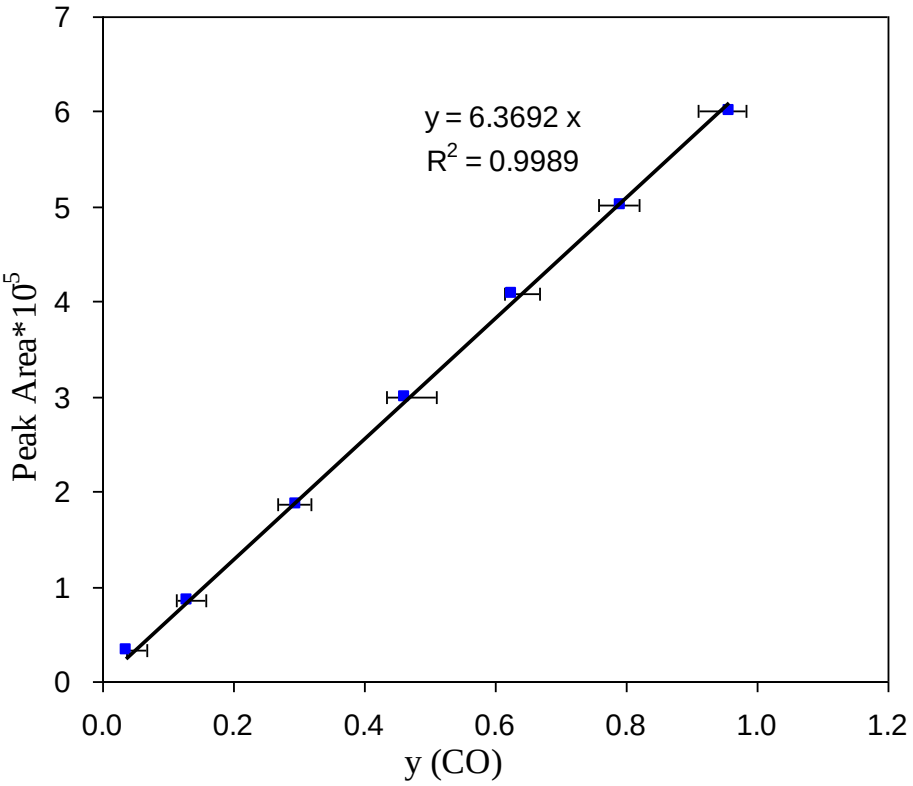

Figure A.5: CO calibration curve

Table A.2: CO calibration data

y, CO	PA, average	Standard Deviation
0.037	32796	1353
0.130	85850	2045
0.295	186623	2287
0.461	300198	3342
0.626	407832	2169
0.791	501801	2505
0.957	601781	2836

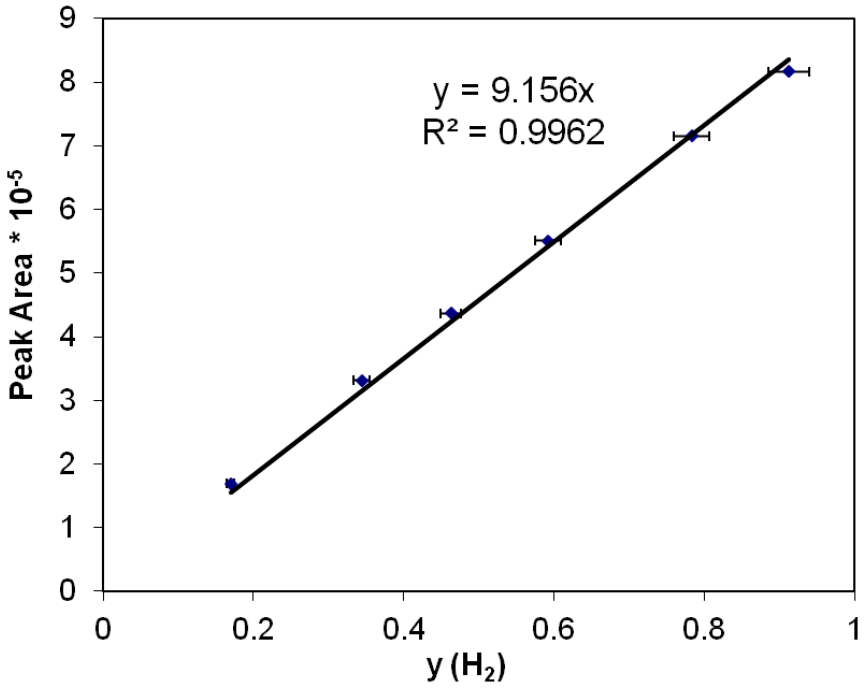

Figure A.6: H_2 calibration curve

Table A.3: H2 calibration data

y (H_2)	PA, average	Standard Deviation
0.17	169181	3356
0.34	331203	7893
0.46	436531	3394
0.59	551114	6564
0.78	715259	2299
0.91	816197	449

Calibration curves for the liquid samples were obtained by manual injections using Hamilton microliter syringes (10 μL, 701N, 80300) with a Hamilton Chaney Adapter (700, 14700) to increase reproducibility. A series of liquid samples with known concentrations

was first prepared and then manually injected into the GC using microliter syringes. At least three repeat injections were made for each concentration to check for reproducibility. Concentrations versus peak area curves were thus generated. The calibration curves and data sheets are shown below. The standard deviation was within 4% at each data point.

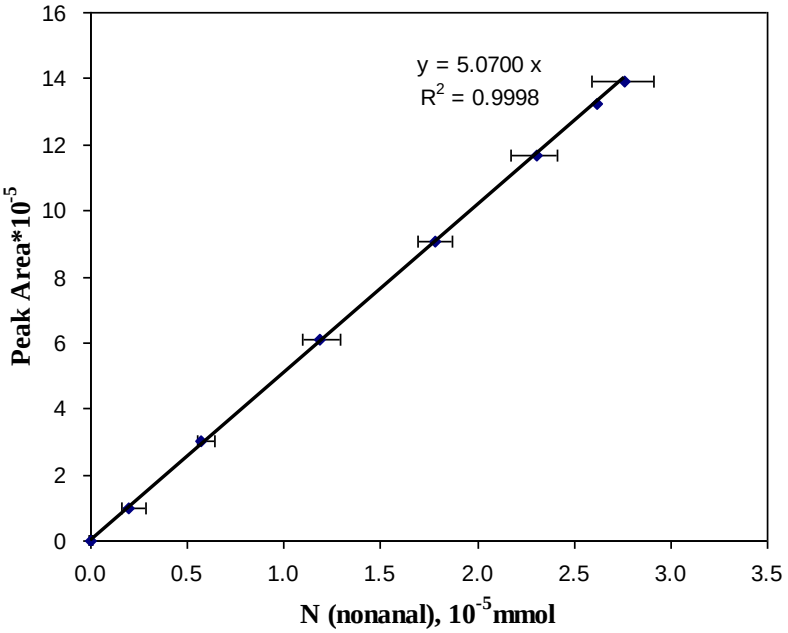

Figure A.7: Nonanal calibration curve

Table A.4: Nonanal calibration data

n (nonanal), 10^{-5} mmol	PA, average	Standard Deviation
2.762	1393516	15625
2.621	1324767	11921
2.304	1168029	8866
1.779	906220	10219
1.185	612192	5140
0.573	304563	6781
0.196	99577	1300

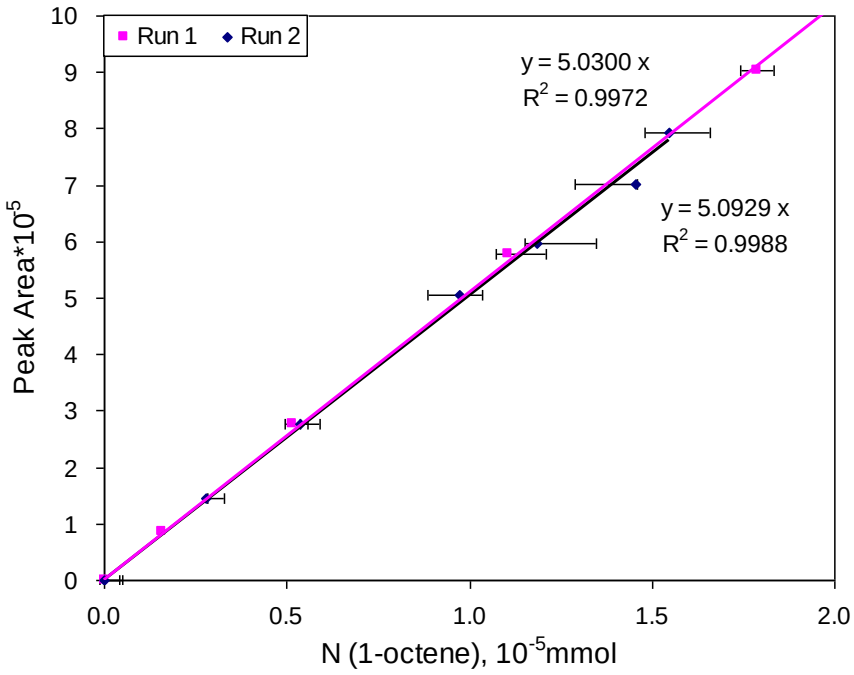

Figure A.8: 1-Octene calibration curve

Table A.5: 1-Octene calibration data (run 1)

n, 1-octene	PA, average	Standard Deviation
0.28	149741	3326
0.54	275627	3338
0.97	505303	7095
1.19	598024	4742
1.45	700748	5157
1.55	792473	7695

Table A.6: 1-Octene calibration data (run 2)

n, 1-octene	PA, average	Standard Deviation
0.16	86347	3156
0.51	276000	2618
1.11	578047	2950
1.79	903246	8104
2.49	1300141	9970
2.93	1448432	8503
3.15	1615072	18354

Appendix B : Prediction of Multicomponent Phase Behavior of CO_2-Expanded Liquids using CEoS/GE Models

The multicomponent systems of 1-Octene hydroformylation in CXL consisting of 1-octene + n-nonanal + H_2 + CO + CO_2 were predicted using CEoS/GE Models.[60] The four combinations of selection are: Peng-Robinson with predictive Soave Redlich-Kwong mixing rule (PR-PSRK), modified Soave-Redlich-Kwong with Modified Huran-Vidal with 2nd order simplification mixing rule (MSRK-MHV2), Soave-Redlich-Kwong with Modified HV by Orbey and Sandler mixing rule (SRK-HVOS) and modified Soave-Redlich-Kwong with Linear Combination HV and MHV1 (MSRK-LCVM). The subsystems that were predicted using these models are listed in Table B.1.

Table B.1: Summary of experimental VLE data used in model evaluation

ID	System	T, ℃	P, bar	Data points
S1	CO_2 + CO + OCT	40-60	80	12
S2	CO_2 + CO + NAL	40-60	80	10
S3	CO_2 + H_2 + OCT	40-60	80	10
S4	CO_2 + H_2 + NAL	40-60	80	10
S7	H_2 + CO + OCT	40-60	6.6 to 6.7	3
S8	H_2 + CO + NAL	40-60	5.8 to 6.5	3
S9	H_2 + CO + CO_2 + OCT	40-60	23 to 65.6	13
S10	H_2 + CO + CO_2 + NAL	40-60	26.9 to 67.1	13
S11	H_2 + CO + OCT + NAL	40-50	6.1 to 6.8	2
S12	H_2 + CO + CO_2 + OCT + NAL	40-50	22.7 to 39.8	5

The following tables compare the experimental data with values predicted by the model that yields the lowest ATAARD (as inferred from Table 2.4).

Table B.2: Comparison of experimental and predicted VLE values for H_2 (1) + CO (2) + 1-octene (3) system using PR-PSRK

		Experimental data[37]				PR-PSRK (Aspen)			
T, ℃	P, bar	x_1	x_2	y_1	y_2	x_1	x_2	y_1	y_2
40	6.6	0.0023	0.0035	0.559	0.433	0.0023	0.0047	0.560	0.432
50	6.7	0.0025	0.0038	0.542	0.453	0.0024	0.0048	0.539	0.449
60	6.7	0.0025	0.0037	0.531	0.457	0.0026	0.0048	0.528	0.453

Table B.3: Comparison of experimental and predicted VLE values for H_2 (1) + CO (2) + nonanal (3) system using PR-PSRK

		Experimental data[37]				PR-PSRK (Aspen)			
T, ℃	P, bar	x_1	x_2	y_1	y_2	x_1	x_2	y_1	y_2
40	5.8	0.0023	0.0038	0.543	0.451	0.0015	0.0033	0.546	0.453
50	6.3	0.0021	0.0034	0.532	0.46	0.0016	0.0036	0.537	0.463
60	6.5	0.0022	0.0038	0.534	0.465	0.0017	0.0037	0.534	0.465

Table B.4: Comparison of experimental and predicted VLE values for H_2 (1) + CO (2) + CO_2 (3) + 1-octene (4) system using PR-PSRK

		Experimental data						PR-PSRK (Aspen)					
T/℃	P/bar	x_1	x_2	x_3	y_1	y_2	y_3	x_1	x_2	x_3	y_1	y_2	y_3
40	23	0.0022	0.0034	0.191	0.138	0.099	0.756	0.0024	0.0040	0.201	0.140	0.100	0.756
40	37.5	0.0025	0.0034	0.337	0.088	0.058	0.851	0.0029	0.0042	0.357	0.091	0.059	0.847
40	45.7	0.0029	0.0037	0.417	0.074	0.054	0.866	0.0033	0.0050	0.437	0.077	0.055	0.865
40	65.1	0.0037	0.0043	0.617	0.061	0.036	0.896	0.0054	0.0058	0.635	0.063	0.037	0.896
50	30.7	0.0023	0.0038	0.248	0.098	0.09	0.805	0.0025	0.0049	0.252	0.099	0.090	0.807
50	38.7	0.0024	0.0037	0.302	0.079	0.062	0.856	0.0029	0.0046	0.329	0.082	0.064	0.850
50	56.9	0.0028	0.0038	0.468	0.058	0.042	0.895	0.0039	0.0051	0.490	0.060	0.043	0.893
50	67.7	0.0032	0.0038	0.587	0.049	0.03	0.916	0.0045	0.0047	0.592	0.048	0.030	0.916
60	27.2	0.0025	0.0036	0.183	0.118	0.096	0.779	0.0028	0.0045	0.197	0.120	0.097	0.776
60	38.3	0.0026	0.0036	0.25	0.063	0.046	0.555	0.0042	0.0056	0.273	0.119	0.083	0.792
60	45.3	0.0027	0.0036	0.325	0.072	0.054	0.868	0.0034	0.0046	0.349	0.074	0.055	0.864
60	55.6	0.0028	0.0037	0.401	0.057	0.041	0.895	0.0038	0.0047	0.432	0.059	0.042	0.892
60	65.6	0.0030	0.0035	0.491	0.047	0.031	0.914	0.0042	0.0044	0.513	0.048	0.032	0.913

Table B.5: Comparison of experimental and predicted VLE values for H_2 (1) + CO (2) + CO_2 (3) + nonanal (4) system using SRK-HVOS

		Experimental data						SRK-HVOS					
T, ℃	P, bar	x_1	x_2	x_3	y_1	y_2	y_3	x_1	x_2	x_3	y_1	y_2	y_3
40	26.9	0.0023	0.0037	0.298	0.129	0.107	0.758	0.0032	0.0048	0.306	0.131	0.108	0.760
40	39.2	0.0025	0.0037	0.468	0.097	0.073	0.826	0.0035	0.0047	0.451	0.094	0.071	0.835
40	47.8	0.0025	0.0036	0.538	0.079	0.059	0.859	0.0038	0.0049	0.538	0.079	0.058	0.863
40	55.8	0.0029	0.0037	0.609	0.071	0.046	0.88	0.0043	0.0047	0.612	0.071	0.046	0.883
50	28	0.002	0.0033	0.301	0.106	0.1	0.788	0.0028	0.0044	0.292	0.105	0.099	0.796
50	38.4	0.002	0.0033	0.413	0.073	0.063	0.861	0.0028	0.0040	0.408	0.072	0.062	0.865
50	55.8	0.0022	0.0032	0.564	0.051	0.037	0.906	0.0032	0.0037	0.563	0.051	0.037	0.912
50	67.8	0.0025	0.0032	0.66	0.048	0.03	0.919	0.0039	0.0038	0.649	0.046	0.029	0.925
60	26.4	0.0023	0.0038	0.246	0.109	0.118	0.769	0.0028	0.0048	0.240	0.108	0.117	0.774
60	39.5	0.0022	0.0039	0.366	0.079	0.088	0.831	0.0032	0.0055	0.359	0.078	0.086	0.836
60	47.1	0.0022	0.0038	0.445	0.062	0.067	0.867	0.0030	0.0050	0.429	0.060	0.065	0.875
60	57.3	0.0023	0.0038	0.532	0.057	0.042	0.896	0.0036	0.0040	0.510	0.054	0.041	0.905
60	67.1	0.0024	0.0037	0.607	0.043	0.039	0.914	0.0033	0.0044	0.578	0.040	0.037	0.923

Table B.6: Comparison of experimental and predicted VLE values for H_2 (1) + CO (2) + 1-octene (3) + nonanal (4) system using SRK-HVOS

		Experimental data						SRK-HVOS					
T, ℃	P, bar	x_1	x_2	x_3	y_1	y_2	y_3	x_1	x_2	x_3	y_1	y_2	y_3
40	6.1	0.0022	0.0037	0.208	0.543	0.45	0.0052	0.0020	0.0048	0.210	0.55	0.45	0.002
50	6.8	0.0024	0.0039	0.220	0.529	0.47	0.0001	0.0023	0.0056	0.217	0.53	0.47	0.003

Table B.7: Comparison of experimental and predicted VLE values for H_2 (1) + CO (2) + CO_2 (3) + 1-octene (4) + nonanal (5) system using SRK-HVOS

	T, ℃	P, bar	x_1	x_2	x_3	x_4	y_1	y_2	y_3	y_4
Experimental data	40	22.7	0.0022	0.0036	0.251	0.1552	0.129	0.113	0.757	0.0003
	40	36.9	0.0021	0.0035	0.420	0.1214	0.076	0.063	0.86	0.0003
	40	47.5	0.0022	0.0035	0.541	0.1003	0.028	0.027	0.943	0.0001
	50	30.6	0.0025	0.0039	0.304	0.1526	0.120	0.101	0.778	0.0003
	50	39.8	0.0026	0.004	0.405	0.1344	0.090	0.074	0.834	0.0011
SRK-HVOS	40	22.7	0.0018	0.0044	0.2144	0.1621	0.124	0.107	0.768	0.0009
	40	36.9	0.0019	0.0040	0.3673	0.1319	0.071	0.058	0.871	0.0008
	40	47.5	0.0010	0.0024	0.4903	0.1109	0.027	0.026	0.947	0.0009
	50	30.6	0.0024	0.0051	0.2556	0.1621	0.113	0.094	0.792	0.0012
	50	39.8	0.0024	0.0048	0.3406	0.1486	0.082	0.067	0.849	0.0012

Appendix C : Gas Flow Rates, Temperature and Pressure Profiles during Continuous Membrane Filtration

CO_2 flow rate, reactor temperature and pressure during continuous membrane filtration without reaction: A continuous membrane filtration experiment was carried out using CO_2-expanded toluene to see whether or not using the CO_2 mass flow controller is able to maintain the reactor pressure. The results are shown in Figure C.1 and Figure C.2. The reactor was first charged with 60 mL of toluene and 32 bar of CO_2. The CO_2 was then introduced by a mass flow cotroller (Brooks) at a predetermined flow rate of 23 sccm.

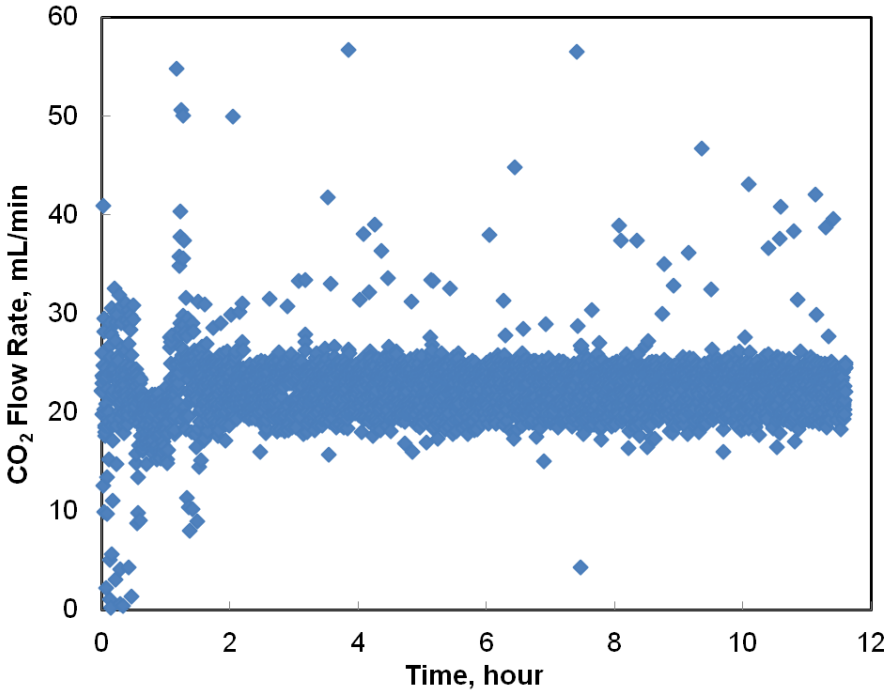

Figure C.1: CO_2 flow rate during continuous filtration of CXL-toluene at 50 ℃, 32 bar

During a continuous filtration of more than 11 hours, the temperature stayed constant at 50 ℃. Even though the flow rate of CO_2 fluctuated around the set point (23 sccm), the pressure of the reactor remained more or less constant after the first 3 hours. These results

proved that the use of mass flow controller was capable to maintain CO_2 pressure during continuous filtration.

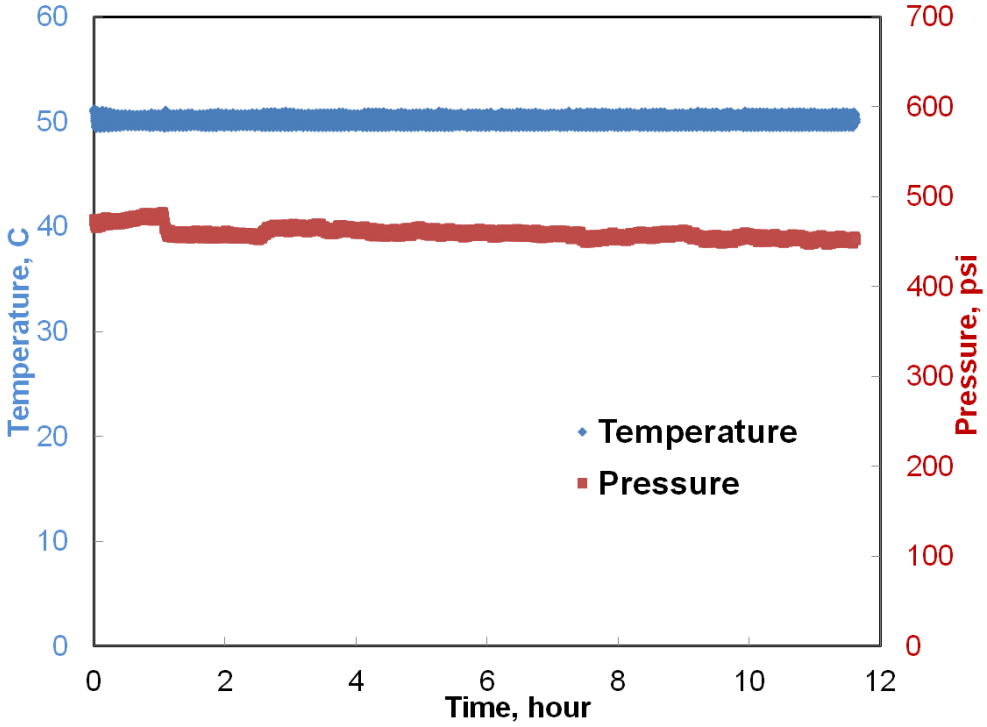

Figure C.2: Reactor temperature and pressure during continuous filtration of CXL-toluene

CO_2 flow rate, reactor temperature and pressure during continuous membrane filtration with reaction: The syngas and CO_2 flow rates, temperature and pressure profiles of an actual continuous reaction are shown in Figure C.3 and Figure C.4. CO_2 flow was set at 15 mL/min. The actual reading of CO_2 flow rate was 15.2 ± 2.3 mL/min. Syngas flow was consumed by the reaction and stablized at 23.4 ± 3.1 mL/min after 4 hours. The more or less constant syngas flow rate shows that the reaction was on steady state. Temperature and pressure were held constant once reaction started.

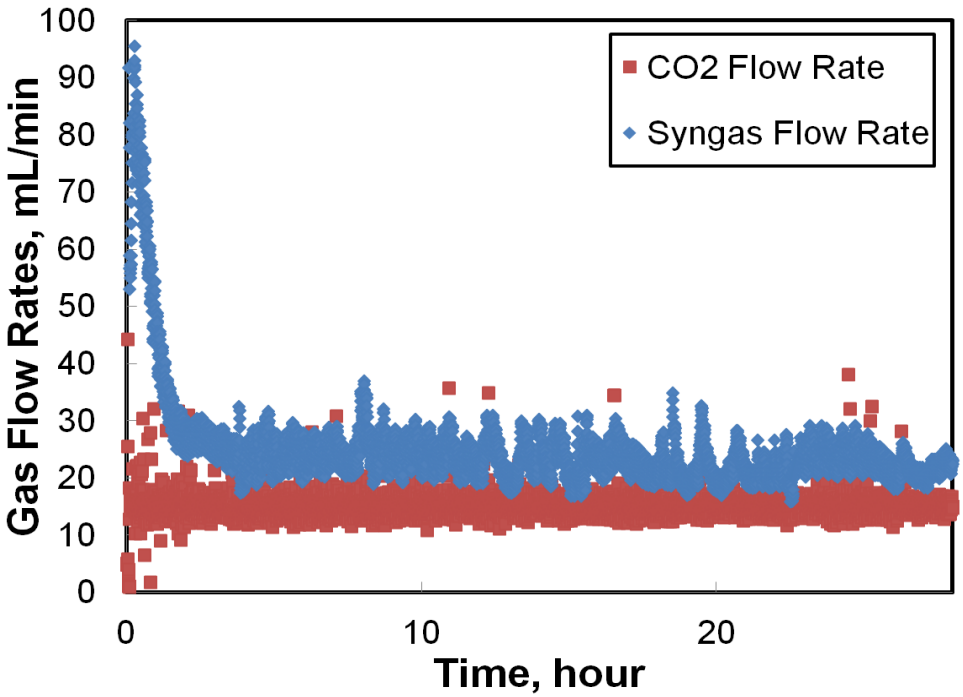

Figure C.3: Syngas and CO_2 flow rates of continuous reaction (CO_2 flow: 15.2 ±2.3 mL/min, syngas flow at steady-state: 23.4 ±3.1 mL/min)

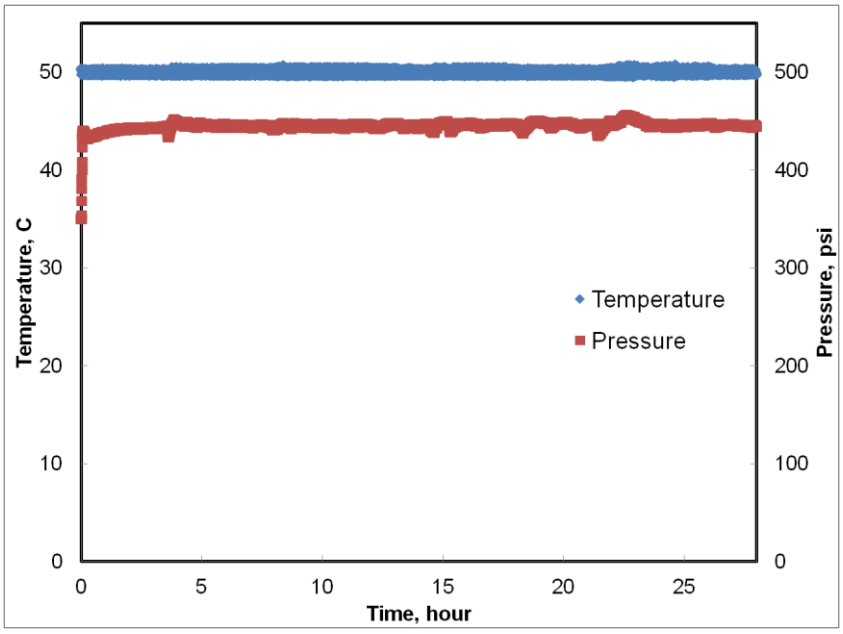

Figure C.4: Temperature and pressure profile of continuous reaction

Appendix D : ICP Analysis Methods

Inductively coupled plasma atom emission spectroscopy (ICP-AES, Horiba Jobin-Yvon, 2000) was used for measuring the concentrations of Rh, P and Si. The operating conditions of ICP is listed in Table D.1. These settings were suitable for analyzing trace elements in organic solvents such as toluene. Auxiliary argon gas was used to prevent carbon deposition from organic samples.

Table D.1: ICP parameter settings

Parameters	Value
Power, W	1300
Plasma flow rate, L/min	16
Auxiliary flow rate, L/min	1.2
Sheath gas flow rate, L/min	0.6
Nebulizer pressure, bar	0.5
Pump speed, rpm	10

Rh and P standards were prepared by dissolving pre-determined amounts of $Rh(acac)(CO)_2$ and triphenylphosphine (TPP) in toluene. A list of standards is shown in Table D.2. Rh was detected at the wavelength of 343.5 nm. P was detected at the wavelength of 253.56 nm. Three repeated measurements were taken at each concentration. The standard deviations for both Rh and P were both less than 5%.

Table D.2: Standards for Rh and P measurement

Number	[Rh], ppm	[P], ppm
1	0.1	0.1
2	1.	1.
3	5.2	5.2
4	40.6	40.4

The calibration curves (Figure D.1 and Figure D.2) using these standards show a linear relationship for both Rh and P.

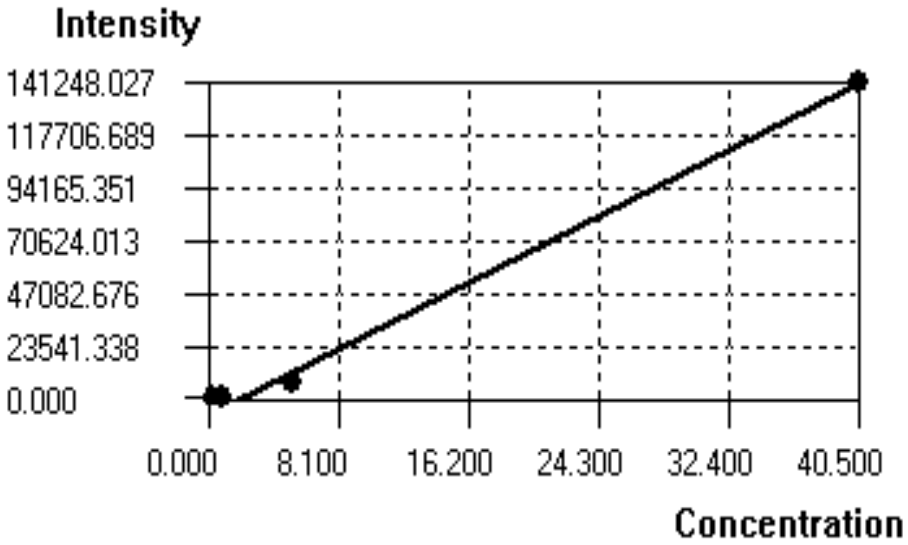

Figure D.1: ICP calibration curve for Rh

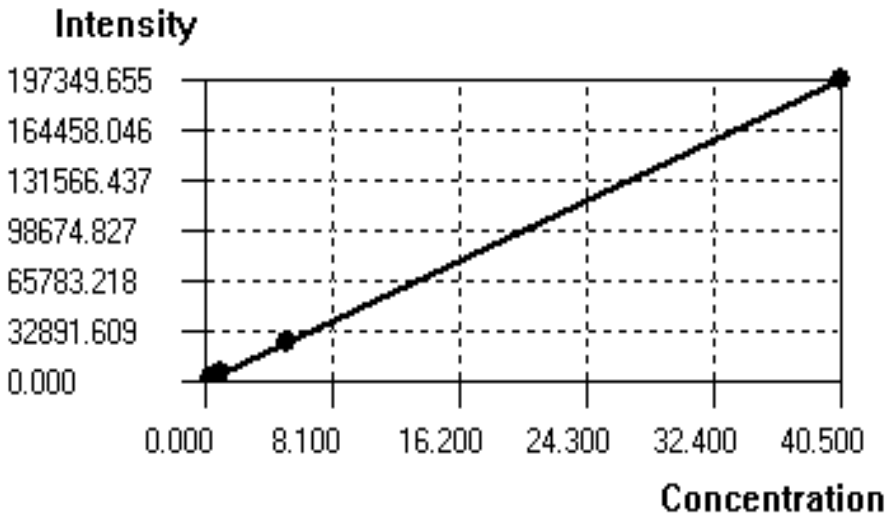

Figure D.2: ICP calibration curve for P

Si standards were prepared separately using trimethylsilane and toluene. Due to the relatively high volativity of trimethylsilane, both toluene and trimethylsilane were kept in the refridgerator before use. The standards were stored in the fridge after prepared. The list of standards for Si is shown in Table D.3 and the calibration curve is shown in Figure D.3. Si was measured at the wavelength of 251.6 nm. The standard deviations from three repeated measurements were less than 3%.

Table D.3: Standards for Si measurement

Number	[Si], ppm
1	5
2	19.7
3	100.2

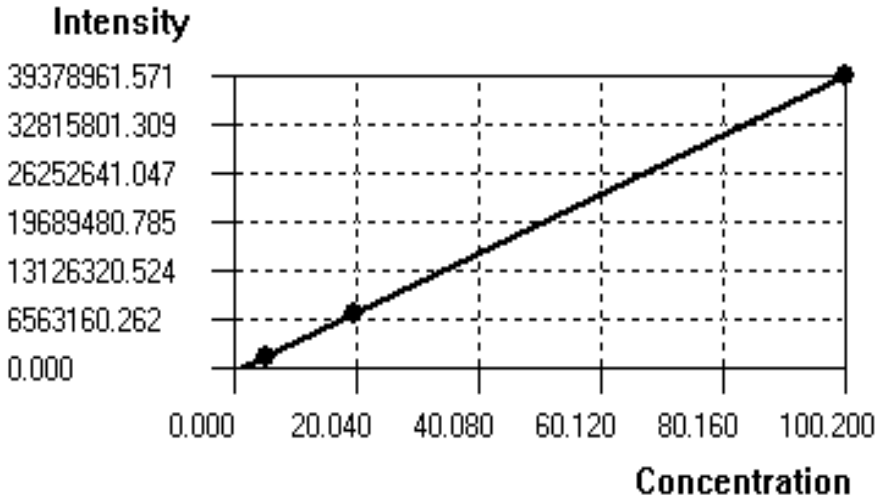

Figure D.3: ICP calibration curve for Si

Appendix E : Details of Economic Analysis

The total capital investment is calculated using the rational shown in Table E.1:

Table E.1: Calculations of total capital investment

Units		percentage
Purchased Cost, $ PC		
purchased-equipment delivery	per. Of PC	0.1
concrete foundations	per. Of PC	0.1
piping	per. Of PC	0.6
steel support	per. Of PC	0.1
instrumentation	per. Of PC	0.1
insulation	per. Of PC	0.1
electrical	per. Of PC	0.1
painting	per. Of PC	0.0
equipment setting	per. Of PC	0.1
Installation equipment costs, $ IEC	PC + above	
freight	per. Of PC	0.0
yard improvements	per. Of PC	0.1
environmental control	per. Of PC	0.0
buildings	per. Of PC	0.4
Direct costs, $ DC	IEC + above	2.8
engineering costs	per. Of DC	0.2
construction overhead	per. Of DC	0.3
contingency	per. Of DC	0.2
contractor's fee	per. Of DC	0.2
Indirect Costs, $ IDC	above	0.7
Auxiliaries/Off-site, $ AO	per. Of DC	0.3
Fixed Capital Investment, $ FCI	DC + IDC + AO	
Working Capital, $ WC	per. Of TCI	0.2
Total Capital Investment, $ TCI	per. Of TCI	1

The total production cost is calculated using the rational shown in Table E.2:

Table E.2: Calculations of total production cost

	Remarks	Percentage
Variable Production Costs, $ VPC		
raw materials		
Direct operating labor, DOL		
Supervisory and clerical labor, SCL	of operating Labor	15%
Utilities		
electricity		
steam		
water, cooling		
Plant maintenance and repairs, PMR	of FCI	7%
operating supplies	of Maintenance & Repairs	15%
laboratory charges	of operating Labor	15%
patents and royalties	of TPC	4%
catalysts		
solvents		
subtotal: variable production costs, VPC		sum of above
Fixed charges, $ FCH		
depreciation	w/o	
taxes (property)	of FCI	2%
financing (interest)	of FCI	1%
insurance	of FCI	8%
rent	of FCI	5%
subtotal: fixed charges, FCH		sum of above
Plant overhead costs, $POC		
safety and protection		
general plant overhead		
payroll overhead, and so on		
subtotal: plant overhead const, POC of DOL		60%
Total operating costs, $ OC		VPC + FCH + POC
General Expenses, GE		
administrative costs	of DOL	25%
distribution and marketing costs	of TPC	10%
research and development costs	of TPC	5%
Total General Expenses, $ GE		sum of above
Total production Cost, $ TPC		OC + GE

Prices of raw materials are listed in Table E.3.

Table E.3: Raw material unit prices

Chemical	Unit Price, $/lb
olefins	0.88
syngas	0.5 (cent/ft^3)
CO_2	0.1 (cent/ft^3)
Rh	20800
toluene	0.59
Co	14.8
Formic acid	0.36

The utility prices were obtained assuming the plants were built in Kansas and listed in Table E.4.

Table E.4: Unit price of utilities

utilities	Unit Price
electricity	0.066 $/kwh
steam	10 $/1000 lb
cooling water	0.1 $/1000 gal